1-1-2014

Epithelial Cell Shape Changes During Lung Branching Morphogenesis: The Role of Wnt/Fzd2 signaling in directing new branch formation

Rachel S. Kadzik
University of Pennsylvania, rkadzik@mail.med.upenn.edu

Epithelial Cell Shape Changes During Lung Branching Morphogenesis: The Role of Wnt/Fzd2 signaling in directing new branch formation

Abstract
Formation of the intricately branched mammalian lung requires precise coordination between the epithelium and mesenchyme over the course of development. This coordination is mediated by molecular signaling between the two tissue compartments. How these signaling pathways coordinate changes in cellular and tissue morphology to give rise to the highly ramified branched network of the lung is not well understood. In this work, I show that signaling through Frizzled 2 (Fzd2) is required for promoting changes in epithelial cell shape that lead to tissue-level changes needed for branching morphogenesis in the lung. Through analysis of both fixed lungs and live imaging lung explants, I was able to identify the changes in individual cell morphology and epithelial tissue organization that occur during new domain branch formation. Using this model, I characterized the defect in branching morphogenesis that arises due to loss of Fzd2 in the lung epithelium. I found that Fzd2 affects apical localization of phospho-myosin light chain 2, and through the RhoA pathway mediates changes in cell shape that lead to thickening of the lung epithelium and ultimately bending of the epithelium. These studies provide a mechanistic link between the Wnt signaling pathway and changes in cell morphology that lead to branching morphogenesis of the lung epithelium.

Degree Type
Dissertation

Degree Name
Doctor of Philosophy (PhD)

Graduate Group
Cell & Molecular Biology

First Advisor
Edward E. Morrisey

Keywords
Branching, Epithelial, Fzd2, Lung, Morphogenesis, Wnt

Subject Categories
Cell Biology | Developmental Biology

EPITHELIAL CELL SHAPE CHANGES DURING LUNG BRANCHING MORPHOGENESIS: THE ROLE OF WNT/FZD2 SIGNALING IN DIRECTING NEW BRANCH FORMATION

Rachel S. Kadzik

A DISSERTATION

in

Cell and Molecular Biology

Presented to the Faculties of the University of Pennsylvania

in

Partial Fulfillment of the Requirements for the

Degree of Doctor of Philosophy

2014

Supervisor of Dissertation:

_____

Edward E. Morrisey, Ph.D., Professor of Medicine

_____

Daniel Kessler, Ph.D., Associate Professor of Cell and Developmental Biology
Graduate Group Chairperson

Dissertation Committee:
Peter Klein, MD, Ph.D., Professor of Medicine
Catherine Lee May, Ph.D., Adjunct Assistant Professor of Pathology and Lab Medicine
Ken Zaret, Ph.D., Joseph Leidy Professor
Amin Ghabrial, Ph.D., Assistant Professor of Cell and Developmental Biology

EPITHELIAL CELL SHAPE CHANGES

DURING LUNG BRANCHING MORPHOGENESIS:

THE ROLE OF WNT/FZD2 SIGNALING IN DIRECTING

NEW BRANCH FORMATION

ACKNOWLEDGMENTS

The work contained in this thesis could not have been completed without the help and support of a number of people. I am grateful for the advice and guidance provided by my advisor, Ed Morrisey. Additionally, there were many colleagues in the Morrisey lab who provided helpful scientific discussions about overarching concepts as well as technical assistance with experimental design and data analysis. The current and former lab members who were particularly important include Dave Cohen, Tien Peng, and Mayumi Miller. I am deeply indebted to Shelby Blythe, who provided unfailing emotional and scientific support through the long days and nights that were required for finishing this work.

ABSTRACT

EPITHELIAL CELL SHAPE CHANGES
DURING LUNG BRANCHING MORPHOGENESIS:
THE ROLE OF WNT/FZD2 SIGNALING IN DIRECTING
NEW BRANCH FORMATION

Rachel S. Kadzik

Edward Morrisey

Formation of the intricately branched mammalian lung requires precise coordination between the epithelium and mesenchyme over the course of development. This coordination is mediated by molecular signaling between the two tissue compartments. How these signaling pathways coordinate changes in cellular and tissue morphology to give rise to the highly ramified branched network of the lung is not well understood. In this work, I show that signaling through Frizzled 2 (Fzd2) is required for promoting changes in epithelial cell shape that lead to tissue-level changes needed for branching morphogenesis in the lung. Through analysis of both fixed lungs and live imaging lung explants, I was able to identify the changes in individual cell morphology and epithelial tissue organization that occur during new domain branch formation. Using this model, I characterized the defect in branching morphogenesis that arises due to loss of Fzd2 in the lung epithelium. I found that Fzd2 affects apical localization of phospho-myosin light chain 2, and through the RhoA pathway mediates changes in cell shape that lead to thickening of the lung epithelium and ultimately bending of the epithelium. These studies provide a mechanistic link between the Wnt signaling pathway and changes in cell morphology that lead to branching morphogenesis of the lung epithelium.

TABLE OF CONTENTS

List of Tables

List of Figures

CHAPTER 1: Introduction

A portion of this introduction and Figure 1.1 were published in a review in *Cell Stem Cell*[1].

Summary

Significant effort from many labs has contributed to our understanding of the signaling pathways that direct formation of the lung. Despite this insight into the biochemical signals that underlie patterning and differentiation of the lung, very little is understood regarding how these signals are translated into physical changes in cell morphology and cell behavior to give rise to the structurally complex branched lung. As the structure of the lung is intimately tied to its proper function, understanding the steps in this morphogenetic process is important for addressing defects that arise during embryogenesis. This introductory chapter will summarize the current understanding of the major molecular pathways required for branching morphogenesis during lung development. I will also highlight the outstanding questions in the field regarding this molecular network as well as the morphogenetic movements that lead to formation of the branched respiratory airways.

Lung development: a brief overview

The adult lung is a highly structured organ whose primary function is to promote gas exchange between the surrounding environment and the circulating blood to allow for terrestrial life. The lung is constructed such that the air from the external environment is passed through a series of branched tubules prior to delivery to the alveoli, where gas exchange with the vasculature occurs. The arborization of the airways serves multiple functions, including allowing for the entering air to be warmed,

moistened and filtered for particulates. In addition, the highly branched network forms a large terminal gas exchange surface in a spatially efficient manner. As such, appropriate patterning of the branched lung epithelium along with the closely aligned vascular network is vital for lung function.

The lung is composed of endoderm-derived epithelial cells that constitute the luminal surface of the airways and alveolar spaces. Surrounding the epithelium are mesenchymal derivatives including airway smooth muscle, pulmonary fibroblasts, and vascular endothelium [2]. During development, the epithelium and mesenchyme are involved in a complex circuit of paracrine and autocrine signals that act to drive morphogenesis and patterning of the developing airway structure [3]. Initial specification of the presumptive lung field is determined by signals from the surrounding mesenchyme, which act to pattern the foregut endoderm. Within 24 hours of specification of the lung the foregut endoderm undergoes a series of morphogenetic movements to give rise to the trachea and the two main stem bronchi. These bronchi ultimately form the 5 lobes of the murine lung: 1 lobe derived from the left bronchus and 4 lobes from the right. Through a series of stereotyped branching processes, these lobes will eventually form the highly arborized respiratory tree [4]. By E16.5 in mice, the primary branching of the lung is complete. Subsequent cell differentiation continues through the early postnatal period to generate more than 40 different cell types in the mature lung [2]. Throughout these processes, signals between the mesenchyme and epithelium inform cell specification, determination, and differentiation as well as direct morphogenetic changes that are essential for development and maturation of the lung.

Molecular Regulation of Lung Development

It is generally understood that development of the lung requires epithelial and mesenchymal interactions induced by molecular signaling between the compartments. While the requirement for a number of these molecular components has been established through knockout analysis, how these signaling pathways interact and how these molecules affect cell biology to shape the developing lung remain areas of active investigation.

The lung initially arises from the anterior foregut endoderm region, which itself arises from the definitive endoderm that develops soon after gastrulation. The definitive endoderm folds to form the gut tube which is patterned along the anterior-posterior and dorsal-ventral axes through paracrine signals from the surrounding mesoderm [5]. As described above, one of the earliest steps in lung development is delineation of the initial respiratory lineage from the foregut endoderm. Specification of the anterior foregut occurs through the action of signaling pathways, including Wnt, Retinoic acid, Fgf, and Bmp in the surrounding mesenchyme acting on the foregut. Integration of these signals leads to specification of the presumptive lung region via expression of Nkx2.1 in the ventral region of the foregut epithelium and restriction of Sox2 expression to the dorsal region [6]. Following specification, the ventral foregut epithelium undergoes a morphogenetic process that leads to a pinching of the foregut endodermal tube to give rise to two new tubes: the dorsal esophagus that leads to the stomach, and the ventral trachea, which leads to the lung. As the trachea and esophagus separate, the two initial buds of the lung epithelium are visible arising from the tracheal region of the foregut endoderm.

Examination of lungs shortly after the two initial buds form show that at this early stage the lung is relatively simple, essentially two epithelial sacs, surrounding a lumen that is continuous with the trachea. This lumen, surrounded by a single-cell layered epithelium, is maintained throughout the branching morphogenesis of the developing lung, and as such presents a different model of branching morphogenesis from salivary gland [7] and mammary gland [8]. From these two simple epithelial sacs, the 5 lobes of the mouse lung form, 4 lobes on the right: the cranial, medial, accessory and caudal, and one lobe on the left. During the pseudoglandular stage, from E9.5 to E16.5, these lobes undergo a series of morphogenetic changes coordinated between the epithelium and the mesenchyme to give rise to the finely branched epithelial airways.

As the lung epithelium grows and branches during the pseudoglandular stage, it is patterned along the proximal-distal axis. The epithelial cells lining the proximal airways express the transcription factor Sox2, and the distal progenitor cells express Sox9 (Fig 1.1). The Sox2-expressing proximal progenitor cells will later differentiate into the ciliated and secretory cells that line the upper airways [9, 10]. Sox9, along with Id2, mark distal multipotent progenitor cells that give rise to all the epithelial cells of the lung [11]. Sox9 plays an important role both in branching morphogenesis and differentiation of the distal cells into the alveolar lineages [12, 13]. The proximal to distal patterning of the lung epithelium is directed and maintained by molecular signaling between the mesenchyme and epithelium through a number of signaling pathways, including Fgf, Wnt and Bmp [13-15].

Following the pseudoglandular stage, around E16.5 in the mouse, branching morphogenesis slows and reaches completion. During the canicular (E17.5-18.5) and saccular stages (E18.5-p5) the proximo-distal patterned epithelium proceeds to undergo

differentiation into the cells that make up the mature, functional lung (Fig 1.1). As described above, the proximal progenitor epithelial cells differentiate into the secretory and ciliated cells of the upper airways that express CC10 and FoxJ1 respectively. SM22a expressing smooth muscle cells, derived from the mesenchyme, surround and support the main bronchioles. At the distal tips of the branched airways, the terminal buds narrow, and undergo further division into small saccules. The cells of the distal epithelium differentiate and go through a series of extensive morphogenetic changes to give rise to the functional gas exchange unit of the lung, the alveoli. The distal epithelial cells become either alveolar epithelial type I cells (AEC1) or alveolar epithelial type II cells (AEC2) (Fig1.1). The AEC1 cells are flat and thin-walled and through close association with the underlying vascular endothelial cells provide the interface that allows for gas exchange. The AECII cells are cuboidal and secrete surfactant that reduces surface tension required for maintenance of the alveolar unit. Molecular signaling pathways including Fgf10, Retinoic acid, and Notch have emerged as critical molecular components needed for maturation of the cell types that compose the alveolar unit [16]. While many of the molecular components of this process have been characterized, the mechanical forces and cellular rearrangements contributing to alveolar development are just beginning to be investigated [17].

A Map for the Branched Lung

Work from the Krasnow lab [4] established that the branching pattern during the pseudoglandular period is highly reproducible and therefore presumably stereotyped and genetically hard-wired. This work highlighted 3 basic types of branching morphogenesis: domain branching, planar bifurcation and orthogonal bifurcation. These modes of branch formation are deployed at different times during establishment of the airway tree to establish the intricate pattern of the mature lung. Domain branch

formation occurs earliest in development, and is characterized by daughter branches budding laterally from the main bronchial tubule. Domain branching establishes the underlying skeleton of the arborized respiratory tree that develops into the main bronchioles of the lung. At the bud tips, the growing terminal bud expands, flattens and undergoes bifurcation, either within the plane of the parent branch (planar bifurcation) or perpendicular to the plane of the parent branch (orthogonal bifurcation). The three modes of branch formation are used in specific sequence to give rise to the stereotyped branching pattern of the lung. This careful analysis of the developmental history of the lung resulted in a lineage diagram for the 5,000 branches of the bronchial tree that is useful for analysis of defects in lung branch formation.

Epithelial-Mesenchymal signaling interactions are required for branching morphogenesis

Initial evidence that signaling between the epithelium and mesenchyme drives branch formation in the lung was derived from tissue transplant experiments in the 1960s. In these experiments, distal lung mesenchyme was placed adjacent to tracheal epithelium, which normally does not undergo branching morphogenesis. The transplanted distal mesenchyme was sufficient to promote branching morphogenesis in the tracheal epithelium [3, 18, 19]. Later work established that isolated lung epithelium could actively branch if cultured with mesenchyme on the opposite side of a filter, suggesting that a diffusible biochemical agent produced by the mesenchyme promotes epithelial branching [20]. Isolated respiratory epithelium is unable to survive in explant culture without mesenchyme, but the denuded epithelium can survive if supplied with Fgf10, Fgf7 or Fgf1. Furthermore, the isolated lung epithelium, cultured in matrigel supplied with either Fgf10 or Fgf1, will undergo branching morphogenesis [21, 22]. Interestingly, epithelium cultured with Fgf7 fails to branch, but instead the tissue forms

large cystic structures. These results demonstrate that the different Fgf ligands expressed in the lung can have distinct effects on epithelial behavior. These series of experiments provide strong support that Fgf acts as the mesenchymal signal that promotes survival and branching morphogenesis of the respiratory epithelium [22].

Fgf Signaling

Fgf ligands induce their downstream biological cascades by binding to and activating Fgfrs, receptor tyrosine kinases. Fgf signaling can act in diverse developmental processes including mesoderm induction and maintenance, cell migration, somite development and proliferation [23]. There are a number of downstream pathway cascades that can be activated with Fgf binding to its receptor including the phospholipase C (PLC) pathway and the Ras/ERK pathway [23]. Because of the diversity of downstream targets, unraveling the particular downstream effects in a tissue-specific manner is an important, but incompletely understood, aspect of the role of Fgfs in lung development. Formation of an active Fgf/Fgfr complex requires heparan sulfate, and localization of heparan sulfates in the lung remains a relatively unexamined aspect of control of Fgf signaling in respiratory development [24, 25]. Numerous members of the Fgf ligand family are expressed in the lung during development, and it has been proposed that each Fgf has a particular role during specific temporal points in lung development. Fgf9 is expressed in the mesothelium and epithelium and has an effect on mesenchymal proliferation and branching morphogenesis [26]. Other Fgf ligands are expressed in the lung mesenchyme, including Fgf10 [21, 22], Fgf1 [27], and Fgf7 [28] [21] [22, 29], and these ligands affect proliferation in both the epithelium and mesenchyme. The Fgf receptor, Fgfr2b, is expressed in the lung epithelium and has a role in branching morphogenesis of the lung [27, 30, 31]. Both Fgf10 and Fgf7 can bind to Fgfr2b, and recent work has suggested that Fgf10 binding to Fgfr2b activates

migration while an Fgf7-Fgfr2b complex promotes proliferation [32]. Although Fgf7 is expressed in the lung mesenchyme, Fgf7 mutant mice do not have a reported lung phenotype [33], which may indicate redundancy with other Fgfs expressed in the lung. Despite the numerous Fgfs expressed in the lung, Fgf10 in the mesenchyme and its cognate receptor Fgfr2b in the epithelium, have emerged as the Fgf ligand/receptor interaction with the most profound effect on branching morphogenesis in the lung.

Evidence for the Fgf10-Fgfr2b-Sprouty Branching Circuit

Research over the last 40 years focusing on the molecular signals required for development of a branched lung has established a central role for Fgf signaling in this process. Analysis of the Fgfr2b knockout mouse revealed a requirement for Fgf signaling through this receptor in early lung development. Loss of Fgfr2b causes complete lung agenesis, although the trachea separates from the esophagus. The tracheal tube forms a blind trachea without any additional bronchial tubes or budding of the endoderm. Further insight into the requirement for FgrR2 in lung development was evaluated by analysis of a dominant-negative Fgfr2 expressed in the lung epithelium [30, 34], or conditional deletion of Fgfr2b using an SPC-cre [35], a Cre line which is active after initial lobation of the lung. Analysis of these mutants allows for evaluation of the requirement for Fgf signaling after the two initial lung buds form. The two major bronchi develop if Fgfr2b is lost after lung specification, and these bronchi extend the length of the lung, but fail to undergo any additional branching. The conditional loss of Fgfr2b in the epithelium further clarifies that Fgf signaling through this receptor is required for the organized branching pattern of the lung. Epithelium with conditional loss of Ffgr2b undergoes late stage branching, but branch formation is completely disorganized. These data support a role for Fgf signaling through Fgfr2b in the molecular

branching circuitry that drives both the initial budding of the lung from the trachea and new branch formation later in development.

Evidence that Fgf10 is the ligand that interacts with Fgfr2b in early lung development comes from two independent analyses of Fgf10 knockout mice. Fgf10 mutant lungs recapitulate the Fgfr2b knockout, displaying complete lung agenesis and formation of a blind trachea [36, 37]. Unfortunately, we currently do not have tools that allow for analysis of the role of Fgf10 in branching morphogenesis after the initial lung bud formation [35, 38]. But, analysis of an Fgf10 hypomorph [38] shows fewer and shorter branches with loss of Fgf10, and complete loss of the accessory lobe. Conditional loss of Fgf10 in the lung mesenchyme using the Dermo1-cre caused only partial loss of Fgf10, but did result in secondary branching defects and complete loss of the cranial lobe [35]. These results demonstrate a requirement for Fgf10 signaling in the initial budding of the lung from the trachea, and strongly suggest a role for Fgf10 in later branching processes.

Downstream of the Fgf10/Fgfr2 interaction, Fgf10 signaling activates the Ras/ERK pathway, and phosphorylated ERK (pERK) is distinctly localized to the growing distal tips of new epithelial branches [13]. During initial lobation of the lung, Fgf signaling through the Ras pathway has been proposed to affect the orientation of cell division and epithelial tubule diameter [39]. The role of Fgf signaling through the Ras/ERK pathway in secondary and tertiary branching processes has yet to be elucidated.

Another downstream target of Fgf signaling is Sprouty. In the lung, Sprouty acts as both a downstream target of Fgf signaling and a negative regulator of Fgf signaling [39-42]. Sproutys act as intracellular negative regulators of Fgf signaling, potentially by

affecting MAPK phosphorylation [43]. Focal regions of Sprouty2 expression are increased in the epithelium prior to new bud formation [42]. This specific expression pattern of an Fgf target gene provides additional support for a role for Fgf signaling in new bud development. Furthermore, double knockouts of Spry1/2 [39] and Spry2/4 [44] exhibit defects in branching morphogenesis and lung formation, similar to what is seen with loss of Fgfr2b. These results suggest that both activation of Fgf10 signaling and reciprocal down-regulation of Fgf signaling via Sprouty is required for proper branching to occur.

An Fgf based signaling network for new branch induction

The knockout analyses detailed above lead to a proposed Fgf based signaling circuit that directs the stereotyped branching program in the lung. In this signaling network, Fgf10, expressed in the mesenchyme, (Fig1.2, A) signals to the epithelium through the Fgfr2b receptor and activates Sprouty2 in epithelial cells. In addition to activating the negative regulator Spry2, Fgf10 signaling promotes epithelial expression of Shh and Bmp4, two signaling molecules that have been proposed to downregulate Fgf10 expression in the lung mesenchyme [15, 45-47]. As the epithelial buds grow and extend into the surrounding mesenchyme, the mesenchyme immediately adjacent to the growing branch does not express Fgf10, though the more distal mesenchyme continues to express Fgf10. This halo of Fgf10-free mesenchyme is likely mediated through the activity of Shh and Bmp4 from the epithelium. When the growing epithelial bud reaches nearly to the edge of the mesenchyme, Fgf10 expression appears to be bifurcated due to this region of inhibition surrounding the epithelium. It has been proposed that the new focal regions of Fgf10 expression promote planar bifurcation of the growing bud tip, further promoting branching morphogenesis. The expression pattern of Fgf10 has been interpreted as a pre-patterning of the mesenchyme to establish the location of domain

branching. But, careful evaluation of the timing of Fgf10 expression in the mesenchyme reveals the distinct punctate pattern arises after new domain branch outgrowth, rather than preceding new branch formation [22]. These results support a model for a dynamic signaling network that drives branching morphogenesis rather than new branch locations determined solely by Fgf10 patterning in the mesenchyme. This model presents a complex signaling and negative feedback circuit that is required for proper branching morphogenesis of the lung epithelium.

Although the described circuit is the generally accepted model for branch formation based on years of experimental data and knockout analysis, this model has a number of aspects that require further examination. As proposed, Fgf10 act as the sole generator of this pattern, but recent data has suggested that correctly patterned branching can occur even with broad, low level, expression of Fgf10 [48]. These results are in agreement with experiments using isolated epithelium in Matrigel supplemented with ubiquitous Fgf10, where individual branches form, but without the patterning observed in vivo [22]. A remaining question in development of the respiratory tree is the mechanism mediated by Fgf signaling that promotes branch outgrowth in the lung. In the drosophila trachea, which also uses an Fgf (branchless/breathless) network for branching morphogenesis, the epithelial cells extend filopodia and migrate through the surrounding cells towards the Fgf10 source [49]. In the lung, no cellular extensions are observed extending into the surrounding mesenchyme, and the epithelium is maintained as a sheet of cells [50] (and our observations). This leaves open the question regarding the cellular biology that underlies Fgf10 acting as a chemoattractant for the lung epithelium. These issues highlight the many outstanding questions regarding the mechanics of new bud formation as well as what factors confer specificity and control of the location of the new bud along the main epithelial tube.

Wnt signaling pathways

As mentioned above, a number of molecular signaling pathways are important for lung development. While there is a clear role for Fgf signaling in establishing the branching pattern in lung development, the requirement for Wnt signaling in this process remains obscure. Analysis of the phenotypic consequences of inactivation or activation of the Wnt signaling pathway has primarily focused on the effect of Wnt signaling on specification and cell fate determination.

The Wnt signaling pathway is activated when a Wnt ligand binds its receptor at the cell surface. The primary Wnt receptors include Frizzleds, of which there are 10 identified in the mouse. Once the ligand-receptor interaction has occurred, a number of different downstream signaling pathways are activated. These pathways are delineated as the canonical, or β–catenin dependent pathway and the non-canonical, or β–catenin independent pathways (Fig 1.3).

The best understood of Wnt pathways is the canonical or β–catenin dependent Wnt pathway. Activation of the canonical Wnt pathway occurs when the Wnt ligand binds to the Fzd/LRP co-receptor at the cell surface and recruits the Disheveled protein (Dvl). Activation of Dvl causes the inactivation of a complex of proteins consisting of serine-threonine kinase glycogen synthase kinase 3B (Gsk3B), casein kinase 1 alpha (Ck1a), Axin2 and adenomatosis polyposis coli (APC). Without Wnt ligand binding, this complex phosphorylates β–catenin, targeting it for proteosomal degradation. Upon Wnt pathway activation, inhibition of this complex results in accumulation of β–catenin and subsequent translocation to the nucleus. In the nucleus, β–catenin complexes with the Tcf/Lef family of transcription factors to activate target gene expression [51].

Canonical Wnt signaling frequently effects cell proliferation or cell fate specification; in contrast, the non-canonical Wnt pathways control components of cell migration and polarity that have effects on tissue morphogenesis. Non-canonical Wnt signaling serves as an umbrella term for any effect of Wnt signaling that does not require β–catenin. Wnt signaling through these non-canonical pathways can include the planar cell polarity (PCP) pathway, which directs how cells align within the plane of a tissue. Convergent extension (CE), another non-canonical pathway, drives the lengthening and narrowing of a tissue as a result of cell intercalation. Both of these pathways involve changes in cell shape and behavior controlled by alterations in the cellular cytoskeleton, frequently mediated through RhoA activation [52-56]. Based on studies in Drosophila, the core components of the PCP/CE pathway have been identified and include the Frizzled receptor, Disheveled, Vangogh-like (vang), Celsr (Flamingo), and Ptk7(Prickle).

In addition to the PCP/CE pathway, a Wnt/calcium- dependent pathway has been described. The Wnt/Ca^{2+} pathway signals through Fzd receptors to heterotrimeric G-protein receptors activating phosphoinotisol signaling pathway to release intracellular calcium stores [57-59]. Release of Ca^{2+} activates downstream calcium-sensitive proteins such as PKC [60], CamKII [59] and calcineurin/NFAT [61]. It remains unclear what role the calcium pathway plays in mammalian development, or if the Ca^{2+} exists in mammalian systems.

A number of studies have demonstrated that several non-canonical pathways, including the Wnt/NF-AT [61], Wnt/JNK [62],Wnt/Siah [63], and the Wnt/TAK1/NLK pathway[64], can antagonize Wnt/β-catenin signaling, indicating possible cross-talk between the non-canonical and canonical pathways. While relatively little work has

focused on the role of non-canonical Wnt signaling in the developing lung, some analysis has been completed evaluating the requirement for components of the PCP pathway.

Wnt signaling in lung development

There are 19 Wnts in vertebrates, and the expression patterns of 5 Wnts have been characterized in the lung: Wnt2, Wnt2b; Wnt 7b; Wnt5a; and Wnt11. Loss of Wnt2 and Wnt2b, Wnt7b, and Wnt5a as well as loss of β–catenin all cause various defects in lung development, establishing a role for Wnt signaling in promoting proper lung development. Wnt11, is expressed in both the lung epithelium and mesenchyme [65], but the Wnt11 knockout has no reported lung phenotype. Most of the analysis of Wnt signaling in lung development has relied on analysis of knockout of single Wnts, although recent work from our lab has highlighted the interaction of multiple Wnt ligands during respiratory development [66, 67].

Analysis of loss of β–catenin at different time points in lung development using conditional knockout mice has demonstrated that the Wnt/β–catenin pathway has a vital and temporally specific role in respiratory organ development. Loss of β–catenin in the foregut endoderm prior to lung specification causes complete lung agenesis [67, 68] due to a failure to specify the Nkx2.1-positive respiratory epithelium. Later in development, loss of epithelial β–catenin after lung specification leads to a loss of distal progenitor cells and a concomitant expansion of proximal cell types [14]. This is accompanied by a reported defect in branching morphogenesis, which may be due to the expanded proximal progenitors being unable to respond to mesenchymal signals that promote branching. Hyperactive Wnt/β-catenin signaling in embryonic lung endoderm causes a switch in lineage commitment from lung to intestinal cell types [69]. These studies using both loss and gain of function of Wnt/β–catenin signaling suggest the predominant role

for Wnt/β–catenin in lung epithelium development is to direct lung specification, differentiation and maintenance of distal progenitor cell types. As defects in specification can affect cell behavior, parsing the interplay between specification and downstream morphological defects remains a challenge in the field.

Wnt2 and Wnt2b are expressed in the splanchic mesoderm surrounding the foregut endoderm at E7.5-E9, prior to lung specification. Complete loss of Wnt2/2b in the mesoderm surrounding the anterior foregut endoderm results in complete lung agenesis due to loss of ventral expression of Nkx2.1, expansion of the dorsal (esophageal) marker Sox2, and a failure of the tracheolaryngeal groove to form. These results, along with the β–catenin results above, demonstrate that Wnt2/2b acts through canonical Wnt signaling to specify the foregut endoderm to lung fate early in development [67]. Analysis of Wnt2 null phenotype reveals a role for this ligand alone in later stages of lung development. Wnt2 mutant lungs are hypoplastic with reduced smooth muscle development surrounding the airways [70]. Wnt2 and Wnt2b expression is restricted to the mesenchyme at all points in development, but their dual role in later aspects of lung development remain relatively unexamined due to the early requirement for these ligands in lung specification.

Wnt7b is expressed throughout the epithelium during lung development. Loss of Wnt7b has effects on both the epithelium and mesenchyme, affecting proliferation in both compartments [71, 72], but does not affect proximal to distal patterning of the lung. Loss of Wnt7b causes decrease of Axin2 and Lef1 expression, downstream targets of Wnt/β–catenin dependent signaling in both the epithelium and the mesenchyme. Decrease in these Wnt target genes suggest that at Wnt7b may be acting through the canonical Wnt pathway in lung development, but does not exclude the possibility that

Wnt7b could also act through the non-canonical pathway. Loss of Wnt7b causes a branching defect such that the right medial lobe arises from the cranial lobe rather than the main bronchi [71] (and my observations). Characterization of a Wnt7b hypomorph suggests that Wnt7b signaling from the epithelium to the mesenchyme affects mesenchyme-derived vascular smooth muscle development [73]. Based on these studies, the primary role for Wnt7b in lung development appears to be regulation of proliferation and vascular smooth muscle development.

Previous work from our lab demonstrated Wnt2/Wnt7b act together in lung development to promote lung development after specification [66]. Loss of both Wnt2 and Wnt7b causes loss of branching morphogenesis in the lung after formation of the initial right and left lobes. Additionally, Wnt2/7b double knockouts have significantly reduced smooth muscle development. Analysis of the double knockout focused on canonical Wnt signaling in the mesenchyme, and defects in epithelial development were not examined. Work remains to establish if the defect in branching morphogenesis with loss of Wnt2/Wnt7b is due to the loss of smooth muscle or due to unreported defects in the epithelium.

Wnt5a has traditionally been thought of as a non-canonical Wnt based on the axis duplication test in Xenopus [74], but cell culture work has shown that Wnt5a can activate β–catenin dependent Wnt signaling, depending on receptors expressed in the receiving cells [75]. Wnt5a in the lung is highly expressed in the mesenchyme around the developing trachea at E11.5, and at lower levels in the lung mesenchyme and epithelium around the branching tips as development proceeds [76]. Wnt5a mutant animals have a very distinct defect in lung development characterized by lung hyperplasia, increased proliferation, and overbranching of the distal airways, without

any change in cell specification [76]. Loss of Wnt5a disrupts some signaling components of the branching circuit, namely a slight increase in Shh expression and incongruously, an increase in Fgf10 expression, as assessed by Northern blot. Overexpression of Wnt5a in the lung epithelium causes decreased branching, shortened outgrowth of new buds and complete loss of the accessory lobe [77]. In addition to defects in branching morphogenesis there were disruptions in the molecular branching circuit. Specifically, Fgf10 expression was increased and Shh expression in the epithelium was decreased. These results lead to the conclusion that Wnt5a is required for down-regulation of Shh expression in the lung epithelium late in development. Despite these findings, whether Wnt5a has a direct role, or indirect role via regulation of Shh, in regulating branch formation requires further investigation.

Non-canonical Wnt signaling in the development of branched organs

In addition to effects through the β–catenin dependent Wnt signaling pathway, Wnt signaling can elicit β–catenin-independent effects on target cells. Rather than affecting cell proliferation or cell fate specification, these alternative Wnt signaling pathways control various aspects of cell migration and polarity which, in turn, can have profound effects on tissue morphogenesis [78]. Molecular analyses of the alternative Wnt pathways has been challenging because these pathways generally lack a robust transcriptional readout. Instead, non-canonical Wnt signaling often leads to cytoskeletal and migratory changes, which can be difficult to characterize and quantify. Despite these caveats, some work has been completed evaluating the requirement for non-canonical Wnt signaling proteins in branching morphogenesis in the mouse kidney and lung.

Some preliminary evaluation of the requirement for the Wnt/PCP/CE components has been completed in branched organs such as the kidney. At this point,

due to the difficulty in determining an appropriate read-out of PCP/CE signaling in these complex organs, there are limited conclusions to be drawn from the available studies. In the kidney, defects in non-canonical Wnt signaling have been reported to cause decreased branching of kidney tubules as well as cause cyst formation. The underlying cellular biology driving these defects is still being examined, but loss of Wnt9b in the kidney [79] causes a disruption in the orientation of cell division. Recent findings have suggested canonical Wnt signaling can control orientation of cell division [80], so assigning a non-canonical role to Wnt9b activity in the kidney may require re-evaluation. Loss of Wnt11 (typically thought to act as a non-canonical Wnt) in the kidney causes decreased branching. This defect in branching morphogenesis is mediated through Gdnf expression, and it remains unclear if Gdnf is a canonical or non-canonical Wnt target [81]. Loss of a core PCP component, Vangl2, in the kidney results in reduced branching and dilated tubules, although this mutant does not develop cystic kidneys [82]. As these results from the kidney make clear, the role and mechanism for non-canonical Wnt signaling acting in branching morphogenesis requires significant additional investigation.

Evaluation of the requirement for non-canonical Wnt signaling in the lung has primarily focused on analysis of mutants of core PCP proteins. Loss of Vangl2 or Celsr1 causes reduced branching morphogenesis, defects in the shape of the major lobes of the lungs, and collapsed lumens of epithelial branches [83]. These studies were completed in the complete knockout, which may have defects in diaphragm development and pleural compartment, potentially confounding interpretation of these results. Of interest, lung explants not subject to the defects in diaphragm development, display defects in branching morphogenesis and a subtle increase in tubule lumen size. Both Vangl2 and Celsr1 are expressed apically in the lung epithelium, but no analysis of their

subcellular distribution within the apical plane has been completed, leaving open the question if the lung epithelium exhibits planar polarity. Loss of another protein that can act within the PCP pathway, Scribble, also results in fewer branches with a narrowed epithelial lumen [84]. Although these studies have demonstrated that core components of the PCP pathway are required for proper arborization of the respiratory epithelium, the mechanism underlying these defects have not been characterized. Furthermore, until it is established that the lung epithelium exhibits planar polarity, an alternative role for these core components in tissue morphogenesis needs to be considered.

Elucidating the tissue specific effect of the Wnt signaling pathway in lung development has remained a challenge, likely due to crosstalk between signaling pathways, including the Fgf pathway. There is evidence for Fgf affecting Wnt expression and canonical Wnt signaling can affect Fgfr2 expression. Fgf9, expressed in the lung epithelium and mesenchyme, regulates Wnt2 expression in the mesenchyme as well as having an effect on branching and mesenchymal growth[26, 85]. Additionally, a screen for downstream effects of Fgf10 signaling in the lung epithelium during bud formation identified Fgf10 as having a positive affect on β-catenin expression and a negative affect on Fzd2 expression[86]. Evidence that Wnt/b-catenin signaling can affect Fgf signaling comes from use of an inhibitor of canonical Wnt signaling, Dkk. Overexpression of Dkk, or deletion of β-catenin, in the lung epithelium results in a decrease in both Fgfr2 expression and p-ERK staining[87]. Additionally, as described above, both loss and overexpression of Wnt5a can cause an increase in Fgf10 expression in the lung. While it is evident that there is crosstalk between the Wnt and Fgf signaling pathways, much work remains to elucidate how these pathways interact during lung development.

There are a few limitations to the approaches used to date to evaluate the requirement for Wnt signaling in the lung. Analysis of the effect of Wnt signaling at the level of the ligand makes it difficult to determine the requirement for Wnt signaling in the epithelium verses effects on the mesenchyme. Additionally, the role for β-catenin in the cell-cell adhesion complex in addition to its role in Wnt signaling complicates assessment of β-catenin knockout phenotypes. In this dissertation I approached the question of evaluating Wnt signaling in the lung from the perspective of the Wnt receptor, Fzd2. Analysis of Wnt signaling at the level of the receptor allows for evaluating tissue specific effects of Wnt signaling, which is not possible when evaluating Wnt ligand mutants. Additionally, by evaluating Wnt signaling by knockout of the receptor, I have not biased my analysis to the canonical Wnt pathway and potentially can evaluate either the canonical and non-canonical pathway, depending which downstream pathway is active in the epithelium.

Frizzled Receptors

Frizzleds are seven-pass transmembrane proteins that function as the principal receptors for Wnt ligands. There are 10 Frizzled receptor genes expressed in the mouse, and 5 are expressed in the lung: Fzd1, Fzd7, Fzd2, Fzd4 and Fzd10 [73]. Although a number of targeted loss of function mutations of Fzd genes have been undertaken, no effect on lung development has been reported. Of the Fzd genes expressed in the lung, Fzd1, Fzd7 and Fzd2 form a distinct subfamily of mammalian Fzd genes and have highly similar protein sequences [88]. Previous work in our lab found that Fzd2 is a downstream target of Gata6 and may have an affect on lung development [89]. Furthermore, loss of Gata6 caused increased Wnt/β-catenin signaling as assessed by the BatGal reporter, and overexpression of Fzd2 caused decreased TopFlash reporter

expression. These results suggested that Fzd2 might play a role in lung development through activation of non-canonical Wnt signaling pathways.

Fzd2 is expressed in both the lung epithelium and the lung mesenchyme [89] (Fig 3.2). While Fzd2 was originally considered a non-canonical Wnt receptor, a number of studies, both in vitro and in vivo, have demonstrated that Fzd2 can act in both pathways. Results from in vitro work showed that selectivity of the branch of the Wnt pathway activated is dependent on the co-receptors expressed and the Wnt ligands available [75]. Wnt5a signaling through Fzd2 and Ror1/2 can activate non-canonical signaling through Rac and down-regulate canonical Wnt signaling [90]. In contrast, in the presence of Wnt3a, Fzd2 can activate canonical Wnt signaling [90-92].

In vitro work on the role of Fzd2 in Wnt signaling has primarily identified non-canonical Wnt pathways as downstream targets of signaling through Fzd2. Overexpression of Fzd2 in Xenopus embryos elicits activation of the calcium pathway, causing increased intercellular Ca^{2+} release [57, 58] and activating CAMKII [59]. Additionally, recent work on a LacZ knock-in into the Fzd2 locus demonstrates a role for Fzd2 in palate closure and heart development, without activation of canonical transcriptional targets [93]. Double knockout of Fzd2 and the closely related Fzd7 cause defects in convergent extension during gastrulation, suggesting that Fzd2, in conjunction with other Fzd receptors, may act through non-canonical Wnt signaling[94]. This group did not report any effect of loss of Fzd2 on lung development. The conflicting data on the downstream effects of Fzd2 in vivo and in vitro highlights the need for analysis of Fzd2 function in a tissue-specific manner in vivo.

As I have highlighted throughout this introduction, while many aspects of the signaling pathways involved in lung development have been evaluated, how these

signaling molecules are translated into the morphogenetic changes needed for lung development has not been well examined. In this dissertation, I provide a detailed description of the changes in tissue morphology and cellular biology that drive changes in the lung epithelium during branching morphogenesis in the lung. I analyze a mutant for a receptor in the Wnt signaling pathway and identify the defects in cellular biology and Fgf signaling that underlie defects in branching morphogenesis. This analysis provides a link between the Fgf and Wnt signaling pathways and changes in cellular biology that drive tissue level deformations necessary for branching morphogenesis in the lung.

Figure 1.1 Signals Direct Lung Development into Specific Differentiated Cell Types of the Adult Lung.

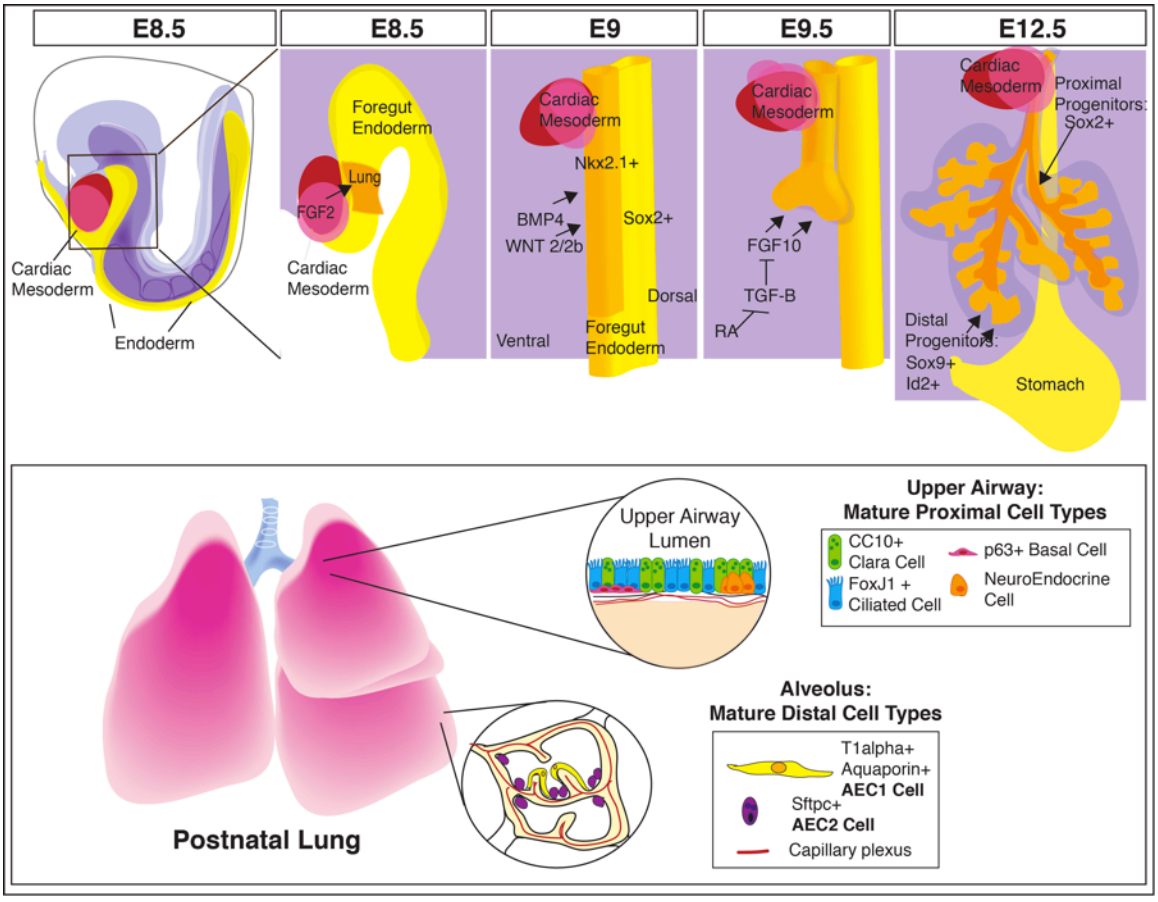

Figure 1.1 Signals Direct Lung Development into Specific Differentiated Cell Types of the Adult Lung.

The foregut endoderm gives rise to the lung epithelium. Fgf signals from the cardiac mesoderm pattern the foregut endoderm into organ specific fields. High levels of Fgf signaling promote lung and thyroid specification, and lower levels promote liver specification. Bmp and Wnt signals from the splanchnic mesoderm promote expression of Nkx2.1 in the ventral endoderm. At E9.0 the trachea bifurcates from the foregut endoderm and the primary lung buds form. Fgf10 signals from the mesenchyme drive lung bud outgrowth and is in turn regulated by retinoic acid repression of Tgf-β signaling. By E12.5 the 5 lobes of the mouse lung have formed, and stereotyped branching morphogenesis has begun. Proximal progenitor cells express Sox2 and will give rise to the cell types that populate the upper airways (club cells, ciliated cells, neuroendocrine cells). Distal progenitor cells express Sox9 and Id2. Early in development (prior to E13.5) these distal cell progenitors can give rise to all the epithelial cells of the lung. Later in development (after E16.5), these distal progenitors will generate the alveolar epithelial lineages including AEC1 and AEC2 cells.

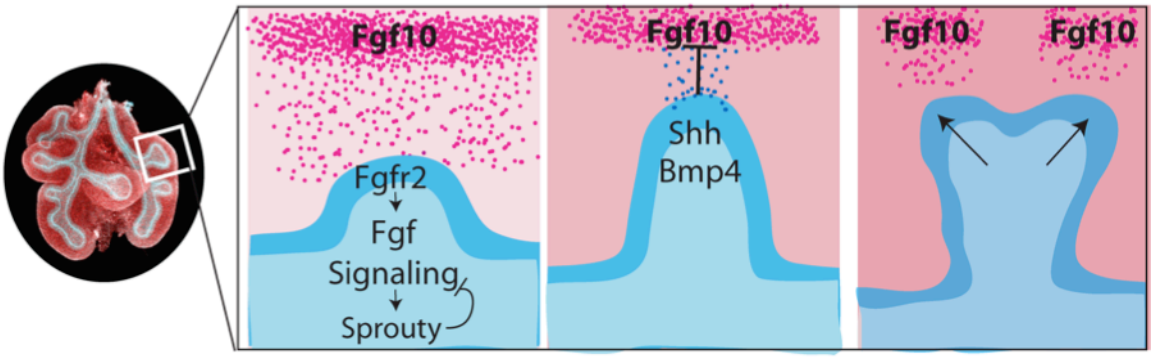

Figure 1.2 Molecular Circuitry for Branching of the Lung

The proposed model for branching morphogenesis requires Fgf10 expression in the mesenchyme to promote new branch formation. Fgf10 signals through Fgfr2 in the epithelium to activate Fgf signaling. One of the downstream targets of Fgf signaling is Sprouty2, which acts to repress Fgf signaling. Fgf10 also promotes expression of Shh and Bmp4 in the epithelium. These molecular signals act to repress expression of Fgf10 adjacent to the epithelium. As the epithelium extends into the mesenchyme, the new bud flattens and bifurcates and grows towards regions of Fgf10 expression.

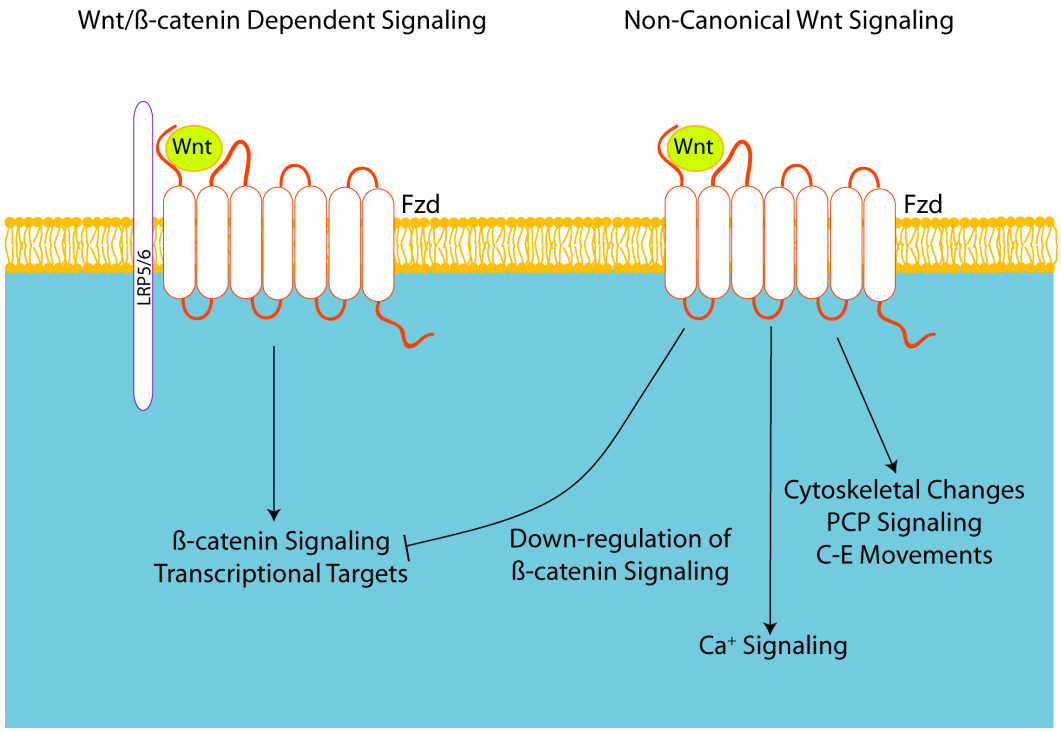

Figure 1.3 Wnt Signaling Pathways

Overview of the Wnt signaling pathways shows Wnt ligands can activate a number of different downstream pathways. In Wnt/β-catenin dependent signaling, the Wnt ligand binds to the Frizzled and Lrp5/6 receptors at the cell surface. The binding of the Wnt ligand releases β-catenin from the destruction complex, and β-catenin translocates to nucleus, where it activates transcriptional targets. The non-canonical Wnt signaling pathway can cause downstream effects that include down-regulation of β–catenin dependent signaling, calcium signaling and changes in cytoskeletal behavior and cell movements.

CHAPTER 2: Changes in Epithelial Behavior Underlying New Domain Branch Formation

Portions of this chapter were published in the *Proceedings of the National Academy of Sciences* [95].

Summary

As reviewed in Chapter 1, the molecular component of branching morphogenesis in the lung has been extensively studied, but how these signaling pathways are translated into effects on cell biology has not been well examined. In this chapter I will describe the changes in both cell morphology and tissue shape that the lung epithelium undergoes during the initial development of the respiratory tree. From this analysis we have developed a model for understanding and evaluating domain branch formation in the lung and changes in cell and tissue morphology in the epithelium that lead to new branch formation.

Introduction

Although a number of the biochemical pathways involved in establishing the arborized airways have been elucidated, the physical forces and changes in cell biology that drive these processes are not well understood. During the pseudoglandular stage, the lung epithelium undergoes a stereotyped branching program to give rise to the elaborately branched respiratory network of the adult lung (Fig 2.1). The branching pattern has been delineated into a series of subroutines [4], all starting with domain branching from the initial lung buds, formed by E10.5. Domain branching is characterized by a new bud arising from the lateral aspect of the bronchiole tubule, and is distinct from later branching modalities which entail bifurcation of distal tip of the

epithelial tube. Domain branches are regularly spaced along the parent branch and added in a proximal to distal manner as the parent branch extends and the lung matures (Fig 2.2). Later in development, domain branches arise dorsally, medially and ventrally to the initial sequence of domain branches, again in a proximal to distal direction. This results in a bottlebrush appearance of branches along the main bronchioles and serves to establish the main scaffolding of the respiratory tree. As these daughter domain branches extend away from the parent tubule, they undergo a series of bifurcations to establish the tertiary branches that fills in the established main arborized skeleton. With this map in hand, we can start to evaluate the changes in cell biology that give rise to morphological changes on the tissue level to form the elaborately branched lung.

Formation of the branches of the lung requires a bending, folding and molding of the lung epithelial tubules. It is unclear at this point the respective force contributions from the mesenchyme and the epithelium in to the process of new branch formation. Explant studies of isolated epithelium in matrigel supplied with Fgf suggest that there are sufficient forces within the lung epithelium to promote branch formation [22]. Despite these results, it is likely that, in vivo, the mesenchyme plays a role in branch formation. Using newly available molecular tools, we were able to characterize the epithelial cell behaviors that contribute to new domain branch formation and propose a model for domain branching in the developing lung.

Live Imaging of the Whole Lung Epithelium

To begin to address the changes that the epithelium undergoes during branching morphogenesis, we undertook live imaging of lung explants. We imaged up to the first 20 hours in culture, because the morphology of the developing lung is relatively well maintained during this period, as compared to fixed samples of the equivalent stage.

With increased time in culture, the lung explant flattens onto the transwell and the surrounding mesenchyme crawls away from the epithelium, potentially affecting the epithelial-mesenchymal interactions that normally occur during branching morphogenesis. Due to this restriction on the time course of live imaging experiments, we primarily focused on the early processes in branching morphogenesis, domain branch formation. We made use of the *R26R*^{mTmG} line, which ubiquitously expresses membrane-localized Tomato-Red under control of the *Rosa* locus, which is flanked by LoxP sites. Upon cre-recombinase expression, the Tomato-Red cassette is removed, and membrane localized GFP is expressed from the *Rosa* locus. The Shh^{cre} line expresses cre-recombinase downstream of the *Shh* promoter and is expressed throughout the foregut endoderm at the time lung specification (approximately E9.5 in the mouse). We generated *Shh*^{cre}*: R26R*^{mTmG} lungs to label the lung epithelium with GFP upon recombination at E9.5, prior to commencement of branching morphogenesis. Over the course of these experiments, we found that the lung was particularly sensitive to phototoxic effects of laser exposure, as such we had to use very low laser power. The level of resolution that we were able to obtain was relatively low, but did allow for live imaging of the processes that the epithelium undergoes during establishment of the respiratory tree. We started imaging at E11.5, when the two major airways of the lung have established the five lobes of the lung. Over the course of the next 13 hours, new branches grow and extend away from the main parent bronchi and the more proximal region of the bud narrows and constricts (Fig. 2.3). Over this period of development, formation of new domain branches in the right caudal lobe and left lobe are observed (Fig. 2.3, arrows). These new domain branches arise not at the tip of the epithelial tube, but rather in the middle of the tube, and as such represents domain branch formation. As these branches form, the epithelial tube kinks and bends at the point where the new

bud will arise (Fig2.3, arrows). We can also observe planar bifurcation of the main bronchiole of the right cranial lobe. As development proceeds, the flattened bud bifurcates and two new buds grow away from the former bud tip (arrowheads in Fig2.3). These live imaging studies provide an overview of the changes that the lung epithelium undergoes during the early pseudoglandular period.

New domain branch formation requires apical constriction and epithelial thickening

During our analysis of early branching, we observed that the epithelium undergoes a number of stereotyped changes prior to new branch formation. At the site of new bud formation, the epithelium thickens, and the epithelial tube deforms and bends (Fig 2.4). Following this, a distinct kink in the epithelium is observed, and a newly formed bud develops; then grows away from the main epithelial tube. As the new branch extends, the region proximal to the bud tip constricts to promote further extension of the branch into the surrounding mesenchyme. The lung epithelium maintains cell-cell adhesion as a continuous sheet throughout these morphological changes, so the tissue-level changes could requires change in cell shape, changes in proliferation and neighbor exchange to accomplish these morphological changes at the tissue level. Proliferation has long been proposed as a motive force behind new branch growth and formation in the lung [96]. In fact, it has been shown that there is increased proliferation in the distal tips of the developing lung epithelium [97]. Despite this proposed mechanism, there is no evidence for a change in proliferation at regions in the epithelium preceding where domain branches form [98, 99]. Rather, increased proliferation is observed after the branches have budded from the epithelium, suggesting a requirement for proliferation in bud outgrowth, but not new branch formation. As such, it is likely that changes in cell

morphology and behavior drive the bending of the epithelial tube to give rise to new domain branches.

The thickening of the epithelium at sites of new branch formation suggested that there were important changes in cell shape and size during this process. To better visualize the individual changes in cell shape that occur prior to and during domain branching, we generated *Shh^{creERT2}:R26R^{mTmG}* mice which allow us to label individual cells in the developing epithelium of the lung (Fig 2.5). The Shh^{creERT2} is an inducible cre recombinase driven by the Shh promoter. By injecting the pregnant dams with limiting amounts of Tamoxifen to induce nuclear localization of the cre-recombinase in cells expressing Shh^{creERT2}, we could induce excision of the Tomato-Red cassette and promote expression of GFP in individual cells within the lung epithelium at E11.5, if the Tamoxifen injections were completed at E10.5. Using this system, we observed a number of spatially distinct cell morphologies in the developing epithelium at E11.5: bottle-shaped cells located primarily at sites of new domain branch point formation, elongated columnar cells in the stalk region, and short columnar cells located at the bud tip (Fig. 2.5). In addition to these cell shapes, we also observed a distinct morphology of cells adjacent to cells undergoing cell division (Fig2.5D). These cells were found throughout the epithelium and they exhibited apical cellular extensions that were deformed due to the rounded mitotic cells. The appearance of these cells that appear to wrap the mitotic cells is notable as they represent a different model of mitotic and neighboring cell behavior than what has recently been reported in the kidney branching epithelium [100]. In the kidney, mitotic cells bud into the luminal space and the daughter cell reinserts into the epithelium a few cells distant from the original cell. In the lung, these cellular projections surrounding the mitotic cells maintain the dividing cells within the lung epithelium, preventing budding into the luminal space. It would be

of interest to examine if these neighboring cells had a role in where daughter cells reinsert into the epithelial sheet, and without live imaging of individual cells it is unknown if daughter cell dispersal occurs in the lung epithelium. Evaluation of $Shh^{creERT2}$:$R26R^{mTmG}$ animals with a limiting dilution of tamoxifen suggests that there is significant cell movement in the developing lung epithelium, as patches of clones are not observed. Investigation as to whether this cell movement is mediated through mitotic events or through neighbor exchange awaits advances in microscopy before this question can be adequately addressed. Cells throughout the lung epithelium migrate to the apical surface prior to mitosis. These mitotic cells have thin cellular projections that maintain contact with the basal surface of the epithelium (Fig2.5E). While elongated columnar cells and bottle cells are located both in the stalk and bending epithelium, quantification of the appearance of labeled cells in distinct regions of the epithelium demonstrates an increased frequency of bottle cells with basally localized nuclei at sites of new bud formation (Figure 2.5F).

The presence of bottle cells and apical-basal cell lengthening are common features of folding epithelial sheets as seen in gastrulation in *Xenopus* [101, 102], neural tube bending [103, 104] }, optic vesicle formation [105], and *Drosophilia* salivary gland development [106]. Consistent with these models, at the site of new bud formation the lung epithelium thickens and adopts a pseudostratified morphology, suggesting the epithelial thickening is due to epithelial cell lengthening and apical constriction.

Apical localization of components of the actin-myosin contractile network

To further investigate evidence for apical constriction occurring in regions undergoing apical-basal cell lengthening and bending, we imaged the luminal surface of the developing epithelial tube. In support of apical constriction in the region undergoing

new branch formation, we found decreased apical surface area of the cells in that region (compare boxes in Fig2.6). Phalloidin staining labeling the actin cytoskeleton shows high levels of the actin cytoskeleton at the apical surface. At the luminal surface, there is a meshwork of actin overlying the cells, which is densest at regions undergoing bending. Moving along the apical-basal axis to regions just basal to the apical surface, actin and E-cadherin are localized to regions of cell-cell contact. Additionally, we found that there was increased apical phospho-myosin light chain 2 (pMLC2) in the lung epithelium in regions undergoing bending as compared to the bud tip (Figure 2.6). Localization of the actin-myosin contractile network and pMLC2 to the apical surface supports the hypothesis that there is increased cortical tension and apical constriction at sites of new bud formation.

Based on examination of live branching epithelium and fixed samples, we propose a model for bending of the lung epithelium to produce new domain branches from the epithelial tube. During branch point formation, lung epithelial cells undergo constriction at their apical ends and lengthen along their apical-basal axes, which causes a thickening of the epithelium at the region where a new bud will form and these processes are required for bending of the epithelial tube (Fig. 2.7).

MATERIALS AND METHODS

Histological preparation

For whole lung branching analysis, embryonic stage was determined by counting somites from the cervical region to the tail. Lungs were dissected from the embryos, and fixed for 1hr in 4% paraformaldehyde in PBS at 4°C for lungs E10.5-13.5 and dehydrated in a descending methanol series. E14.5 lungs and older were fixed in methanol [4]. For

vibratome sections, embryos were staged by counting somites, fixed for 1hr as above, embedded in 4% agarose, and sectioned at 100μm thickness to allow for visualization of the apical surface of the epithelium. To label individual cells with GFP, *Shh*^{creERT2} dams were injected with tamoxifen at 0.1 mg/kg at E10.5 days and dissection was completed 24 hours later.

Immunohistochemistry

Immunofluorescent staining as performed as previously described for vibratome sections, and whole mount lungs [4]. After antibody staining, whole mount lungs were dehydrated in 100% methanol and then mounted in BABB (1 part benzyl alcohol: 2 part benzyl benzoate) and mounted on a slide with a Fastwell spacer and sealed with cover slip[107]. The following antibodies were used for immunohistochemistry and whole mount imaging of lung explants: Alexa-Fluor-655 conjugated phalloidin (Sigma, 1:100), E-cadherin (Sigma, 1:500), SM22a (Abcam 1:200), p-MLC2 (Cell Signaling, 1:100) and GFP (MBL, 1:100).

Live imaging of lung explants

E11.5 embryonic lungs were dissected from embryos of the indicated genotypes. Lungs were dissected away from the heart with the trachea left attached as previously described[108]. Lungs were cultured at the air liquid interface on top of standing inserts (Millicell) in DMEM:F12 media with 0.5% FBS, and 1% penicillin/streptomyocin at 5% CO_2, 37°C**.** A diagram of the explant system design is pictured at Fig2.10. Standing insert legs were cut to 50μm and placed in glass-bottomed Mattek dishes.

Time-Lapse Microscopy

Lungs were imaged using a Zeiss LSM 710 confocal microscope, using a 10x/0.45 Plan-Apochromatic objective lens. Confocal sections (10μm), stack of 5 sections, were obtained every 20 minutes for 16-17 hours. A stage-top environmental chamber was used to maintain humidity, temperature at 37°C, and CO_2 at 5%. Experiments on lung explants were repeated at least 5 times. Representative single experiments are shown. Images collected were analyzed using ImageJ and custom Matlab analysis.

Image Processing and Analysis

3D reconstitution images were assembled in ImageJ from z-stacks of sections. ImageJ was used to quantify mean intensity levels of pMLC2 at cell-cell junctions.

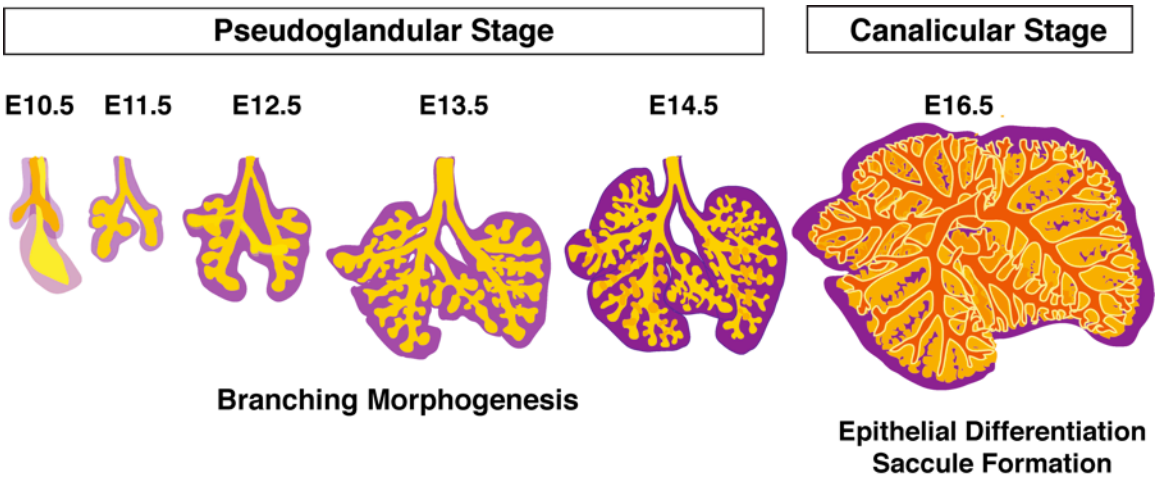

Figure 2.1 Branching Morphogenesis in Lung Development

Drawings of the changes the lung epithelium undergoes during the pseudoglandular period to give rise to the highly branched lung. At E10.5, the lung consists of two simple epithelial sacks. By E11.5, the initial lobation of the lung has occurred, giving rise to the 5 lobes of the mouse lung: the right medial, cranial, caudal and accessory lobes and the left lobe. From E12.5 to E14.5, the lung undergoes secondary and tertiary branching which ceases by E16.5.

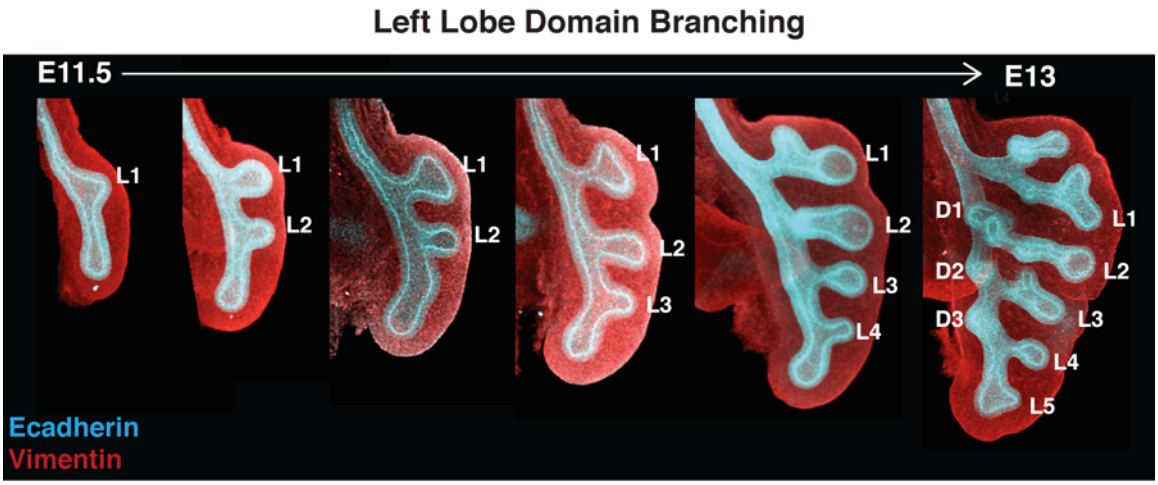

Figure 2.2 Left Lobe Domain Branching

Whole mount control lungs were stained with antibodies for Ecadherin and Vimentin to visualize the lung epithelium during branching morphogenesis. Domain branching is characterized by the formation of a new branch laterally from the side of the extending epithelial tube rather than the tip of the bronchiole. As development progresses, new domain branches are added along the parent epithelial tube in a proximal to distal direction. The regularly spaced domain branching pattern over time has lead to the proposal for a periodicity generator to establish the branching pattern.

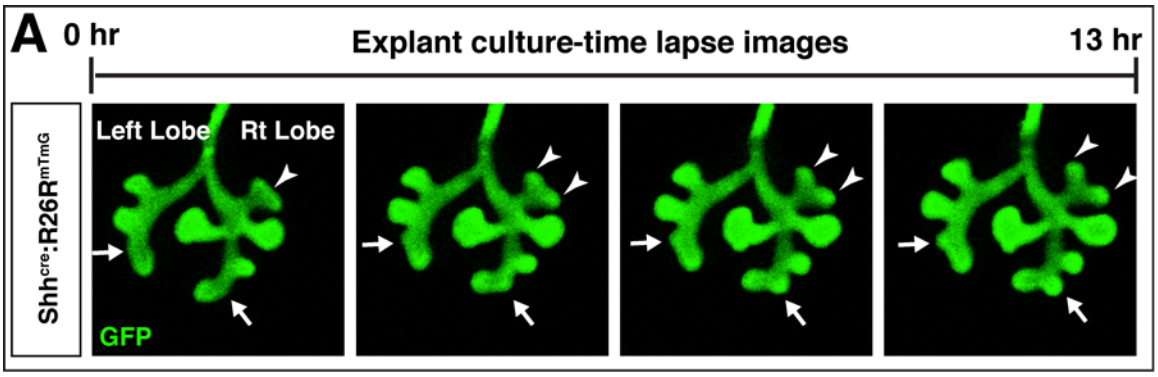

Figure 2.3 Live Imaging of Branching Morphogenesis in the Lung Epithelium

Real time imaging of control Shh^{cre}:$Rosa^{mTmG}$ lungs ex vivo shows changes in the lung epithelium as new domain branches form. Arrows indicate the regions where new domain branches arise in the left lobe and right caudal lobe. The lung epithelium extends and at the site of new bud formation bends before a new bud emerges. Arrowheads on the right cranial lobe highlight a region undergoing planar bifurcation, where new branches arise from the bud tip.

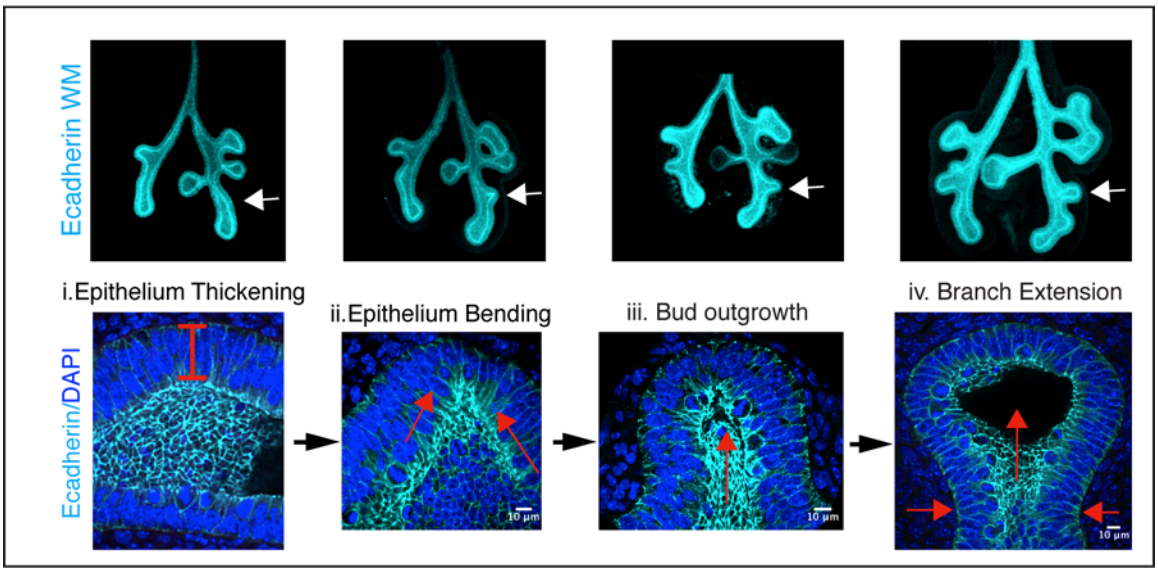

Figure 2.4 Changes in Lung Epithelium During New Branch Formation

At sites of new domain branch point formation, the epithelium first thickens (i), then buckles at a distinct point (ii), then buds and extends away from the founder epithelial tube (iii), and the epithelial tube constricts at the base of this new branch as extension proceeds (iv).

Figure 2.5 Analysis of epithelial cell types in the bending, stalk, and developing bud regions of the epithelium.

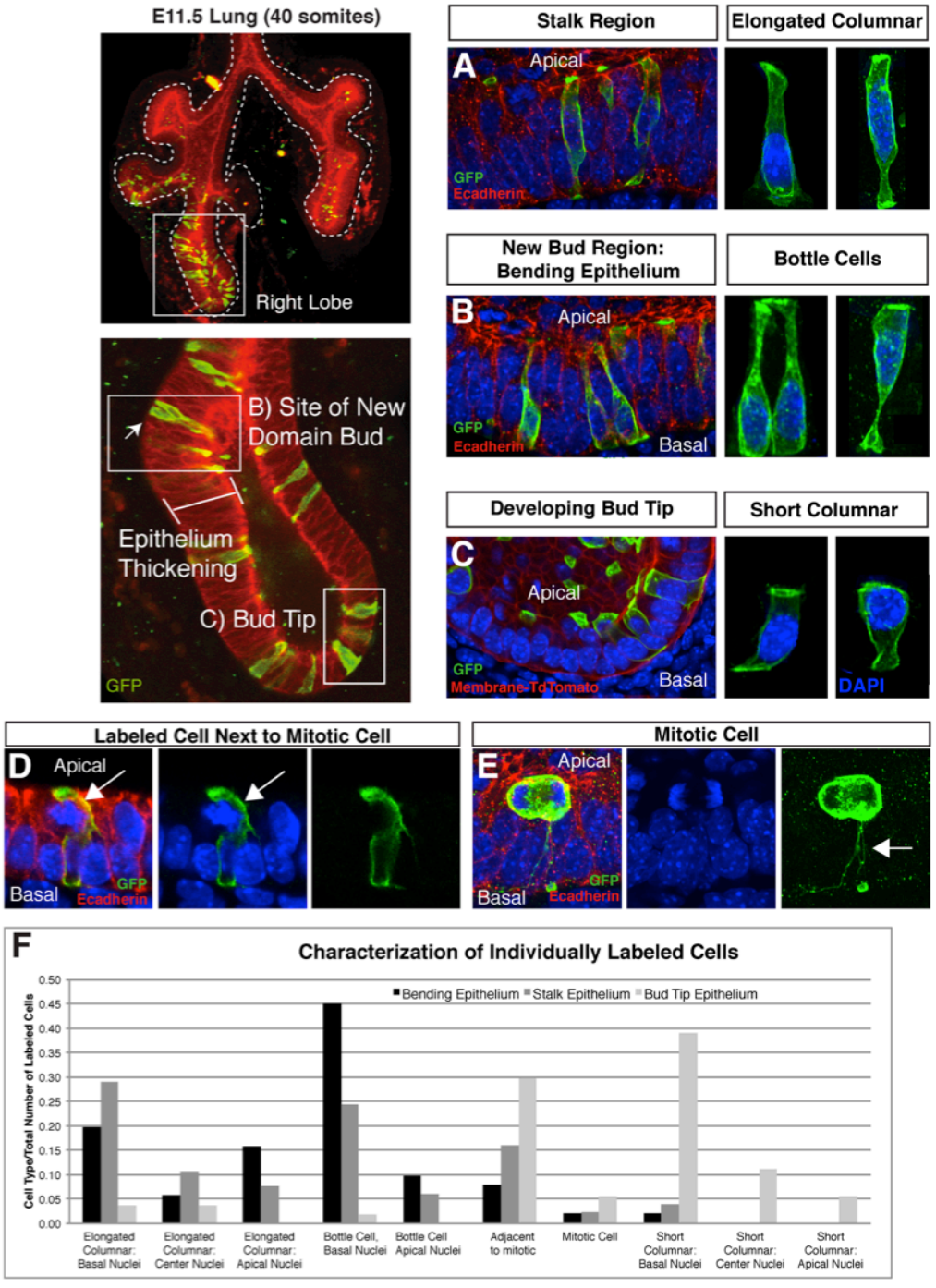

Figure 2.5 Analysis of epithelial cell types in the bending, stalk and developing bud regions of the epithelium. Using the *Shh*^{creERT2}; *R26R*^{mTmG} to randomly label individual epithelial cells in the developing lung epithelium, we characterized a number of cell types found in different regions of the epithelium. The developing bud tip predominantly had a short columnar morphology, with the nuclei migrating up to the apical surface for cell division (C). In the developing stalk and at regions of new bud formation, we observed predominantly elongated columnar cells (A) and bottle cells, with significant elongation either apically or basally, depending on the nuclear location (B). We quantified the frequency of each individual cell type in each of the three regions and found an increase in bottle cells with basally localized nuclei in regions of the epithelium undergoing bending (F). Throughout the epithelium, we noted the morphology of labeled cells immediately adjacent to cells undergoing mitosis (D). These labeled cells maintained contact with both the apical and basal surfaces and their apical necks were deformed due to the adjacent mitotic cell. This morphology is of interest as it suggests in the lung the mitotic cells remain within the epithelial sheet and do not bud into the lumen, in contrast to what is observed in the developing kidney (Packard et al., 2013). Mitotic cells localize to the luminal (apical) surface during cell division, but maintain thin processes that contact the basal surface (arrows in E). Images of individual cells are 3-D projections of GFP-labeled cells, cropped to the cell(s) of interest.

Figure 2.6 Actin-Myosin Localization at the Luminal/Apical Surface of the Lung Epithelium

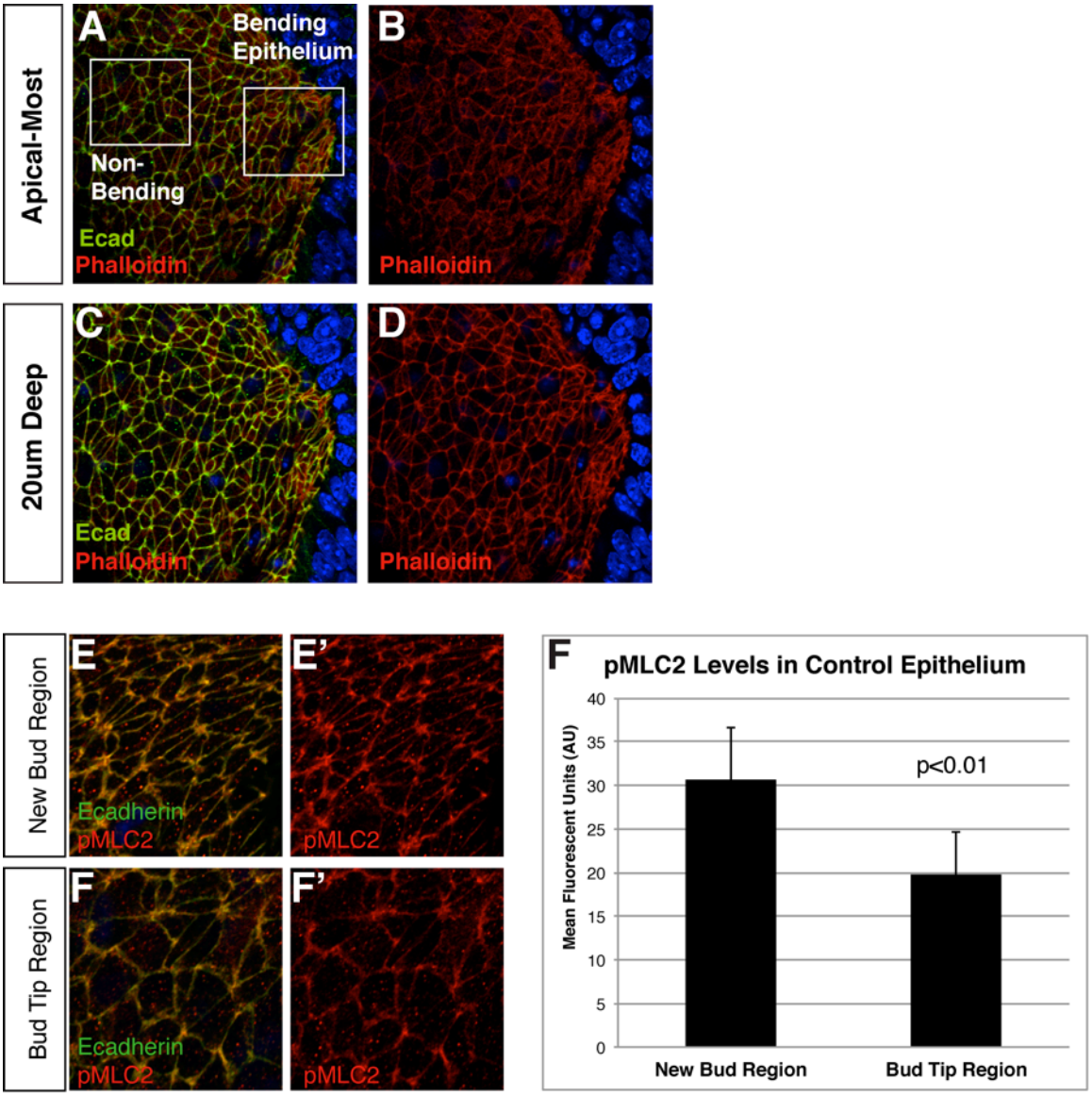

Figure 2.6 Actin-Myosin Localization at the Luminal/Apical Surface of the Lung Epithelium

Enface images of the luminal surface of regions of new bud formation were analyzed for phalloidin and E-cadherin expression and localization (A-D). Comparing cell outlines in regions where the epithelium is undergoing active bending versus non-bending epithelium show that there is decreased surface area of the epithelial cells in regions where new buds are forming. Phalloidin staining for actin demonstrate a fine network that spans multiple cells at the most apical surface of the epithelium (A-B). This actin localization is increased in regions undergoing bending. Moving basally into the cell body, actin and E-cadherin are localized to the cell-cell junctions.

Enface images of the epithelial surface of regions of new bud formation or at the bud tip were analyzed for pMLC2 expression (E-F). Edges of cell-cell contacts were measured and mean fluorescent intensity was determined using ImageJ. There was significantly increased pMLC2 localization at cell-cell edges in regions undergoing bending of the epithelium, $p<0.01$ using a two-tailed students t-test (G). More than 3 embryos and over 50 edges per region were analyzed.

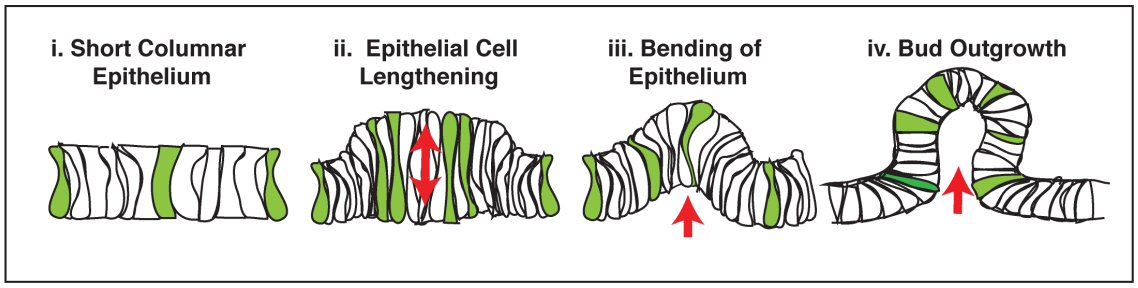

Figure 2.7 Model for Epithelial Tissue Morphogenesis During New Branch Formation in the Lung

Diagram of how the epithelial sheet that composes the developing lung airways deforms at sites of new branch point formation: epithelial cells lengthen along the apical-basal axis leading to a bend in the epithelial sheet (E). This results in the formation of new bud or branch point in the epithelial tube. As the new bud extends, the cells in the bud tip once again adopt a short columnar morphology.

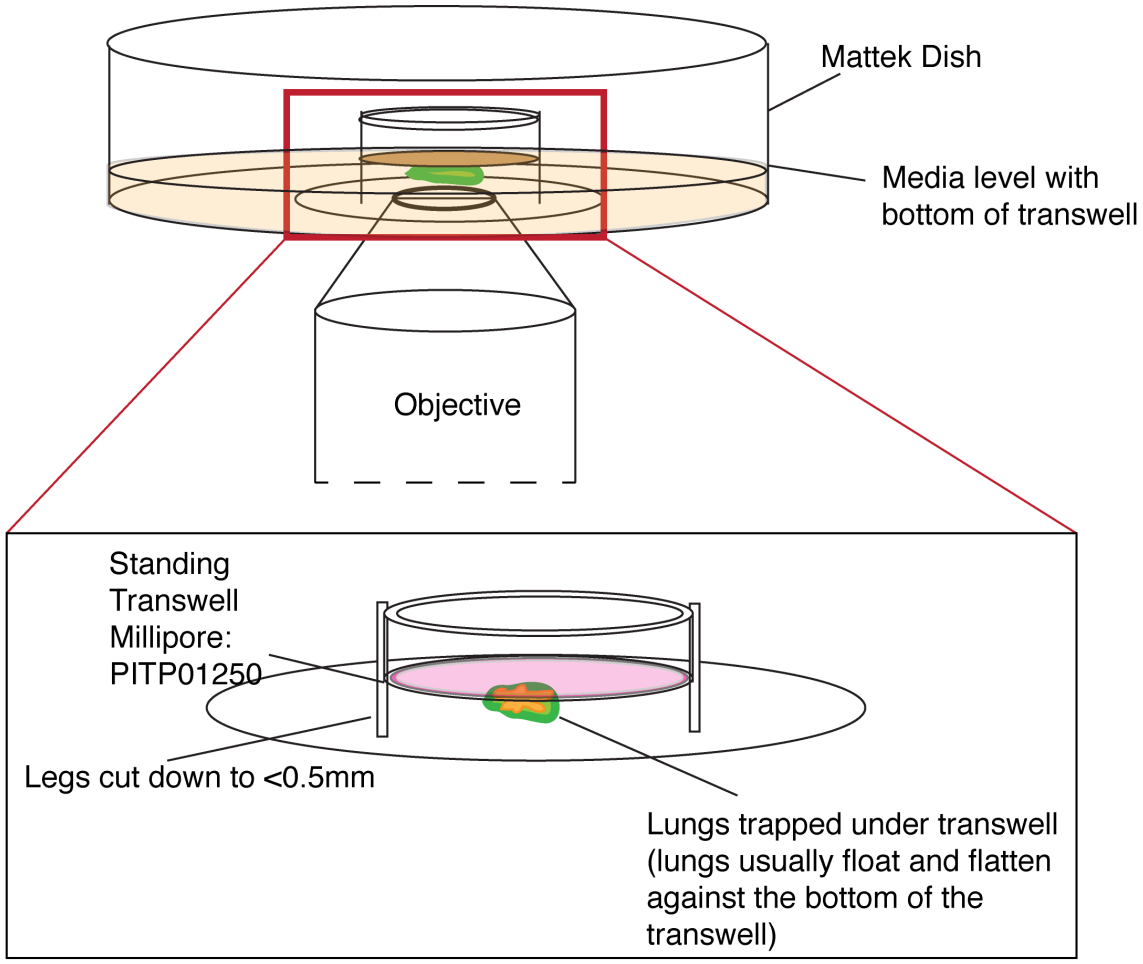

Figure 2.8 Diagram of Lung Explant Culture System

E11 lungs are placed in media in a glass bottomed Mattek dish . Use of an objective with a large working distance is recommended to allow for imaging of the lung. The floating lungs are covered with a standing transwell to stabilize the lungs and also to allow lungs to be adjacent to the air-liquid interface. Lungs usually flatten onto the transwell over the course of imaging. To prevent artifacts due to phototoxicity, the lowest laser power possible to visualize the tissue of interest, decreased size of z-stack, fastest acquisition settings, and the longest time period between imaging events is recommended.

Chapter 3: The role of Fzd2 in lung epithelial development

Portions of this chapter were published in the *Proceedings of the National Academy of Sciences* [95].

Summary

Changing the morphology of a simple epithelial tube to form a highly ramified branching network requires changes in cell behavior that lead to tissue-wide changes in organ shape. How epithelial cells in branched organs modulate their shape and behavior to promote bending and sculpting of the epithelial sheet is not well understood and the mechanisms underlying this process remain obscure. We show that the Wnt receptor Fzd2 is required for domain branch formation during the initial establishment of the respiratory tree. Live imaging and transcriptome analysis of lung branching morphogenesis demonstrate that Fzd2 promotes changes in epithelial cell length and shape. These changes in cell morphology deform the developing epithelial tube to generate and maintain new domain branches. Fzd2 controls branch formation and epithelial tube shape by regulating Rho signaling and localization of phospho-myosin light chain 2, in turn controlling epithelial cell shape changes during morphogenesis. These studies demonstrate the importance of Wnt/Fzd2 signaling in promoting and maintaining changes in epithelial cell shape that affect development of a branching network.

Introduction

Development of many epithelial-derived organs requires a process of bending, folding, and reorganization of a primitive epithelial sheet or tube to generate a functional three-dimensional organ. The mammalian lung is derived from a simple endoderm tube through a complex series of morphological changes that generates the highly arborized

airways required for postnatal respiration. In humans, the first 16 generations of branching are thought to be genetically hard-wired which is supported by work on mouse lungs showing that the branching pattern across multiple mouse strains is highly reproducible [4, 109]. Despite such insight, little is understood about the genetic control of the molecular and cellular mechanisms underlying branching morphogenesis in the lung.

The epithelial cells that line tubular branching networks can be thought of as a large planar epithelial surface that must undergo changes in cell morphology in specific subregions for proper branch formation to occur. Several pathways have been implicated in regulating epithelial cell behavior in a plane including the Wnt signaling pathway. While the canonical Wnt signaling pathway regulates gene expression through nuclear translocation of β-catenin and its subsequent co-activation of LEF/TCF transcription factors, non-canonical Wnt signaling involves a less well-defined signaling network that leads to alterations in epithelial cell shape and cytoskeletal structure. Non-canonical Wnt signaling is known to regulate epithelial cell shape changes in other systems such as convergent-extension movements during *Xenopus* development [110, 111] and bending of the neural plate [112]. Whether such pathways regulate branching networks that underlie the formation of multiple organs including the lung is unknown.

In the current study, we show that the Wnt receptor Fzd2 plays a key role in regulating epithelial cell behavior and tube morphology necessary for formation of new branch points during airway morphogenesis. Fzd2 is essential for regulating changes in epithelial cell shape and cell lengthening along the apical-basal axis which we show is critical for formation of new domain branch points and maintaining proper airway tube shape in the developing lung. Loss of Fzd2 leads to decreased apical expression of

phospho-myosin light chain 2 (pMLC2) indicative of decreased Rho signaling, which is required for thickening of the lung epithelium prior to new branch formation. Importantly, activation of Rho signaling can rescue the loss of Fzd2 signaling during lung branching morphogenesis. Together, our data highlight a previously unappreciated mechanism in the formation of branched networks by Wnt signaling through control of epithelial cell shape.

Loss of Fzd2 in the lung epithelium causes the formation of distal cysts in the lung

Fzd2 is expressed at high levels in the developing lung epithelium and has been implicated in regulating epithelial differentiation down-stream of Gata6 [89]. To further assess the role of Fzd2 in the developing lung, we generated a *Fzd2*$^{flox/flox}$ allele and crossed these mice into the *Shh*^{cre} allele (Fig. 3.1) [113]. The *Shh*^{cre} allele is a knock-in of the cre-recombinase into the Shh locus, and as such, expresses cre-recombinase as early as E9.5, at the time of lung specification in the mouse. Fzd2 expression in *Shh*^{cre}*:Fzd2*$^{flox/flox}$ mutants is efficiently reduced in the lung epithelium by E12.5 as observed by in situ hybridization and quantitative real-time PCR (Q-PCR) (Fig. 3.2). We have tested 5 antibodies for Fzd2 in the lung and in cell culture, and have not identified any that specifically reflect Fzd2 protein expression or localization. This is likely due to the high sequence similarity between Fzd2, Fzd7 and Fzd1. Because of this sequence similarity, there is only one unique 25 amino acid sequence that is found in Fzd2, but not in Fzd7 or Fzd1. We have tested antibodies raised against this sequence on paraffin sections and vibratome sections in mutant and control lungs as well as in cell culture with shRNA knockdown of Fzd2 and have not obtained positive results. In paraffin sections and in cell culture there does appear to be some staining, but this labeling is observed in the Fzd2 null epithelium and in the Fzd2 shRNA knockdown cells, indicating

this staining is either background or that this antibody may have cross-reactivity with Fzd1 or Fzd7. As such, protein levels and subcellular localization of Fzd2 in the lung epithelium cannot be assessed with the molecular tools currently available.

We observe specification and formation of the lung with loss of Fzd2, suggesting that Fzd2 is not the Wnt receptor in the epithelium required for lung specification by Wnt2/2b. While initial lung formation occurs in *Shh*^{cre}*:Fzd2*$^{flox/flox}$ mutants, by E14.5 mutant lungs contain multiple large cysts in the distal regions of the lung (Fig. 3.3). By E18.5, *Shh*^{cre}*:Fzd2*$^{flox/flox}$ mutant lungs are smaller than controls and large cysts continue to be visible in the distal parts of the lung (Fig. 3.3). In contrast to other examples of cystic lungs in the developing embryo [14, 114], *Shh*^{cre}*:Fzd2*$^{flox/flox}$ mutants are viable, but contain large cysts in the distal regions of their lungs (Fig. 3.3). Interestingly, these cysts are consistently localized to the most distal regions of the lung, and are primarily found in both of the left and the right caudal lobes.

Fzd2 and Fzd1 show partial redundancy in maintenance of the cystic phenotype in the late pseudoglandular period

The cystic phenotype is not fully penetrant and partially resolves as development proceeds, with distinct cysts observed in 63% of lungs at E12.5 and distinct cysts in only 40% of lungs at E15.5 in *Shh*^{cre}*:Fzd2*$^{flox/flox}$ mutants. This decrease in presentation of the phenotype as development proceeds suggests that there is some resolution of the cystic phenotype during the pseudoglandular period. This resolution of the cystic phenotype may be due to redundancy with other Fzd receptors. A number of other Fzd receptors are expressed in the lung, including the closely related Fzd1 and Fzd7 (Fig 3.4, A). Time course analysis of Fzd receptors expressed in the lung during development (Fig 3.4, A) show that Fzd2 expression increases from E9.5 to E14.5, but plateaus at E14.5 to E18.5.

In contrast, Fzd1 expression continues to increase from E14.5 to E18.5. Additionally, loss of one copy of Fzd1 in addition to complete loss of Fzd2 increases the penetrance of the cystic phenotype, although it does not increase the severity of the phenotype (Fig 3.4). Due to the breeding restrictions with the *Shh*^{cre} allele (it demonstrates mosaic expression when passed through the female germ line) and the close proximity of the Shh and Fzd1 alleles on the 11th chromosome, we were unable to obtain sufficient numbers of Fzd2$^{F/F}$; Fzd1$^{-/-}$; Shh$^{cre/+}$ animals to perform analysis on, but additional breeding to obtain these animals would be useful. These results suggest some redundancy between Fzd2 and Fzd1 in later presentations of the phenotype, but do not account for the incomplete penetrance at early stages. Fzd7 also has high sequence similarity with Fzd2 and has been shown to have some functional redundancy [94] using a different Fzd2 knock-out allele. Future investigation into the requirement for both Fzd2 and Fzd1 in later stages of this phenotype as well as analysis of the Fzd2/Fzd7 double knockout would be useful for characterizing the role of these Fzd receptors in epithelial lung development.

Fzd2 is required for formation of lateral domain branches during lung branching morphogenesis

Development of cystic regions in the embryonic lung could represent a failure of the airway branching program during establishment of the arborized respiratory tree. To determine if there were defects in branching morphogenesis in *Shh*^{cre}*:Fzd2*$^{flox/flox}$ mutant lungs, we examined embryonic lungs from E10.5 to E16.5 using whole mount immunostaining for E-cadherin and vimentin to mark the developing epithelium and mesenchyme, respectively. At E10.5 (36-40 somites) when the initial right and left lobes bud from the trachea, there is no discernable difference between *Shh*^{cre}*:Fzd2*$^{flox/flox}$ mutant and control lungs (Fig. 3.5, A, F). By E11.5 (48 somites), when the initial lobation of the right and left lobes has commenced, the *Shh*^{cre}*:Fzd2*$^{flox/flox}$ mutant lungs

are shorter and wider than the control lungs and do not exhibit constriction of the epithelial tube distal to the formation of new branch points (Fig. 3.5, B, G). In normal lung development, new lateral branches are added along a founder branch in a stereotyped pattern to establish the main bronchial airways in a process described as domain branching. By E12.5 (54-60 somites), *Shh*^{cre}*:Fzd2*$^{flox/flox}$ mutant lungs have failed to undergo proper lateral domain branch formation, and large cysts have formed instead of new distal branches (Fig. 3.5 D-E, I-J). Closer examination of *Shh*^{cre}*:Fzd2*$^{flox/flox}$ mutant lungs shows that loss of Fzd2 expression leads to failure to add domain branches as development proceeds, and the branches that do form are wider and exhibit cystic morphology as compared to controls (Fig. 3.5 K). This loss of domain branches can be quantified and reveal an approximate 50% decrease in new domain branch formation in *Shh*^{cre}*:Fzd2*$^{flox/flox}$ mutants (Fig. 3.5). These data suggest that the formation of the distal cysts in the Fzd2 mutants are due to defects in domain branch formation in early lung development. Specifically, because new domain branches fail to bud from the epithelial tube, but the epithelium continues to grow, cystic regions form instead of new domain branches. These results raise the interesting possibility that distal cysts in the Fzd2 mutant reflect a morphological defect in the initial branching program.

Tertiary internal domain branching occurs in Fzd2 conditional knockout lungs

Although Fzd2 is required for domain branch formation early in development, later branching modalities appear to occur in Fzd2 lungs. These findings may provide an explanation as to why the cystic regions appear to regress later in development and the *Shh*^{cre}*:Fzd2*$^{flox/flox}$ mutants are able to survive with functional lungs. As development advances, the mode of branching morphogenesis changes from domain branching from the main bronchioles to planar bifurcation and orthogonal branching that occur at the

developing bud tip, and additional domain branching along the established airways. In addition to the change in the mode of branching morphogenesis, the cell types in both the epithelium and mesenchyme change as development proceeds.

Early in development, when we observe defects in domain branch formation with loss of Fzd2, there are few smooth muscle cells surrounding the lung epithelium. As development proceeds, smooth muscle cells wrap the developing epithelial branches and change the physical environment in which branching morphogenesis occurs. Smooth muscle development in the *Shh^{cre}:Fzd2$^{flox/flox}$* mutant does not appear to be affected (Fig 4.3). Of interest is that although *Shh^{cre}:Fzd2$^{flox/flox}$* epithelium is defective in domain branch formation early in development, internal domain branches later in development do form in *Shh^{cre}:Fzd2$^{flox/flox}$* lungs (Fig 3.6). Fewer of these internal domain branches are formed, likely due to physical restrictions of shorter main branches in the *Shh^{cre}:Fzd2$^{flox/flox}$* mutant as compared to control (Fig 3.6). One possibility is that the formation of internal domain branches later in development is subject to different molecular signals or different physical forces that are not defective in Fzd2 null lungs. Although internal domain branches form, the bud tips, which are not surrounded by smooth muscle, fail to undergo planar bifurcation in *Shh^{cre}:Fzd2$^{flox/flox}$* epithelium (Fig 3.6 A, D) at the same time points. Despite the defect in planar bifurcation, defective infolding of the dilated cysts does occur late in development (Fig 3.6 G), but this may represent the process of sacculation rather than branching morphogenesis, as it is observed at E16.5. The recovery of some modes of branching morphogenesis in the Fzd2 null epithelium suggests that there may be a variety of mechanisms to promote bending and budding of the epithelium.

Proximal-distal patterning and cell differentiation are not significantly altered upon loss of Fzd2 in lung epithelium

Defects in branching morphogenesis are frequently associated with defects in proximal-distal patterning of the lung epithelium, making it difficult to determine if the primary effect is morphological, or due to defects in cell specification [14, 15, 115]. To determine if proximal-distal patterning of the lung epithelium was disrupted by loss of Fzd2, we examined expression of markers of proximal (Sox2) and distal (Sox9) lung epithelial progenitors [115-117]. Sox2 expressing epithelial cells are restricted to the proximal region of control lungs at E12.5 and E14.5 (Fig 3.7). Conversely, Sox9 expressing epithelial cells are found in the most distal regions of the branching lung epithelium of control lungs at E12.5 and E14.5 (Fig 3.7). This pattern of appropriate proximal-distal patterning is maintained at all stages of development observed, including the E18.5 lung just prior to birth (Fig 3.7). These data show that in contrast to loss of Wnt/β-catenin signaling[14, 67, 68] during lung development, Fzd2 does not regulate cell fate determination in the lung but rather plays a distinct role in epithelial morphogenesis.

The adult cystic phenotype is similar to a human disease, CCAM

In contrast to embryonic development, cysts in adult *Shh*^{cre}*:Fzd2*$^{flox/flox}$ mutant lungs are lined predominantly with proximal cell types, Scgb1a1 expressing secretory cells, and lack Sftpc expressing alveolar epithelial type 2 distal cells (Fig 3.8 C', D'). These data suggest that while initial proximal-distal patterning of *Shh*^{cre}*:Fzd2*$^{flox/flox}$ mutant lung epithelium is established during development, it is not maintained in the postnatal cysts. This may be due to a requirement for Fzd2 in lung repair in the adult animal. The lung epithelium in the cysts may be subject to increased epithelial injury during

respiration after birth. The cystic regions in the adult animal exhibit a number of defects in morphology, which are likely, in part, due to epithelial injury. Surrounding the large cystic regions in the *Shh^{cre}:Fzd2$^{flox/flox}$* adult animal, there is thickened smooth muscle (Fig 3.8 C, D), and the morphology of the epithelium is folded and convoluted (Fig 3.8 C', D'), similar to the morphology of the upper bronchioles. These morphological changes in the large cystic regions are of interest as they display phenotypic similarities to a human disease, congenital cystic adenomatoid malformations. Cystic regions characterize CCAM, either micro, as in Type II, or large cystic regions, as in Type I in fetal and neonatal lungs. Both Fzd2 CKO cysts and Type I CCAM are lined with cuboidal epithelial cells surrounded by thickened mesenchyme (Fig 3.8, B, F). The cuboidal epithelial cells that line the cystic regions in both CCAM and Fzd CKO lungs express markers for proximal cell types (Fig 3.8 G-G"). In addition to the phenotypic similarities between CCAM cysts and *Shh^{cre}:Fzd2$^{flox/flox}$* mutant cysts, the temporal presentation between *Shh^{cre}:Fzd2$^{flox/flox}$* mutants and CCAM is similar, with large cysts arising during the pseudoglandular period, and these cysts frequently resolving by birth. CCAM type I defects can cause to fetal hydrops and lead to increased susceptibility to postnatal lung infection. CCAM type I is frequently treated by pre- or neo-natal excision of the cystic region or treatment with steroids. We currently do not have a mouse model for CCAM; as such, the *Shh^{cre}:Fzd2$^{flox/flox}$* mutant may prove to be an appropriate model for this disease to allow for investigation into treatments to promote resolution of the cystic region.

Loss of Fzd2 does not significantly change Wnt/β-catenin signaling in lung epithelium

Fzd2 has been shown to activate both β-catenin dependent as well as β-catenin independent Wnt signaling [91-94]. Therefore, we evaluated the effect of loss of Fzd2 expression on canonical Wnt signaling using the Wnt-reporter line *TOPGAL* [118]. *Shh^{cre}:Fzd2$^{flox/flox}$:TOPGAL* mutant lungs did not exhibit a significant change in LacZ histochemical staining compared to control lungs (Figure 3.9). Use of the *BATGAL* reporter [119] also did not reveal any significant change in canonical Wnt signaling with loss of Fzd2 in lung epithelium (Figure 3.9). Although we have an *Axin-2* knock-in reporter mouse for assessing Wnt signaling, we were unable to use the *Axin-2* reporter because the *Axin-2* locus is approximately 5 cM from the *Fzd2* locus. Because reporter constructs may only report some of the Wnt/β-catenin dependent signaling occurring in the cell, we also performed Q-PCR for known Wnt targets in the developing lung. QPCR and a microarray did not reveal a significant change in canonical Wnt signaling activity (Figure 3.9). These findings are consistent with a previously reported global Fzd2 null allele that demonstrated loss of Fzd2 does not significantly affect Wnt/β-catenin signaling [93].

Because the Fzd2 phenotype is only partially penetrant and there is likely redundancy between Fzd2 and other Fzd receptors in the receiving cell, we assessed if loss of one copy of *β–catenin* in addition to complete loss of Fzd2 could worsen the branching defect. This analysis would highlight if part of the Fzd2 phenotype is due to canonical Wnt signaling. To assess this, we analyzed *Fzd2$^{F/F}$; β-catenin$^{F/+}$; Shh$^{cre/+}$* lungs at E12.5 and E13.5 (Figure 3.10). We found that loss of β–catenin in addition to complete loss of Fzd2 did not have any notable affect on branching morphogenesis or the

appearance of cysts in the lung. Furthermore, loss of β–catenin in addition to loss of Fzd2 did not change the penetrance of the cystic phenotype. These results strongly suggest that defects in β-catenin independent Wnt signaling pathways are responsible for the phenotype observed with loss of Fzd2.

Fzd2 does not interact with Wnt5a

There are a number of Wnt ligands expressed in the developing lung, including Wnt7, Wnt2/2a, Wnt5a, and Wnt11. Of these, knockout phenotypes for Wnt7b, Wnt2/2a and Wnt5a have been described, but no defects in branching morphogenesis or cyst formation have been reported. Early in development, Wnt5a is expressed around the trachea. As development proceeds, Wnt5a is expression is concentrated in the distal mesenchyme surrounding the branching epithelium [76]. Wnt5a null animals have defects in lung development that have been described as an overbranching defect late in development [76]. In contrast, Wnt5a overexpression causes the formation of cystic regions in the lung, which is phenotypically similar to loss of Fzd2 [77]. While we do not see an increase in Wnt5a expression with loss of Fzd2, signaling through Fzd2 may act to repress downstream signaling effects of the Wnt5a pathway.

To evaluate if decrease of Wnt5a may rescue the Fzd2 phenotype, we evaluated loss of Wnt5a in addition to complete loss of Fzd2. Loss of one copy of *Wnt5a* did not have any effect on the Fzd2 phenotype (Fig 3.11). Furthermore, in evaluating the Wnt5a phenotype, we noted that loss of Wnt5a has an effect on early branching morphogenesis not previously described. Analysis of the *Wnt5a*$^{-/-}$ mutant lung reveals disruption in the direction of growth of the proximal domain branches. In control lungs, new domain branches grow away from the main bronchiole tube at an angle of 90 degrees or less. In Wnt5a null lungs, the branches extend at angles in excess of 100 degrees. This

displacement appears to predominantly affect the most proximal branches (Fig 3.11). During the establishment of the lateral domain branch pattern, the periodicity of branching does not appear to be disrupted with loss of Wnt5a, as the same number of domain branches are formed. But, the domain branches are notably shorter as compared to control. Loss of both Fzd2 and Wnt5a appear to have an overlay of the two distinct branching phenotypes, with the lungs demonstrating both the displaced orientation of the domain branches (due to loss of Wnt5a) with fewer branches and cystic regions in the distal epithelium (due to loss of Fzd2). These results suggest that Fzd2 and Wnt5a do not have a genetic interaction in lung branching morphogenesis.

Loss of Fzd2 disrupts the paracrine signaling program for branching morphogenesis of the lung

To further assess the molecular changes that underlie the branching defects with loss of Fzd2, we determined the changes in the transcriptome of $Shh^{cre}:Fzd2^{flox/flox}$ mutant lungs at E12.5. These data revealed changes in signaling factors known to regulate lung branching morphogenesis including Fgf10 (Fig. 3.12). Previous work has described a model for paracrine signaling interactions required to promote lung branching, which includes an important role for Fgf10 signaling as well as Bmp4 and Shh (Fig. 3.12) [37, 120]. This proposed model describes a role for Fgf10 in establishing the site of new bud formation [121], although there remain a number of questions as to how Fgf10 mediates changes in the lung epithelium to give rise to new buds [48]. Q-PCR analysis shows that Bmp4 is up regulated and Fgfr2 and Shh are down regulated in $Shh^{cre}:Fzd2^{flox/flox}$ mutant lungs at E12.5 (Fig. 3.12). In situ hybridization analysis shows that Fgf10 expression is elevated and its domain is expanded in $Shh^{cre}:Fzd2^{flox/flox}$ mutant lungs at E12.5 (Fig. 3.12). While the Q-PCR analysis demonstrates changes in Bmp4, Fgfr2b and Shh expression levels with loss of Fzd2, the RNA localization pattern for

these genes is not changed as assessed by in situ hybridization (Fig. 3.12). Increased Fgf10 signaling can have a number of downstream effects, including increased proliferation, changes in the orientation of cell division, increased Sprouty2 expression, and changes in cell migration [38, 97, 122]. To evaluate if the increased Fgf10 expression affected any of these described Fgf downstream pathways, we assessed these processes in *Shh^{cre}:Fzd2$^{flox/flox}$* mutant lungs (Figure 3.13). Proliferation and orientation of cell division were not affected with loss of Fzd2. Additionally, we did not see a significant change in Sprouty2 expression as assessed by QPCR. The expanded Fgf10 expression could be due to decreased Shh expression, which is thought to down regulate Fgf10 expression. Additionally, increased Fgf10 expression could be a feedback response to the decreased Fgfr2 expression, which may decrease activation of the Fgf pathway in the epithelium. Either, or both, of these changes could result in the observed disruption of the Fgf10 branching circuit. As Fgf10 is expressed exclusively in the lung mesenchyme, the increased Fgf10 expression is due to a non-cell autonomous response to changes in the Fzd2 deficient lung epithelium. These data show that loss of Fzd2 specifically in the lung epithelium leads to alterations in the branching molecular circuitry. Regardless of the cause of the defect in change in Fgf10 localization, we wanted to identify the cell biological defect that resulted in failure to form new domain branches and formation of cystic regions in the lung.

The increase in Bmp4 expression and decrease in Fgfr2 expression in *Shh^{cre}:Fzd2$^{flox/flox}$* mutants could lead to an insensitivity to Fgf signaling even in the presence of increased Fgf10 ligand. This would explain the lack of change in described downstream Fgf signaling with increased Fgf10 expression. To assess if loss of Fzd2 had an affect on the chemoattractive effects of Fgf10, we exposed control and *Shh^{cre}:Fzd2$^{flox/flox}$* mutant lung tips to Fgf10 soaked beads and measured their ability to

extend epithelial branches towards these beads. The epithelium from *Shh^{cre}:Fzd2$^{flox/flox}$* mutant lungs buds and extends towards the Fgf10 soaked beads, but are dilated and have a less distinct tubular morphology compared to the control lung buds (Fig 3.14). These results demonstrate that the Fzd2 null lung epithelium is able to respond to the chemoattractant effects of Fgf10 signaling. Although the Fzd2 null epithelium grows towards the source of Fgf10, it exhibits a defect in the ability to organize and maintain a distinct tube to promote proper extension towards a focal region of Fgf10 expression. These data suggest that the increase in Fgf10 expression is secondary to defects in Fzd2 deficient lung epithelium. This failure of the Fzd2 null lung epithelium to properly organize and extend as a distinct tube can also be seen in vivo at early stages of lung development (Fig 3.5). Thus, lung epithelium in *Shh^{cre}:Fzd2$^{flox/flox}$* mutants exhibits an epithelial cell intrinsic defect in the ability to properly form, extend, and maintain a new distinct branch point independent of increased Fgf10 expression or changes in cell proliferation.

Fzd2 is required for maintaining tube dimension and new branch formation through regulation of epithelial cell shape

As described above, we performed live imaging studies to better understand the changes that occur in the lung epithelium as it undergoes branching morphogenesis. Using *Shh^{cre}:Fzd2$^{flox/flox}$:R26R^{mTmG}* mutants to label the lung epithelium with GFP upon recombination driven from the *Shh^{cre}* allele, we imaged newly forming domain branches using a lung explant model system. Starting at the time of explant (E11), the two major airways, or bronchi, of the lung have formed initial buds corresponding to the five lobes of the lung, which looks grossly similar between mutant and control lungs. In contrast to the control lung, *Shh^{cre}:Fzd2$^{flox/flox}$:R26R^{mTmG}* mutants exhibit reduced bud outgrowth, decreased constriction along the epithelial tube and the main lobes of the lung increase

in diameter, but not in length (Fig. 3.15 A and B). This behavior is similar to what is observed in the isolated bud tips from *Shh^{cre}:Fzd2$^{flox/flox}$* mutants growing towards the Fgf10 beads (Fig 3.14). This growth pattern leads to a failure to form new domain branches in *Shh^{cre}:Fzd2$^{flox/flox}$:R26R^{mTmG}* mutant lungs (Fig. 3.15 A, brackets).

We measured branch growth and extension using ImageJ to skeletonize the branching pattern of the developing lung (Fig. 3.15). These data show that the extension of the airway epithelial tube and newly formed branches is significantly decreased in the *Shh^{cre}:Fzd2$^{flox/flox}$:R26R^{mTmG}* mutants as compared to control (Fig. 3.15 D). These live-imaging experiments demonstrate that loss of Fzd2 affects maintenance of epithelial tube morphology, new bud formation, and branch extension in a branching network.

Wnt/Fzd2 is required for sculpting new domain branch points by promoting apical constriction through the RhoA pathway

Using the model defined in Chapter 2, lung epithelial cell behavior and shape was evaluated in *Shh^{cre}:Fzd2$^{flox/flox}$* mutants. Using ImageJ, we determined apical surface area by outlining and quantifying the apical-most surface of E-cadherin-stained epithelial cells. Assessment of apical surface area showed that *Shh^{cre}:Fzd2$^{flox/flox}$* mutant cells had a larger apical surface suggesting a failure to undergo apical constriction (Fig. 3.16 A-C). Moreover, *Shh^{cre}:Fzd2$^{flox/flox}$* epithelium does not thicken at predicted sites of new branch formation while control lungs do (Fig. 3.17 A-C). Predicted sites of new bud formation are based on the Krasnow lung map, but in general, the lung epithelium of the Fzd2-CKO animals does not undergo thickening except in the stalk region, where the epithelium is subject to constrictive forces from the surrounding smooth muscle cells. E-cadherin immunostaining was used to outline individual lung epithelial cells in both control and *Shh^{cre}:Fzd2$^{flox/flox}$* mutants and cell shape as well as length, diameter, and

volume were assessed (Fig. 3.18). As expected, control lung epithelial cells exhibited bottle cell morphology at sites of new branch point formation (Fig. 3.18). In contrast, lung epithelial cells in *Shh^{cre}:Fzd2$^{flox/flox}$* mutants displayed a squat columnar shape throughout the epithelium. These changes did not significantly affect the overall cell volume of *Shh^{cre}:Fzd2$^{flox/flox}$* mutant cells but did result in a 30% decrease in apical-basal cell length (Fig. 3.18 C,D). These results demonstrate that upon loss of Fzd2, lung epithelial cells fail to apically constrict, lengthen along the apical-basal axis, and as a result, the epithelial sheet fails to thicken at the region of new branch formation.

Apical constriction of epithelial cells is driven by the cortically localized contractile actomyosin network linked to cell-cell adhesions [123]. This network involves multiple cytoskeletal and cell adhesion proteins including myosins, actin, cadherins and catenins. Our transcriptome analysis shows that expression of a number of cell adhesion genes are disrupted in *Shh^{cre}:Fzd2$^{flox/flox}$* mutants. Among these, the increase in α-catenin expression was of interest as α-catenin associates with adherens junctions and the actomyosin skeleton [124, 125]. We evaluated the localization of α-catenin in the lung epithelium and found a distinct localization pattern of α-catenin in control lungs. α-catenin is apically enriched in regions that exhibit a pseudostratified morphology: the stalk region, and particularly in regions undergoing new bud formation (Fig 3.19 B-ii, H). In regions at the bud tip, where the epithelial cells display a short columnar morphology, α-catenin is more basal-laterally localized (Fig 3.19 C-ii, H). In agreement with the short columnar cell morphology we see throughout the lung epithelium with loss of Fzd2, the epithelium of the *Shh^{cre}:Fzd2$^{flox/flox}$* mutant lung has basal-laterally localized α-catenin, and does not demonstrate distinct apical localization in the stalk region or in regions where new buds would be expected to form.

Interestingly, we see an increase in basal-lateral β-catenin in *Shh^{cre}:Fzd2$^{flox/flox}$* mutants throughout the epithelium (Fig 3.19 B-D, G-H), but no change in E-cadherin basal-lateral localization. This may represent a shift in α-catenin association with the actin cytoskeleton versus association with cadherin mediated cell-cell adhesions [126] at regions of increased cortical tension in the stalk and bending epithelium.

The analysis of the lung epithelium at new branch points revealed that *Shh^{cre}:Fzd2$^{flox/flox}$* mutant epithelium fails to undergo apical constriction and changes in cell shape that precede new bud formation. As a result, the lung epithelial tube fails to maintain a distinct tubular morphology and extend into the mesenchyme, and new buds form with a less distinct bend and a more rounded morphology. This results in delayed bud formation and a 'cystic' phenotype characterized by rounded new bud tips. We had previously performed a transcriptome analysis and referred to these results to determine if any components of the non-canonical Wnt signaling pathway were changed with loss of Fzd2. Notably, we found 2 factors that had been implicated in affecting the non-canonical Wnt signaling pathway via the Rho pathway were decreased with loss of Fzd2 [112, 127]. QPCR analysis of mutant and control lungs confirmed a 40% decrease in Celsr1 and Arhgef19 with loss of Fzd2 (Fig 3.20). As both of these components have been proposed to affect the RhoA pathway, we evaluated if pMLC2 levels (a target of the RhoA pathway) were changed with loss of Fzd2. We found that pMLC2 levels levels were decreased at the apical surface of Fzd2 null lungs (Fig 3.20 D-F). It has previously been reported that Rho Kinase (ROCK) inhibitors and MLC inhibitors can affect branching morphogenesis in lung explants [50, 98]. We wanted to evaluate if this defect in branching morphogenesis resulted in changes in the lung epithelium cellular morphology similar to what we observe with loss of Fzd2. We found that inhibition of

phosphorylation of MLC2 via ML7 caused a defect in branching morphogenesis and an increase in cyst formation similar to what is seen with loss of Fzd2 (Fig 3.21 G,J). Additionally, inhibition of ROCK (an effector of RhoA signaling) via fasudil also caused defects in branching morphogenesis (Fig 3.21 G) and an increase in cyst formation (Fig 3.21I), albeit with a lower penetrance than treatment with ML7. We analyzed the epithelium of the explants treated with ML7 and fasudil and found that the lung epithelium had greatly expanded regions of short columnar epithelial cells, similar to what is observed with loss of Fzd2. Due to the explant conditions, we were unable to section the explants in order to evaluate the apical surface of the lung epithelium, but transverse views demonstrate the short columnar cellular phenotype (Fig 3.21 Hi-Ki). These results, along with the decreased pMLC2 levels with loss of Fzd2 suggested that the RhoA pathway was affected with loss of Fzd2. To assess if the RhoA pathway was active in the presentation of the Fzd2 null phenotype, we used a RhoA activator, calpeptin [128], in the explant conditions to attempt to rescue cell shape changes and branching in the mutant lungs. We found that treatment of the $Shh^{cre}:Fzd2^{flox/flox}$ mutant explants with (15mM) calpeptin could partially rescue the phenotype in 67% of the explants treated (n=9, 3 independent experiments). While the pattern of domain branching could not be restored, the number of cystic tips was reduced from 44% tips exhibiting a cystic phenotype in DMSO treated $Shh^{cre}:Fzd2^{flox/flox}$ lungs to 24% tips exhibiting a cystic phenotype in calpeptin-treated $Shh^{cre}:Fzd2^{flox/flox}$ lungs ($p=0.05$). We observe an occurrence of 15% cystic tips in the control lungs in the explant conditions, and this is not significantly different than what is observed in the calpeptin-treated $Shh^{cre}:Fzd2^{flox/flox}$ lungs ($p=0.26$). Additionally, we observe an increase in the number of new branches added over a 24 hour period: with an average of 4 new branches in the control, 2 new branches in the DMSO-treated $Shh^{cre}:Fzd2^{flox/flox}$ lungs ($p<0.01$ as

compared to control) and 3 new branches in the calpeptin-treated *Shh^{cre}:Fzd2$^{flox/flox}$* lungs ($p<0.05$ as compared to DMSO-treated *Shh^{cre}:Fzd2$^{flox/flox}$* lungs) (Fig 3.22). Epithelial cells in the calpeptin-treated *Shh^{cre}:Fzd2$^{flox/flox}$* lung epithelium regained their bottle-cell morphology as observed in control DMSO treated explants (Fig. 3.21 Hi and Ki). Taken together, these data reveal a molecular pathway where Fzd2 regulates RhoA signaling, which along with proper expression of Fgf10, is required for changes in epithelial cell morphology to coordinate formation of new branch points (Fig. 3.23).

Discussion

Changing the morphology of the primitive endoderm tube to form the highly ramified respiratory tree requires alterations in individual cells that lead to dramatic changes in organ shape. We show that Wnt/Fzd2 signaling is necessary for controlling changes in cell shape through regulating RhoA signaling. The loss of apical-basal lengthening in Fzd2 mutants results in a more uniform lung epithelial cell shape that leads to a failure in the epithelium to thicken. Failure to form a thickened, pseudostratified epithelium in the Fzd2 mutant lungs results both in a widened epithelial tube as well as a defect in formation of new branches. Our studies indicate that Wnt/Fzd2 signaling plays a critical role in altering epithelial sheet morphology through promoting cell shape changes, which is required for generating complex tissue structures such as the branched network of the lung.

In this study, we have focused on the changes in the epithelium during new branch formation as we specifically deleted Fzd2 in the lung epithelium. New branch formation and maintenance of epithelial tube morphology likely requires coordinated changes between the epithelium and the surrounding mesenchyme. While we observed specific changes in epithelial cell biology with loss of Fzd2, we did not see any changes in

mesenchymal cell biology as assessed by SM22a staining or actin localization, suggesting that the changes in cell biology are restricted to the epithelium (Fig 4.3). However, we did observe changes in mesenchymal Fgf10 expression that likely contribute to the overall defects observed upon loss of Fzd2 in the developing lung. Previous work has suggested that Fgf10 signaling from the mesenchyme acts to promote specific outgrowth where a new branch forms [21, 37, 121], although new research has called into question the requirement for focal localization of Fgf10 for proper branching morphogenesis to occur [48]. Interestingly, the previously reported effects of Fgf10 signaling, including changes in cell proliferation or orientation of cell division, were not changed in Fzd2 deficient lung epithelium suggesting either a different role for this ligand in regulating branch point formation or a lack of responsiveness in the Fzd2 deficient epithelium [38, 39, 97]. The increase in levels and expansion in the domain of Fgf10 expression could be due to decreased Shh or Fgfr2 expression, which provide important feedback signals that control the proper expression of Fgf10 [35, 47]. However, even in the context of a precise focal Fgf10 signal, the Fzd2 deficient epithelium cannot maintain proper branch morphology. Together, these results suggest Fzd2 mutant lung epithelium is intrinsically defective in epithelial morphology required for new branch formation but alterations in Fgf10 signaling could contribute to the overall phenotype in a non-cell autonomous manner.

The formation of new branch points in the developing respiratory tree requires changes in cell behavior in a specific region of the lung epithelium that leads to bending of the epithelial tube. Thickening of the epithelium in a specific region precedes bending of the epithelium, a change in morphology that is observed in other systems where a sheet of cells invaginates to promote complex tissue reorganization required for development [101, 102, 129]. Importantly, Wnt/Fzd signaling has been implicated in

promoting these processes during gastrulation [130-133]. While we observe a defect in the thickening of the lung epithelium with loss of Fzd2, it is unclear at this point if the thickening of the epithelium is required for the bending process to occur, or if it is a secondary effect of volume conservation of a cell with decreased apical surface area [134]. As both of these processes are defective with loss of Fzd2, we cannot distinguish if the failure to form new domain branches is due to a failure in cell shape change due to remodeling at the apical surface or if it is due to a failure of the lung epithelial cells to elongate along the apicobasal axis.

Non-canonical Wnt signaling can modify epithelial cell shape and behavior in epithelial sheets through multiple downstream pathways [112, 132]. In the Fzd2 deficient lung epithelium, the epithelial cells fail to adopt a bottle shape and there was a decrease in the components of the actomyosin contractile network at the apical surface as evidenced by a decrease in pMLC2 apical localization. pMLC2 is a target of the RhoA pathway [135], which has been identified as a component of non-canonical Wnt signaling that can regulate changes in cell morphology by modifying cytoskeletal dynamics [52-56]. In $Shh^{cre}:Fzd2^{flox/flox}$ mutants we found decreased expression of two factors, Celsr1 and Arhgef19, which have been implicated in both non-canonical Wnt and Rho signaling [112, 127]. Along with decreased apical expression of pMLC2, these data indicate decreased RhoA signaling upon loss of Fzd2 expression. Inhibition of either ROCK or pMLC2 causes defects in cellular organization and branching morphogenesis and a Rho-activator could partially rescue the loss of Fzd2, supporting a role for RhoA signaling in orchestrating the cell changes needed for new branch formation.

While the importance of branching morphogenesis has been known for some time, little has been revealed about how changes in cell shape can alter and sculpt the

shape of the growing lung epithelial sheet that composes the branching airways. Our data show that Wnt/Fzd2 signaling is required for regulating lung epithelial cell shape and can contribute to bending of the epithelial tube to generate and maintain new branch points. Such alterations have an important impact on postnatal lung structure that may impede respiration. These data provide both a new model for how cell shape changes promote branching morphogenesis as well as show that Wnt/Fzd2 is essential for these changes.

MATERIALS AND METHODS

Mouse strains and breeding

A targeting vector designed to insert loxP sites upstream and downstream of the single coding exon of Fzd2 was electroporated into R1 ES cells. Homologously recombined clones were detected by Southern blot analysis and injected into C57BL/6 blastocysts as previously described. High percentage chimeras were mated to obtain germline transmission of the *Fzd2*$^{flox/+}$ allele. The neomycin resistance gene was removed by crossing germline line *Fzd2*$^{flox/+}$ mice to the Flper mouse (JAX). Schematic of targeting construct, Southern blot probes and position of PCR genotyping primers are shown in Fig 3.1. *Fzd2*$^{flox/flox}$ mice are fertile and exhibit no overt phenotype. Generation and genotyping of the *TOPGAL* β-catenin activity reporter mice [118], *R26R*^{mTmG}[136], *Shh*^{cre}[113], *Shh*^{creERT2} [113], have been previously described.

Histological preparation

Embryos were dissected, fixed in 4% paraformaldehyde in PBS at 4°C, dehydrated through a descending ethanol washes, embedded in paraffin wax, and sectioned at 6μm. Histological procedures were performed as described[137] [114]. For

whole lung branching analysis, embryonic stage was determined by counting somites from the cervical region to the tail. Lungs were dissected from the embryos, and fixed for 1hr in 4% paraformaldehyde in PBS at 4°C for lungs E10.5-13.5 and dehydrated in a descending methanol series. E14.5 lungs and older were fixed in methanol [4]. For vibratome sections, embryos were staged by counting somites, fixed for 1hr as above, embedded in 4% agarose, and sectioned at 100μm thickness to allow for visualization of the apical surface of the epithelium. For lacZ staining, lungs were dissected out and fixed in 2% PFA for 1 hour, and lacZ staining was performed as previously described for 15 minutes to prevent saturation of the stain [138]. To label individual cells with GFP, *Shh*^{creERT2} dams were injected with tamoxifen at 0.1 mg/kg at E10.5 days and dissection was completed 24 hours later.

Immunohistochemistry and in situ hybridization

Immunofluorescent staining as performed as previously described for paraffin sections, vibratome sections, and whole mount lungs [4]. Whole mount lungs were dehydrated in 100% methanol and then mounted in BABB (1 part benzyl alcohol: 2 part benzyl benzoate) and mounted on a slide with a Fastwell spacer and sealed with cover slip[107]. The following antibodies were used for immunohistochemistry and whole mount imaging of lung explants: Sox2 (Seven Hills, 1:500), Sox9 (Santa Cruz, 1:100), Scgb1a1 (Santa Cruz, 1:20), Sftpc (Chemicon, 1:500), p-Histone-H3 (Cell Signaling, 1:200), α-catenin (Cell Signaling-1:100), and myosinIIa (Cell Signaling-1:50.), Alexa-Fluor-655 conjugated phalloidin (Sigma, 1:100), E-cadherin (Sigma, 1:500), γ-tubulin (Sigma, 1:100), SM22a (Abcam 1:200), and GFP (MBL, 1:100). Further details on histological protocols can be found at the Molecular Cardiology Research Center (http://www.uphs.upenn.edu/mcrc/histology/histologyhome.html). In situ

hybridization probes against Fgf10 [22], Fgfr2, Shh, Fzd2 [89], and Bmp4 [139] radioactive section in situs were performed as previously described [140].

Quantitative Real-Time PCR

Total RNA was isolated from E12.5 lungs using the RNeasy kit (Qiagen) using the manufacturer's protocol. cDNA was synthesized from total RNA using SuperScript Strand Synthesis System (Invitrogen). Q-PCR was performed using the SYBR green system (Applied Biosystems) with primers listed in Table 1. GAPDH or β-actin expression values were used to control for RNA quantity. Data shown are average +/- standard deviation for a minimum of 5 biological replicates for each genotype. Table 1 contains the primer sequences used for Q-PCR.

Microarray

RNA was isolated from E12.5 lungs from *Shh*^{cre} control and ***Shh***^{cre}***:Fzd2***$^{flox/flox}$ embryos (three each) and used to generate biotinylated cRNA probe libraries for Affymatrix Mouse Gene 2.0ST array. Microarray data were analyzed using the Oligo package available at the Bioconductor website (http://www.bioconductor.org). The raw data were background-corrected by the Robust Multichip Average (RMA) method and then normalized by an invariant set method. Differential gene expression between the control and mutant mice was analyzed by the Limma package available at the Bioconductor website. p values obtained from the multiple comparison tests were corrected by false discovery rates. Heatmap displays were created using the freely available MeV package (http://www.tm4.org/mev/).

Live imaging of lung explants

E11.5 embryonic lungs were dissected from embryos of the indicated genotypes. Lungs were dissected away from the heart with the trachea left attached as previously described[108]. Lungs were cultured at the air liquid interface on top of standing inserts (Millicell) in DMEM:F12 media with 0.5% FBS, and 1% penicillin/streptomyocin at 5% CO_2, 37°C**.** Standing insert legs were cut to 50μm and placed in glass-bottomed Mattek dishes.

Time-Lapse Microscopy

Lungs were imaged using a Zeiss LSM 710 confocal microscope, using a 10x/0.45 Plan-Apochromatic objective lens. Confocal sections (10μm), stack of 5 sections, were obtained every 20 minutes for 16-17 hours. A stage-top environmental chamber was used to maintain humidity, temperature at 37°C, and CO_2 at 5%. Experiments on lung explants were repeated at least 5 times. Representative single experiments are shown. Images collected were analyzed using ImageJ and custom Matlab analysis.

Image Processing and Analysis

3D reconstitution images were assembled in ImageJ from z-stacks of sections. Quantification of the domain branching of E-cadherin stained whole mount lung was based on previously reported domain branching pattern [4]. Change in bud length over the course of the live imaging experiment was determined by first skeletonizing the lungs in ImageJ, then making length measurements at equal intervals over the course of the imaging experiment. Kymographs were made using a custom MATLAB program. To determine apical cell area, regions of 100μm^2 size, within 50μm of developing buds or region of predicted bud location, were analyzed. Measurements of apical area were determined in ImageJ by outlining E-cadherin staining at the most apical region of the

cell. Apical to basal cell length and cell volume were determined by outlining cells manually in each plane of a z-stack, with 0.5μm confocal sections. Cell volume was determined by using Cavalieri's estimation. Reconstructed cell outlines, cell volume and apical to basal cell length were made using EDGE[134]. Cell outlines, cell volume and apical to basal cell length were equivalent using either manual or automated (EDGE) results, but the automated results are reported in the figures. Measurements were made in at least 3 animals and over 100 cells per genotype were analyzed for apical area, cell volume, and apical to basal cell height.

Cell proliferation and determination of angle of cell division

Cell proliferation was analyzed by phospho-histone H3 (P04-H3) staining in E11.5 lungs. P04-H3+ cells in the proximal and distal regions of the developing epithelium were evaluated and compared to the total number of nuclei present (as determined by DAPI staining). At least 3 mice each of Shh^{cre} and Shh^{cre}:$Fzd2^{flox/flox}$ were analyzed. Vibratome frontal sections of E11.5 lungs were stained for E-cadherin, DAPI, and γ-tubulin to determine the spindle orientation of dividing cells. Only cells in anaphase were used for analysis. The angle of cell division in comparison to the direction of lung growth was determined using ImageJ. Analysis was performed on sections from at least three different lungs for each genotype.

Fgf10 bead experiment

Distal tips of mutant and control lung were dissected from E11.5 lungs. 75μm agarose beads were incubated with 250ng/ml Fgf10 as described previously[97]. Lung tips were embedded in 50:50 Matrigel (GFR-Collaborative): DMEM/F12 media and Fgf10 soaked beads were placed 75-100μm away from the bud tip. Lungs were incubated

for 48 hours and images taken at 0, 24 and 48 hours. Distance grown and bud width were determined by analysis in ImageJ. Experiments were repeated at least 5 times and representative images are shown.

Table 3.1 QPCR and Genotyping Primers

QPCR Primer Name	**Sequence**
Arhgef19_F	agccaaactgaagctgtcca
Arhgef19_R	aaacttcccgagctccttcc
Axin2_F	cagcccttgtggttcaagct
Axin2_R	ggtagattcctgatggccgtagt
BMP4_F	ccctttccactggctgatca
BMP4_R	gggacacaacaggccttagg
Celsr1_F	aacttctgcgatgggacctc
Celsr1_R	gagggtgtggcatagcttgt
Fgf10_F	cagtaagacacgcaagcatttactg
Fgf10_R	aatctgatccaattcttccatggt
Fgfr2_F	gaatgatgctgggcttttgc
Fgfr2_R	gcttctcagtgagttttataacagc
Fzd2_F	cgctcatcgtgggcatcacgt
Fzd2_R	gccggctgttggtgagacgag
Gapdh_F	aggttgtctcctgcgacttca
Gapdh_R	ccaggaaatgagcttgacaaagtt
Lef1_F	atgcacgtgaagcctcaaca
Lef1_R	agctgcactctcctttagcg
Spry2_F	agccgcgatcacggagttcag
Spry2_R	tgcgaccgttgccactctg
Shh_F	aagtacggcatgctggctcgc
Shh_R	gccacggagttctctgctttcacag
Tcf3_F	acctagcccctcaacgcctgt
Tcf3_R	ccaagcggtcctccatcttgct
Genotyping Primers Name	**Genotyping Primers Sequence**
Fzd2-Flox_F	gcctgctcgctatttttgttggc
Fzd2-Flox_R	aaatgaggagggagaaagaggggg

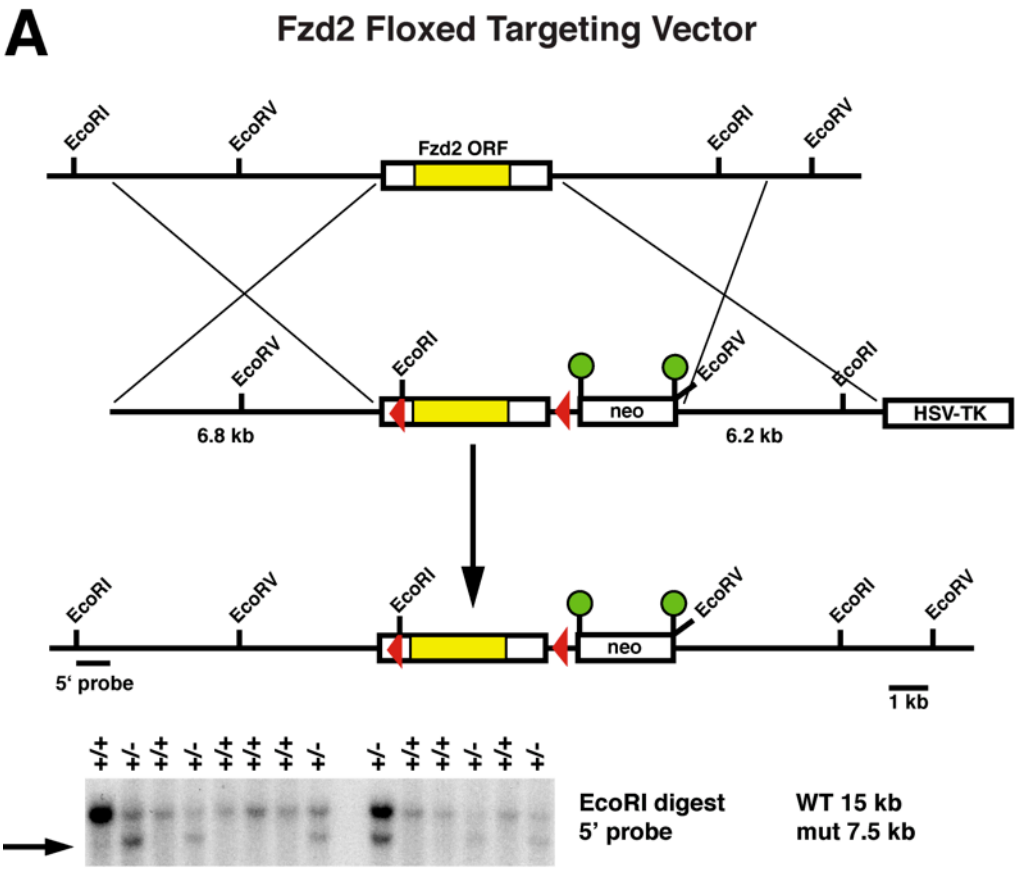

Figure 3.1 Diagram of Fzd2-floxed allele

A conditional floxed allele of Fzd2 was generated by homologous recombination in ES cells which inserted loxP sites in the 5’ UTR and down-stream of the polyadenylation sequence of mouse *Fzd2* (A). Southern blot analysis confirmed correct targeting of both ES cells and germline offspring (A).

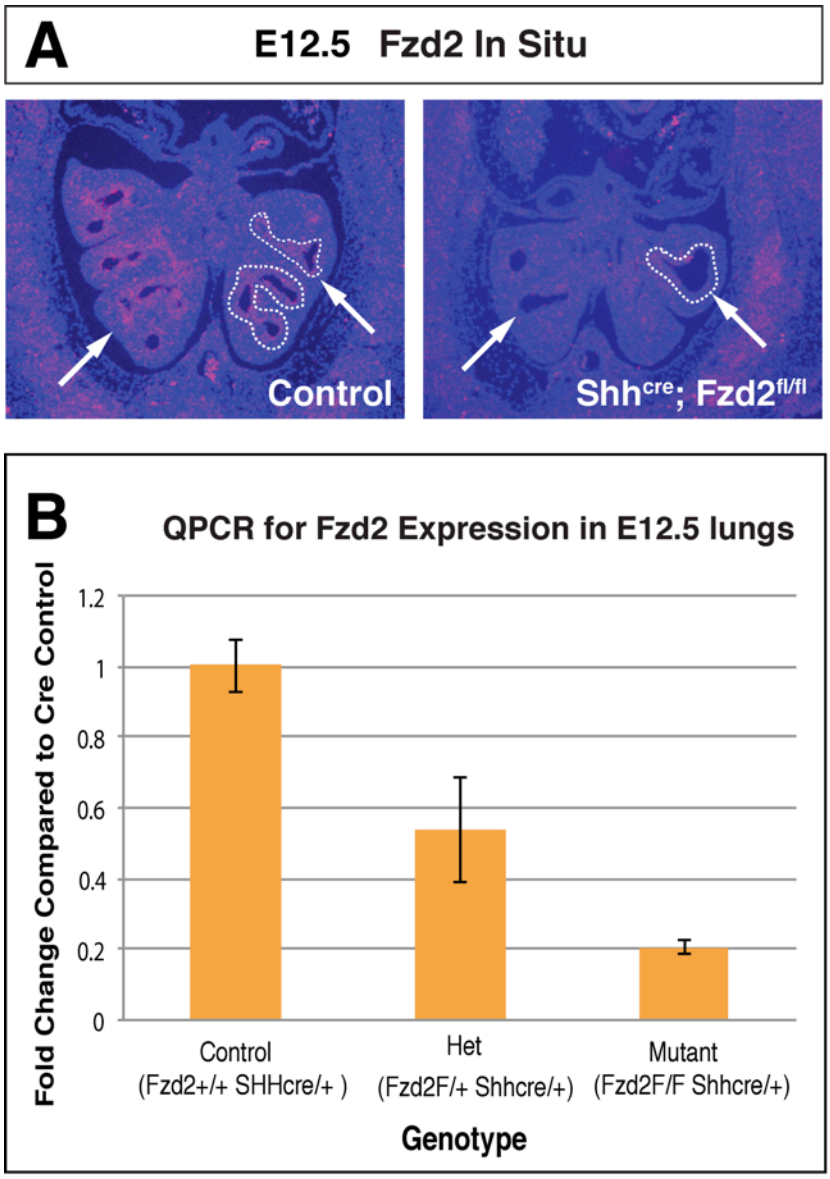

Figure 3.2 Efficient Loss of Fzd2 in the Lung Epithelium by E12.5 with Shh $^{cre/+}$

Expression of Fzd2 in *Shh^{cre}:Fzd2$^{flox/flox}$* mutants is decreased specifically in the developing lung epithelium at E12.5 (A and B, arrows and dotted line). Q-PCR for Fzd2 expression in control and mutant lungs, shows a reduction of approximately 50% in *Shh^{cre}:Fzd2$^{flox/+}$* heterozygotes and 80% in *Shh^{cre}:Fzd2$^{flox/flox}$* mutants at E12.5 (B). The remaining expression is likely due to mesenchymal expression of Fzd2 in the lung.

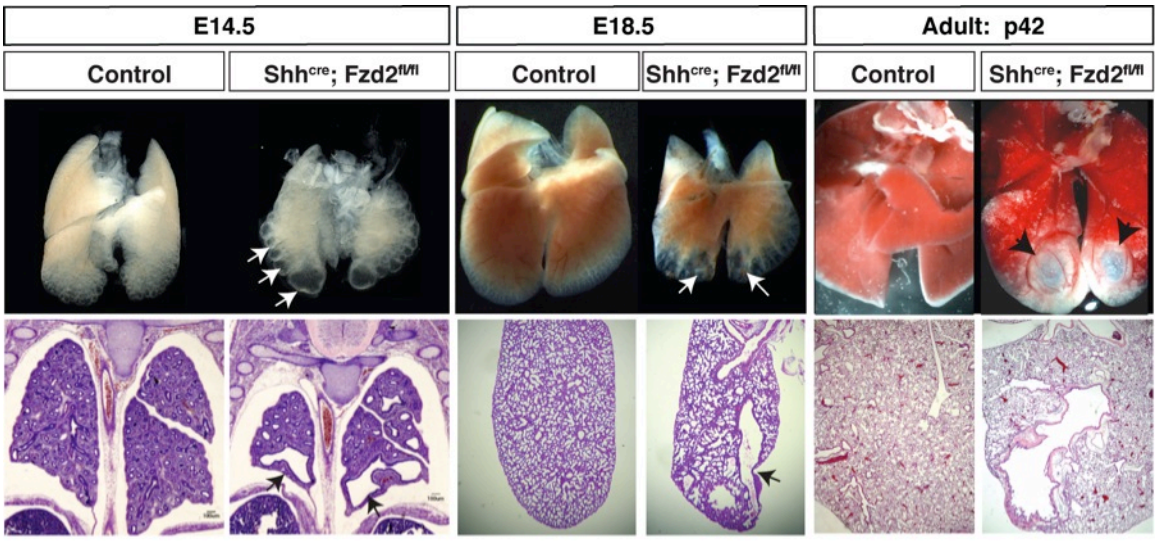

Figure 3.3 Gross Phenotype of Loss of Fzd2 in the Lung Epithelium

At E14.5, *Shh*^{cre}*:Fzd2*$^{flox/flox}$ mutants exhibit cysts in the distal airway region of the whole mount lung (C and D, arrows) and H+E stained histological tissue sections (E and F, arrows). These cysts persist through E18.5 using as seen in whole mount samples (G and H, arrows) and H+E stained histological tissue sections (I and J, arrows). Cysts in the airways of *Shh*^{cre}*:Fzd2*$^{flox/flox}$ mutants are also observed in adult mice at P42, (K and L, arrows) and H+E stained histological tissue sections (M and N, arrows). Controls in all experiments are *Shh*^{cre} mice.

Figure 3.4 Fzd1 and Fzd2 Interaction in the Lung Epithelium

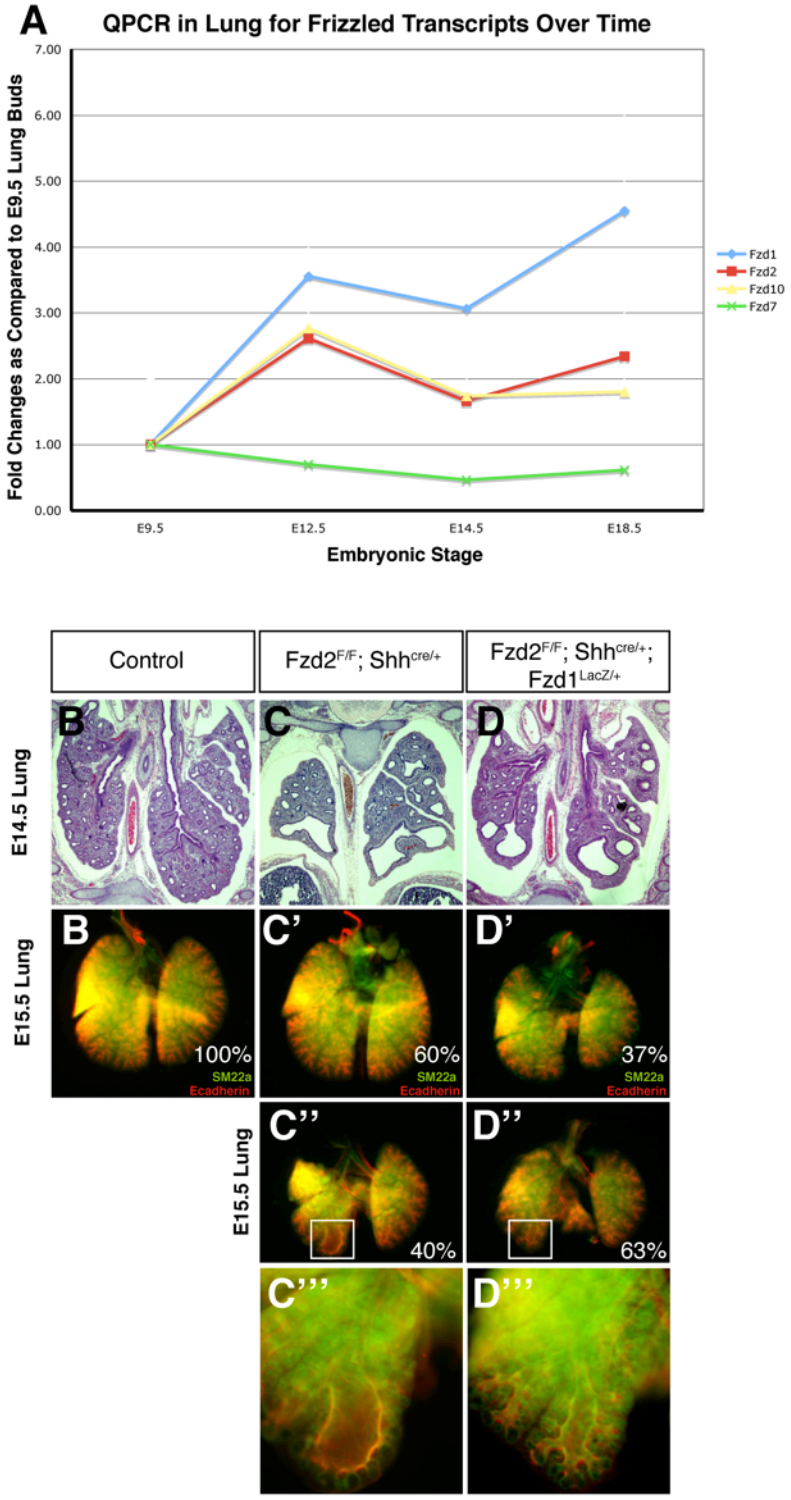

Figure 3.4 Fzd1 and Fzd2 Interaction in the Lung Epithelium

Wild-type lungs from early (E9.5), mid (E12.5 and E14.5) and late (E18.5) embryos were pooled and evaluated for expression of Fzd receptors via QPCR. Expression levels for Fzd2, 10, 7 and 10 at E9.5 were set as 1, and all other time points were compared to this time point to determine how expression changes over the course of development. Fzd2 and Fzd10 expression increases from E9.5 to E12.5, then plateaus until birth (E18.5). In contrast, Fzd1 expression continues to increase as development proceeds. Fzd7 expression is highest at E9.5 and decreases over time.

Loss of one copy of Fzd1 in addition to complete loss of Fzd2 causes increased penetrance of the cystic phenotype. Distal cysts can be seen in $Fzd2^{F/F}$; $Shh^{Cre/+}$ and $Fzd2^{F/F}$; $Shh^{Cre/+}$;$Fzd1^{+/-}$ lungs at E14.5 (B-D). At E15.5, the appearance of distal cysts and lung hypoplasia is observed in 40% of the $Fzd2^{F/F}$; $Shh^{Cre/+}$ lungs (C"). Loss of one copy of Fzd1 in addition to complete loss of Fzd2, causes lung hypoplasia in 100% of the lungs examined, and 63% of the $Fzd2^{F/F}$; $Shh^{Cre/+}$;$Fzd1^{+/-}$ lungs exhibited distal cysts (D" and D'"), although the size of the cystic regions is not increased with loss of Fzd1.

Figure 3.5 Defect in Domain Branching with Loss of Fzd2

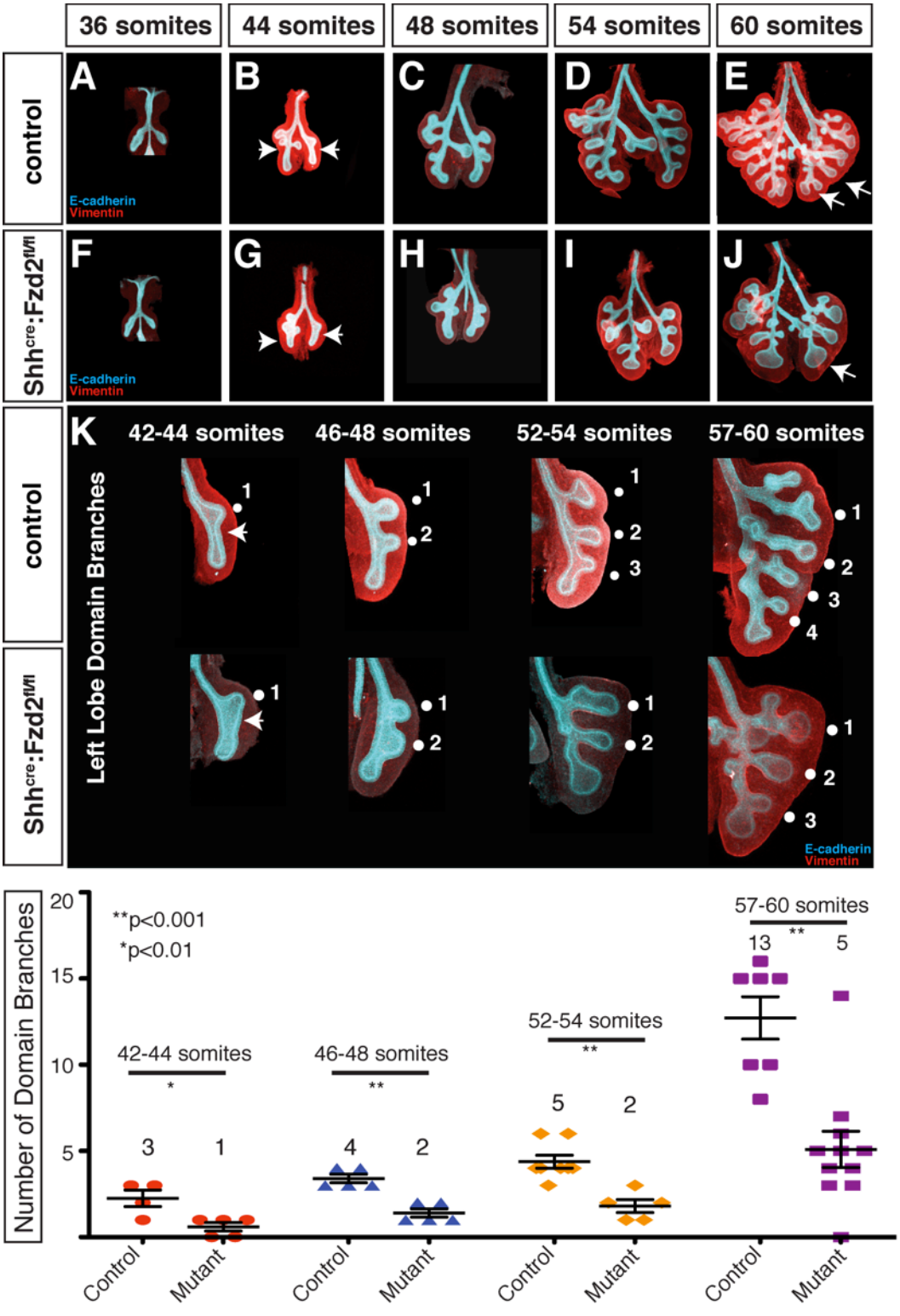

Figure 3.5 Defect in Domain Branching with Loss of Fzd2

Whole mount immunohistochemistry using vimentin to mark mesenchyme (red) and E-cadherin to mark epithelium (cyan) was used to characterize branching morphogenesis in control (A-E) and *Shh^{cre}:Fzd2$^{flox/flox}$* mutants (F-J) from approximately E10.5 (36 somites) through E13.5 (60 somites). The development of cysts in the distal regions of *Shh^{cre}:Fzd2$^{flox/flox}$* mutants correlates with a decrease in formation of domain branches (E and J, arrows). The deficiency in domain branch formation is enumerated and apparent by the 57-60 somite stage (K). Quantification of the number of domain branches during the initial domain branching program (E11-E13.5) shows a reduction in the number of domain branches formed at all time points evaluated in *Shh^{cre}:Fzd2$^{flox/flox}$* mutants (K and L). Scale bars= 500μm**.**

Figure 3.6 Interior Domain Branching in Fzd2-null Epithelium

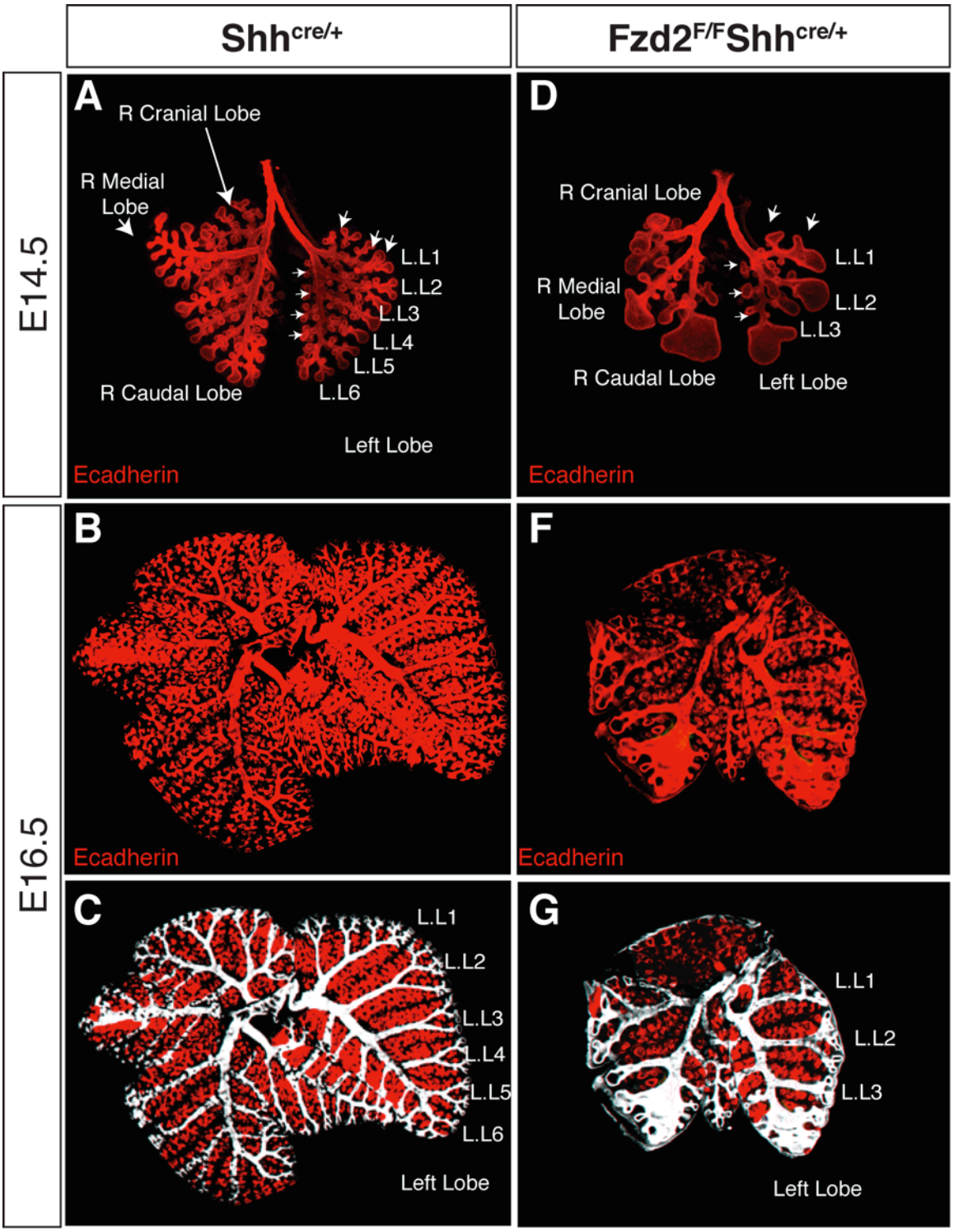

Figure 3.6 Interior Domain Branching in Fzd2-null Epithelium

Whole mount immunohistochemistry using E-cadherin to mark epithelium (red) was used to characterize branching morphogenesis in control (A-C) and *Shh*^{cre}*:Fzd2*$^{flox/flox}$ mutants (D-F) in E14.5 and E16.5 lungs. Major bronchioles are pseudocolored with white in C and G to allow for visualization of the domain branches. Analysis of domain branch formation at E14.5 (A, D) and E16.5 (C,G) demonstrate that the defect in domain branching observed at earlier stages is unchanged. Tertiary branching along the major domain branches form in the E14.5 and E16.5 lungs, although fewer branches have formed (A,D). By E16.5, tertiary branching along the main bronchioles appears grossly normal. At E16.5, the distal cystic regions appear to be undergoing additional, unpatterned budding (G).

Figure 3.7 Fzd2 does not regulate proximal-distal patterning of lung epithelium during development.

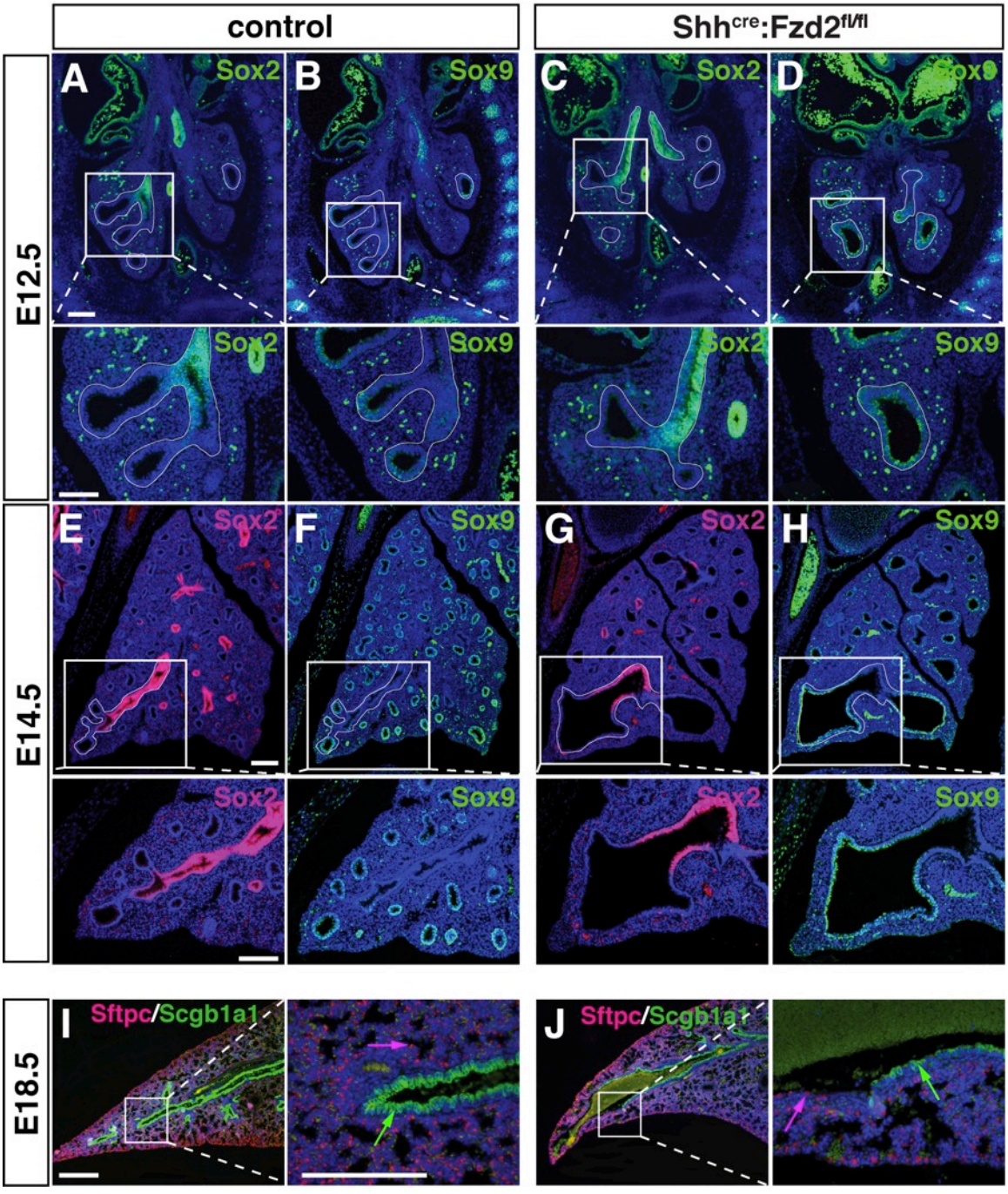

Figure 3.7 Fzd2 does not regulate proximal-distal patterning of lung epithelium during development. Immunostaining for Sox2 and Sox9 was performed to mark the developing proximal and distal lung epithelium, respectively. Sox2 expression is confined to the proximal regions of the developing lung epithelium and Sox9 expression is confined to the distal lung epithelium in control lungs (A-F). While *Shh*^{cre}*:Fzd2*$^{flox/flox}$ mutants have large cysts in the distal regions of their lungs, these cyst still exhibit a proximal-distal patterning as shown by restriction of Sox2 and Sox9 expression to their proximal and distal regions, respectively (C-H). At E18.5, Sftpc expression marks alveolar type 2 cells (pink arrows) while Scgb1a1 marks secretory cells (green arrows) of the proximal airways (I). The large cysts in *Shh*^{cre}*:Fzd2*$^{flox/flox}$ mutants at E18.5 continue to exhibit Sftpc+ cells in the distal most regions while Scgb1a1+ cells line the more proximal regions (J). Scale bars= 500μm.

Figure 3.8 Fzd2 CKO Adult Lung Phenotype and CCAM

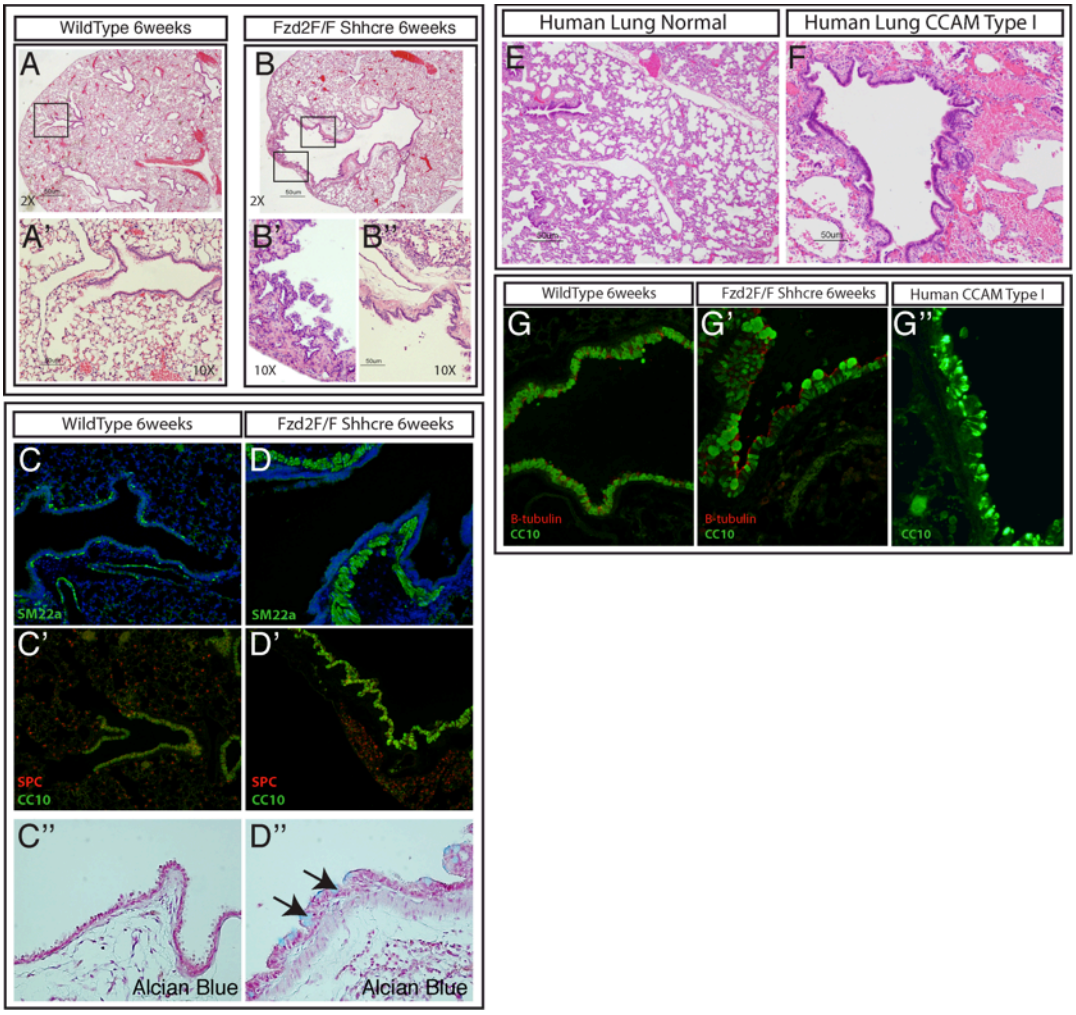

Figure 3.8 Fzd2 CKO Adult Lung Phenotype and CCAM

Mutant animals frequently exhibit a single large cyst in the distal region of the left lung and/or caudal lobe of the right lung (B). Boxed areas of the control and mutant lungs are magnified below. Abnormal cell types surround the cysts, although other areas of the mutant lung appear unaffected.

In control lungs, SM22a is localized to the smooth muscle surrounding the proximal airways and blood vessels (C). In cysts of the mutant lung, thickened smooth muscle surrounds all but the most distal region of the cyst (D). Proximal airways of control lungs are lined with clara cells (CC10 positive) Type II cells (SPC positive) are found in the surrounding alveolar space (C'). In mutant lungs, CC10 positive cells line the cyst to the most distal region and Type II cells are localized normally (D'). Alcian Blue staining of control and mutant lungs. In contrast to control airways, cysts from mutant lungs have increased number of alcian blue positive cells (D"), indicating increased secretory cells lining the cystic regions of the lungs.

CCAM is phenotypically similar in presentation to the cystic region of the Frizzled2 mutant lungs (F). Both CCAM and Frizzled2 cysts are lined with epithelial cells surrounded by thickened mesenchyme.

In control lungs (G) the upper airways are lined with Clara cells (CC10 positive) and ciliated cells (β–tubulin positive). Both of these proximal epithelial cell types are found in the distal cysts in Frizzled2 mutant cysts (G') and CC10 positive cells are also found lining the cysts in CCAM samples (G").

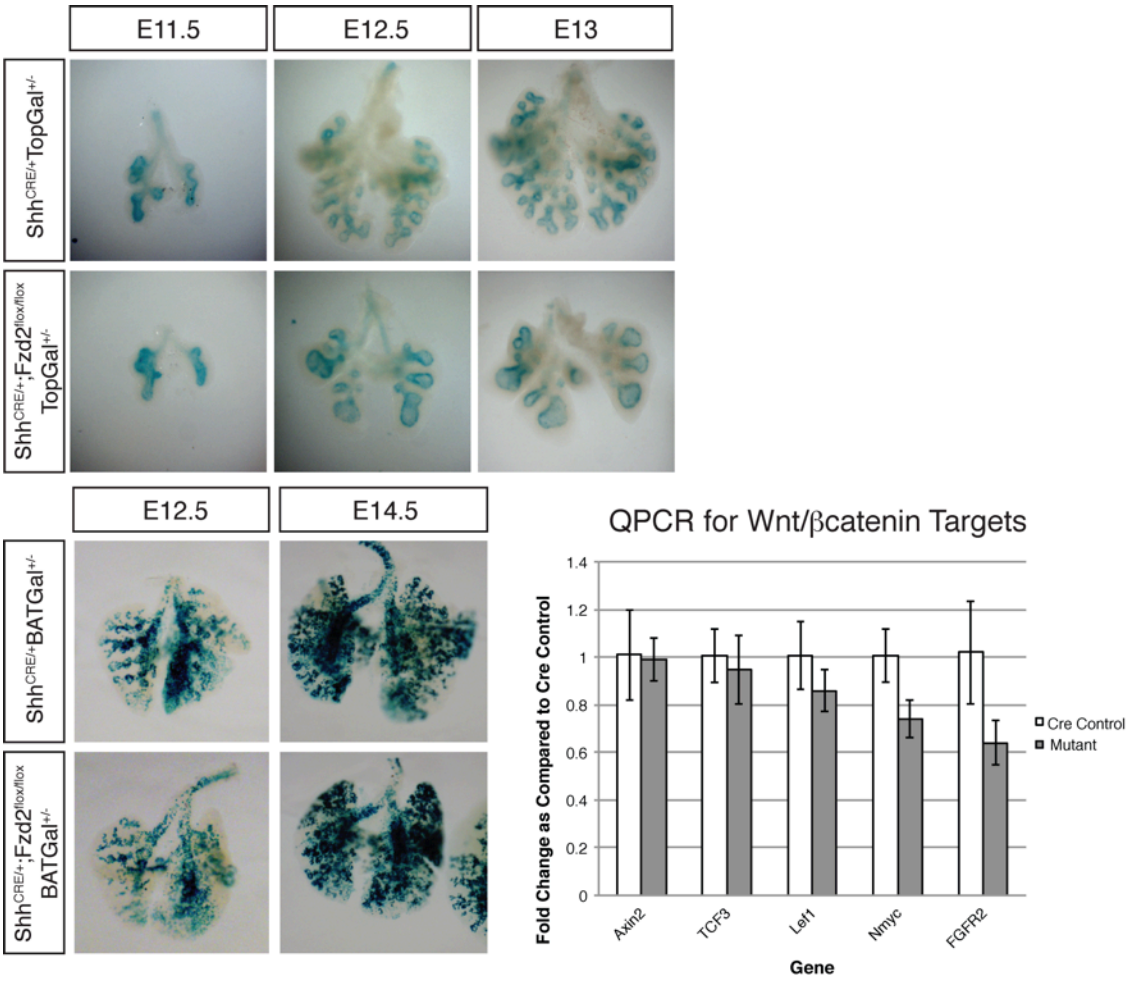

Figure 3.9 Loss of Fzd2 in lung epithelium does not lead to significant alterations in canonical Wnt signaling. *Shh^{cre}:Fzd2$^{flox/flox}$* mutants were crossed to TOPGAL mice to generate *Shh^{cre}:Fzd2$^{flox/flox}$:TOPGAL* mutants. LacZ expression in *Shh^{cre}:Fzd2$^{flox/flox}$:TOPGAL* mutants is not altered as compared to *Shh^{cre}:TOPGAL* controls (upper panels). Similarly, BATGAL reporter did not show any significant difference in activity with loss of Fzd2. Q-PCR for targets of canonical Wnt signaling shows that the expression of the well characterized targets such as Axin2, Tcf3, and Lef1 are not altered in *Shh^{cre}:Fzd2$^{flox/flox}$* mutants.

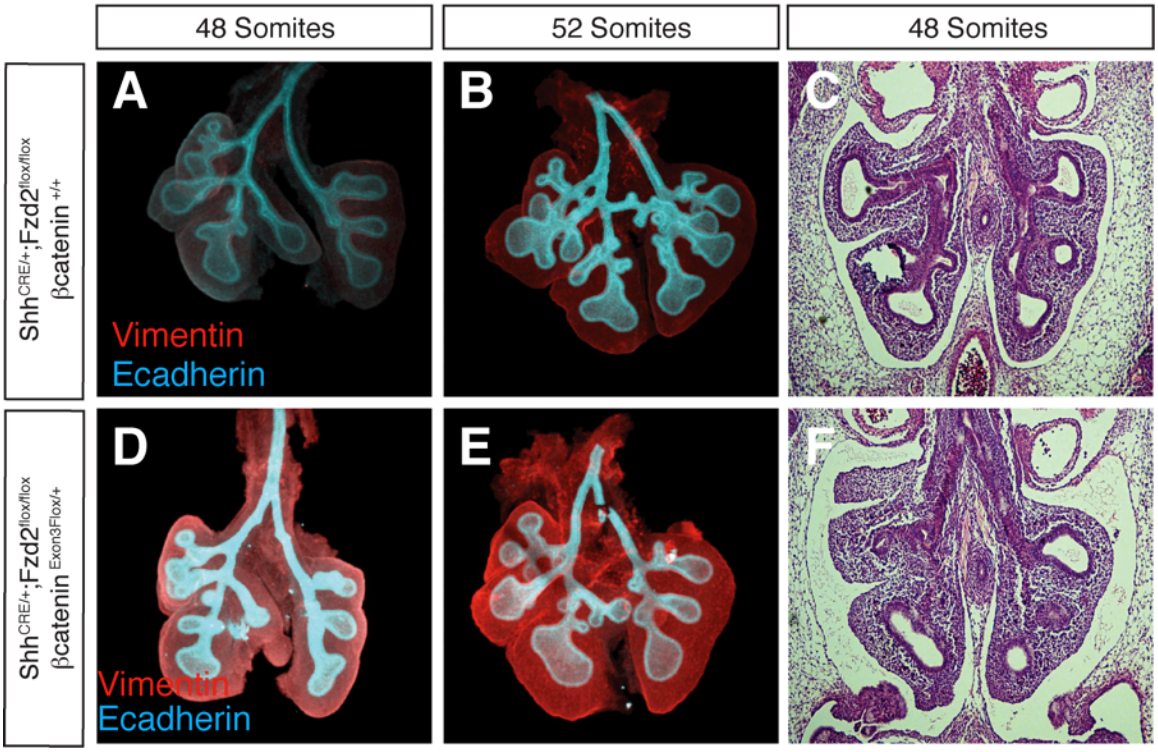

Figure 3.10 Loss of β-catenin Does Not Affect the Fzd2-CKO phenotype

Whole mount immunohistochemistry using vimentin to mark mesenchyme (red) and E-cadherin to mark epithelium (cyan) was used to characterize lung development in *Shh*^{cre}*:Fzd2*$^{flox/flox}$ mutant (A-B) and *Shh*^{cre}*:Fzd2*$^{flox/flox}$ β-catenin $^{flox/+}$ mutants (D-E) at approximately E12.5 (48 somites)-E13(52 somites). Loss of one copy of β-catenin did not increase severity of the defect in branching morphogenesis, hypoplasia or cyst formation in comparison to *Shh*^{cre}*:Fzd2*$^{flox/flox}$ mutants. H+E stained frontal sections show large cystic regions in *Shh*^{cre}*:Fzd2*$^{flox/flox}$ mutant (C) and *Shh*^{cre}*:Fzd2*$^{flox/flox}$ β-catenin $^{flox/+}$ mutants (F).

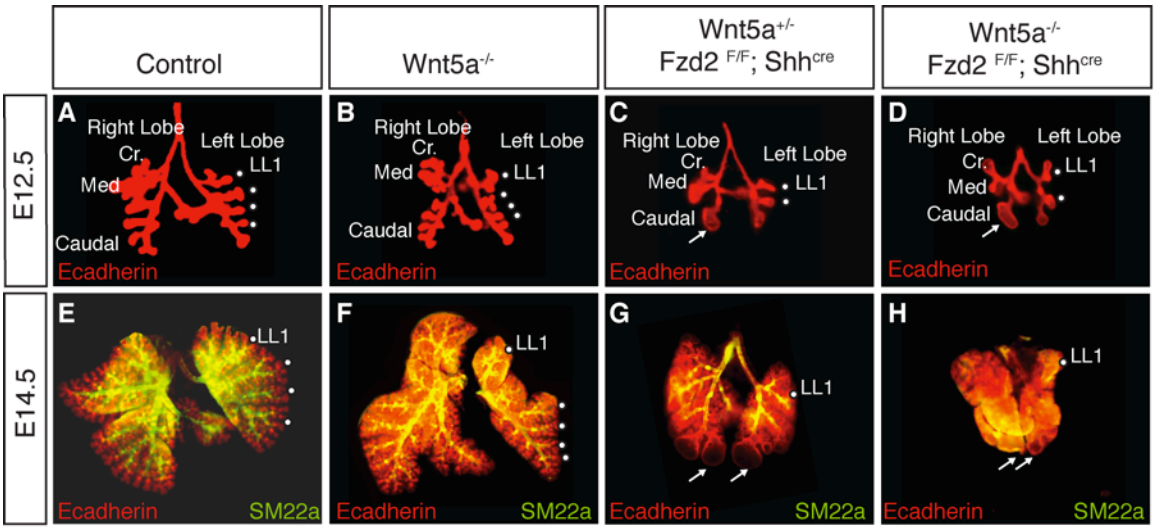

Figure 3.11 Fzd2 and Wnt5a Exhibit Distinct Defects in Branching Morphogenesis

Whole mount lungs were stained with E-cadherin to outline the lung epithelium (E12.5 and E14.5) or Ecadherin and SM22a to label both the epithelium and the smooth muscle (E14.5). At E12.5, Wnt5a mutant lungs do not show a defect in the number of domain branches formed as compared to control (A,B) (4 left lobe domain branches at E12.5). The domain branches that form in Wnt5a null lungs are shorter as compared to control, although the main left bronchi is the same length (A,B). Additionally, the most proximal domain branch (LL1), the right medial, and right cranial lobes are all oriented at a greater angle with respect to the parent branch as compared to control (A,B). Loss of one copy of Wnt5a does not rescue loss of Fzd2 in the lung epithelium either at E12.5 or E14.5 (C,G). Complete loss of Wnt5a in addition to complete loss of Fzd2 displays features of both phenotypes: distal cysts (arrows in D,H), fewer domain branches, and increased domain branch angle.

Figure 3.12 Disruption of the Molecular Branching Program with Loss of Fzd2 in the Lung Epithelium

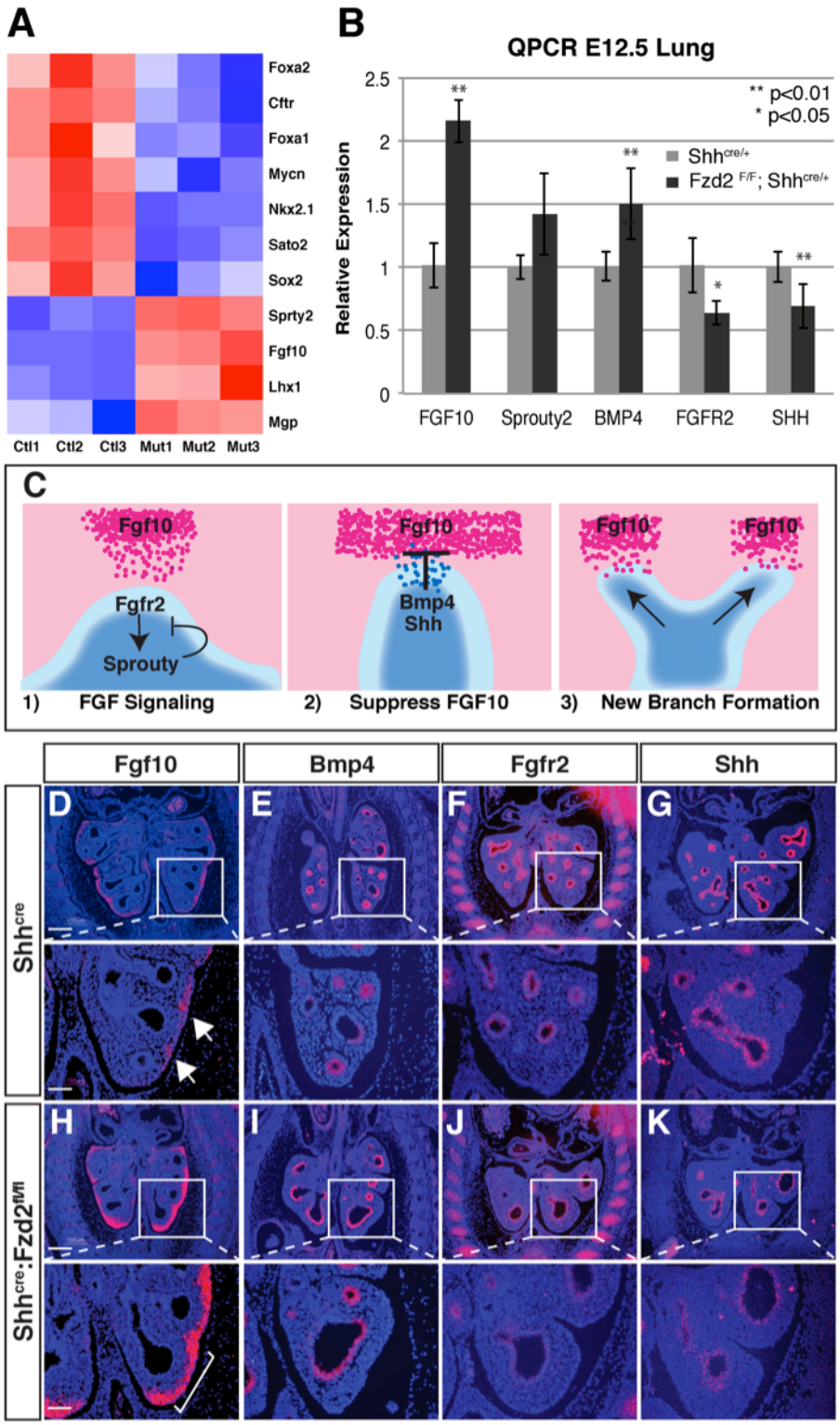

Figure 3.12 Disruption of the Molecular Branching Program with Loss of Fzd2 in the Lung Epithelium

Microarray analysis reveals disruption in expression of multiple signaling factors important for branching morphogenesis including Fgf10 (A). Q-PCR analysis of multiple components of the branching signaling niche reveals increased expression in Fgf10 and Bmp4, and decreased expression of Fgfr2 and Shh (B). Diagram of how the Fgf10, Bmp4, and Shh pathways are thought to interact to control branching morphogenesis with Fgf10 inducing outgrowth of a new bud and Bmp4 and Shh inhibiting Fgf10 activity to form a cleft leading to bifurcation and two new bud points (C). In situ hybridization showing expanded and increased Fgf10 expression, increased Bmp4 expression, and decreased Fgfr2 and Shh expression in control and Shh^{cre}:$Fzd2^{flox/flox}$ mutants (D-K). Scale bars= 100μm

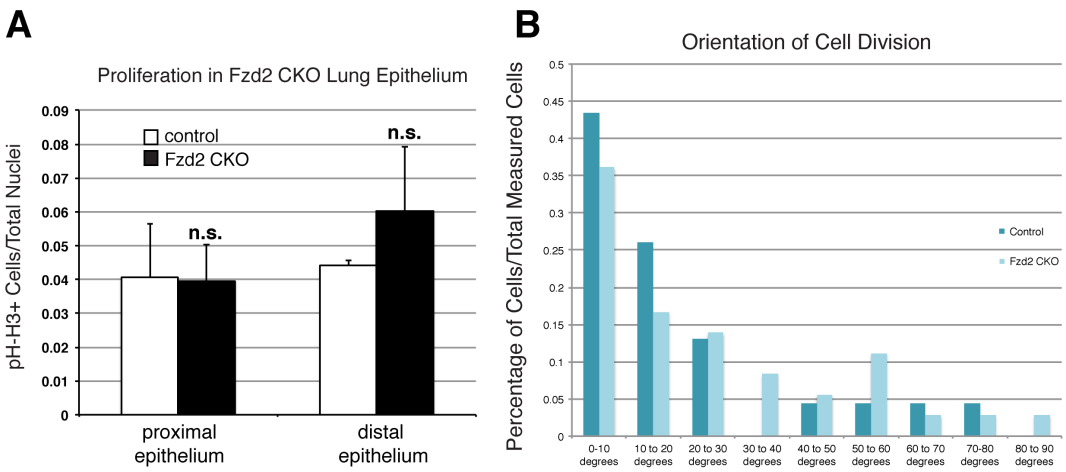

Figure 3.13 Loss of Fzd2 in the developing lung epithelium does not lead to a significant change in cell proliferation or orientation of cell division.

Cell proliferation was assessed using phospho-histone H3 immunostaining at E11.5 in both proximal and distal regions of control and *Shh*^{cre}*:Fzd2*$^{flox/flox}$ mutants (A). Changes observed were not statistically significant (n.s.). Analysis was performed on sections from at least three different lungs for each genotype.

Vibratome frontal sections of E11.5 lungs were stained for E-cadherin, DAPI, and g-tubulin to determine the spindle orientation of dividing cells. Only cells in anaphase were used for analysis. The angle of cell division in comparison to the direction of lung growth was determined using ImageJ. This angle was determined by drawing a line between g-tubulin-stained basal bodies using ImageJ, and compared to overall direction of lung epithelial tube extension in control and *Shh*^{cre}*:Fzd2*$^{flox/flox}$ mutants at E11.5 (B) in accordance with previously described methods (Tang et al, 2011). No significant changes were observed. In both A and B, $p>0.05$. Controls in all experiments are *Shh*^{cre} mice.

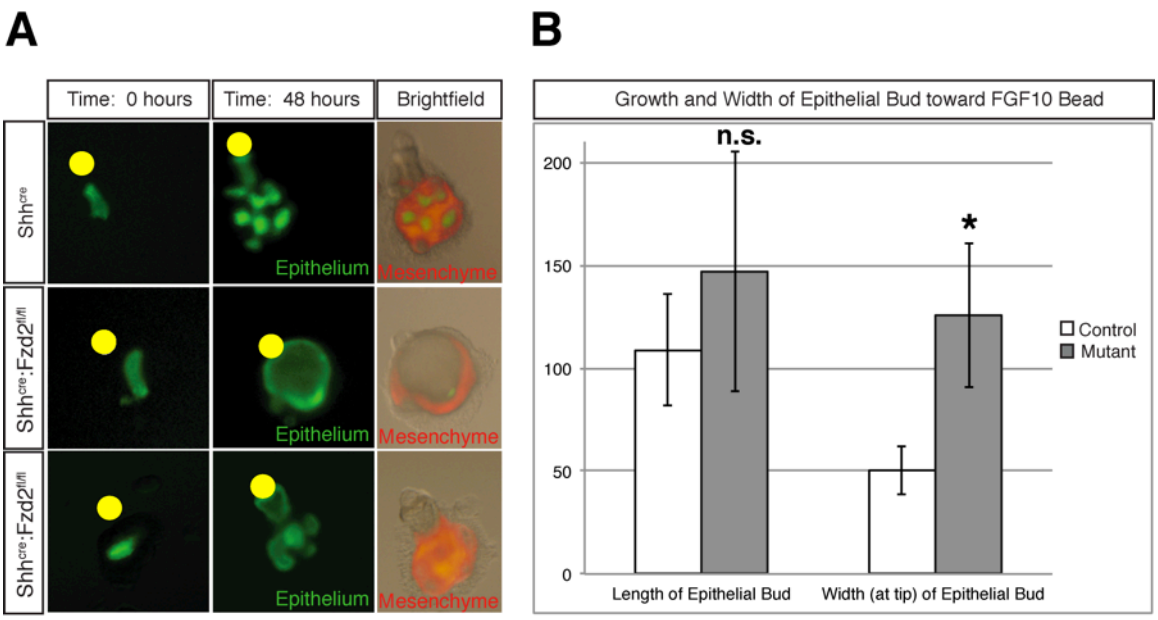

Figure 3.14 *Shh^{cre}:Fzd2$^{flox/flox}$* mutant lung epithelium responds to the chemoattractive effect of FGF10. Lung bud tips, consisting of the lung epithelium and surrounding mesenchyme, were isolated from E11.5 lungs using previously published protocols. Beads soaked in 250ng/ml Fgf10 were placed in Matrigel, within 150um of the bud tips and imaged over the course of 48 hours. While control *Shh^{cre}* epithelium extended a new branch towards the Fgf10 soaked bead, *Shh^{cre}:Fzd2$^{flox/flox}$* mutant epithelium either extended a broad branch or simply grew in a cystic manner towards the beads (A). Epithelium branching at the base of the extending tube seen in the upper and lower panels in A is due to endogenous Fgf10 in the surrounding mesenchyme (pictured in brightfield image). Quantification of the length and diameter of the branching epithelium as it extends towards the Fgf10 soaked beads shows that while the length was not significantly affected, the diameter of the branches was significantly increased in *Shh^{cre}:Fzd2$^{flox/flox}$* mutants (B). *p<0.04, n.s.=not significant, p>0.05. Each experiment was repeated a minimum of 5 times, with representative images shown. Scale bars= 100μm.

Figure 3.15 Live Imaging of Lung Explants

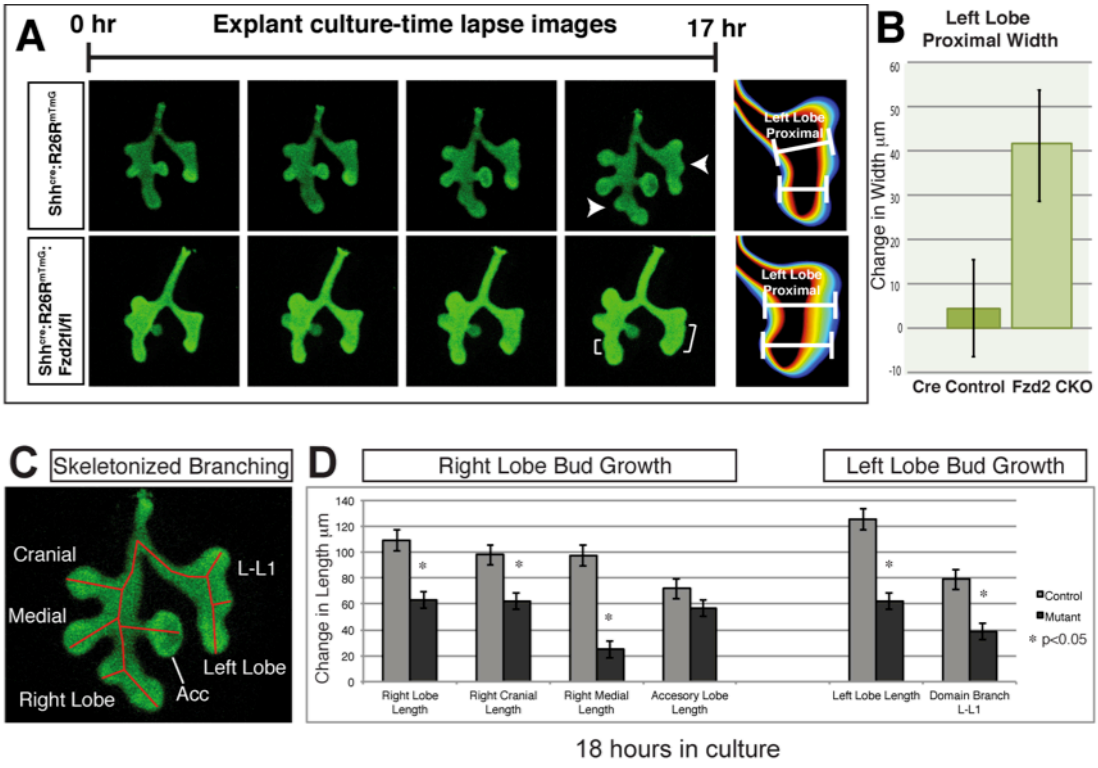

Figure 3.15 Live Imaging of Lung Explants

Real time imaging of control and Shh^{cre}:$Fzd2^{flox/flox}$ mutants ex vivo shows that while control lungs form new domain branch points through extension at predictable sites of bud formation, Shh^{cre}:$Fzd2^{flox/flox}$ mutant lung epithelium expands without bending of the epithelium leading to a wider airway tube (A and B). At sites of new domain branch point formation, the epithelium first thickens (Ci), then buckles at a distinct point (Cii), then buds and extends away from the founder epithelial tube (Ciii), and the epithelial tube constricts at the base of this new branch as extension proceeds (Civ). Using $Shh^{creERT2}$:$R26R^{mTmG}$ mice to mark cells, epithelial cells at sites of new branch points have a broad basal surface and an elongated and narrow apical region. Conversely, epithelial cells at the growing tip are more columnar and shorter with fairly equivalent apical and basal surface areas (D). Diagram of how the epithelial sheet that composes the developing lung airways deforms at sites of new branch point formation: epithelial cells lengthen along the apical-basal axis leading to a bend in the epithelial sheet (E). This results in the formation of new bud or branch point in the epithelial tube. As the new bud extends, the cells in the bud tip once again adopt a short columnar morphology.

Change in bud length over the course of the live imaging experiment (18 hours) was determined by first skeletonizing the lungs in ImageJ, then making length measurements at equal intervals over the course of the imaging experiment. Using a skeletonized branching pattern as a guide (A), quantitative measurements of the developing right and left lobes shows a marked decrease in lengthening of the branches of Shh^{cre}:$Fzd2^{flox/flox}$ mutant lungs (B) over the 18 hour time-lapse experiment.

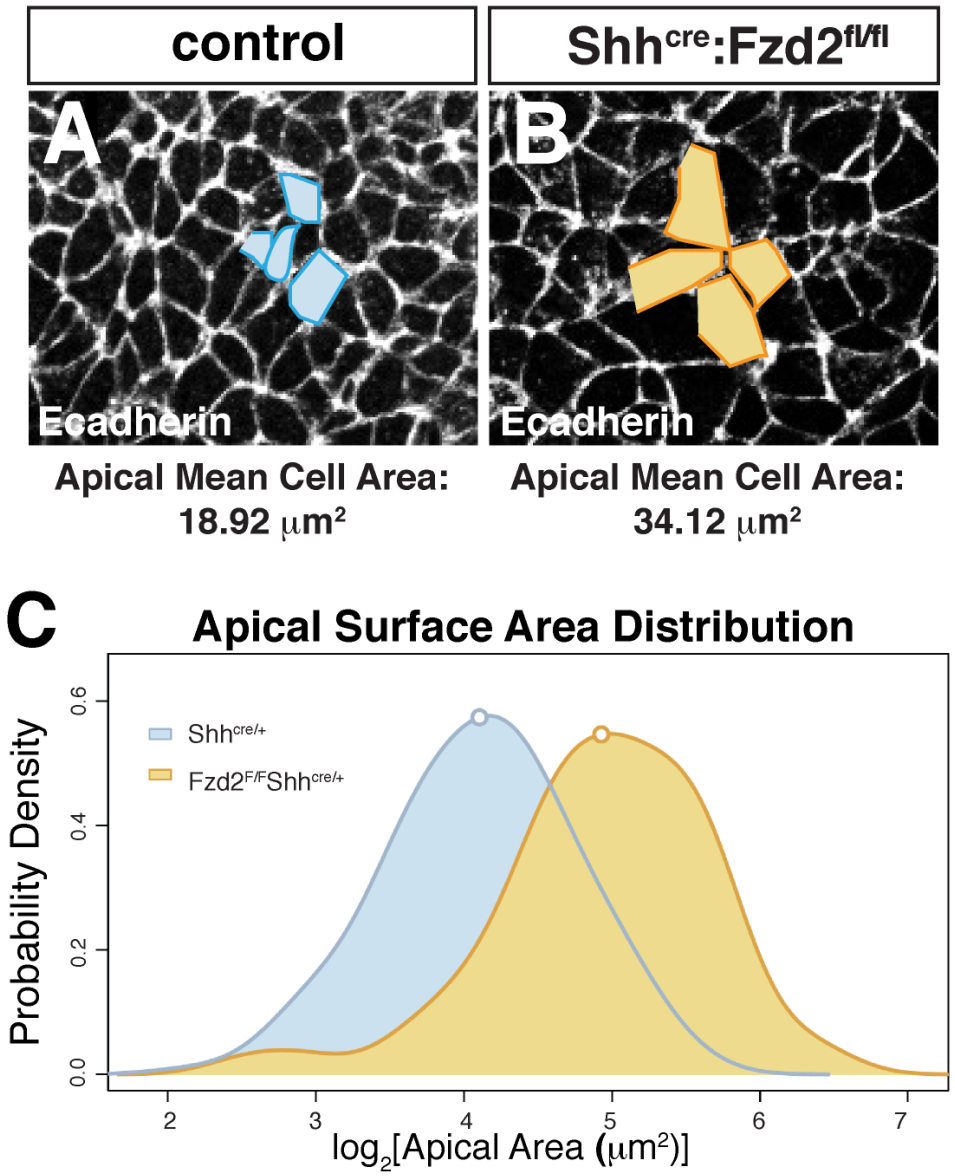

Figure 3.16 Increased Apical Cell Surface Area with Loss of Fzd2

Vibratome sections of E11.5 control and mutant lungs were stained for Ecadherin and imaged to assess the apical surface area of the epithelial cells lining the airway lumen. Average apical surface area was increased in *Shh^{cre}:Fzd2$^{flox/flox}$* mutant lung epithelial cells as compared to control (C).

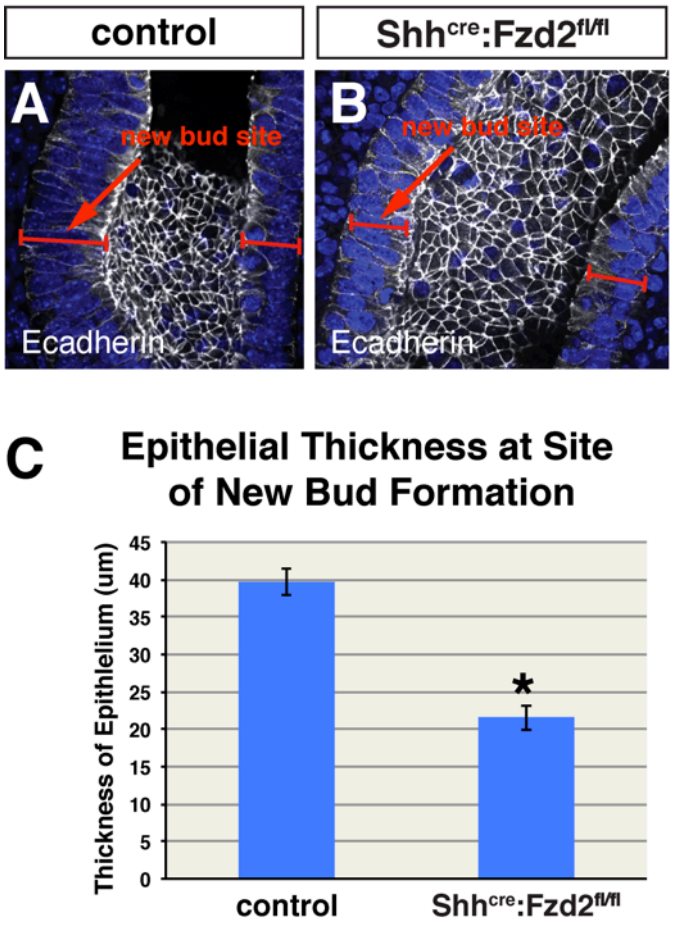

Figure 3.17 Failure of the Lung Epithelium to Thicken at Site of New Branch Formation with Loss of Fzd2

Vibratome sections of E11.5 control and mutant lungs were stained for Ecadherin and imaged to assess the changes in epithelial thickness that precedes new domain branch formation. The epithelial thickening observed in normal and control lungs at sites of new branch point formation was absent in *Shh^{cre}:Fzd2$^{flox/flox}$* mutant lungs (A-C).

Figure 3.18 Defects in Cell Morphology at Sites of New Branch Formation with Loss of Fzd2

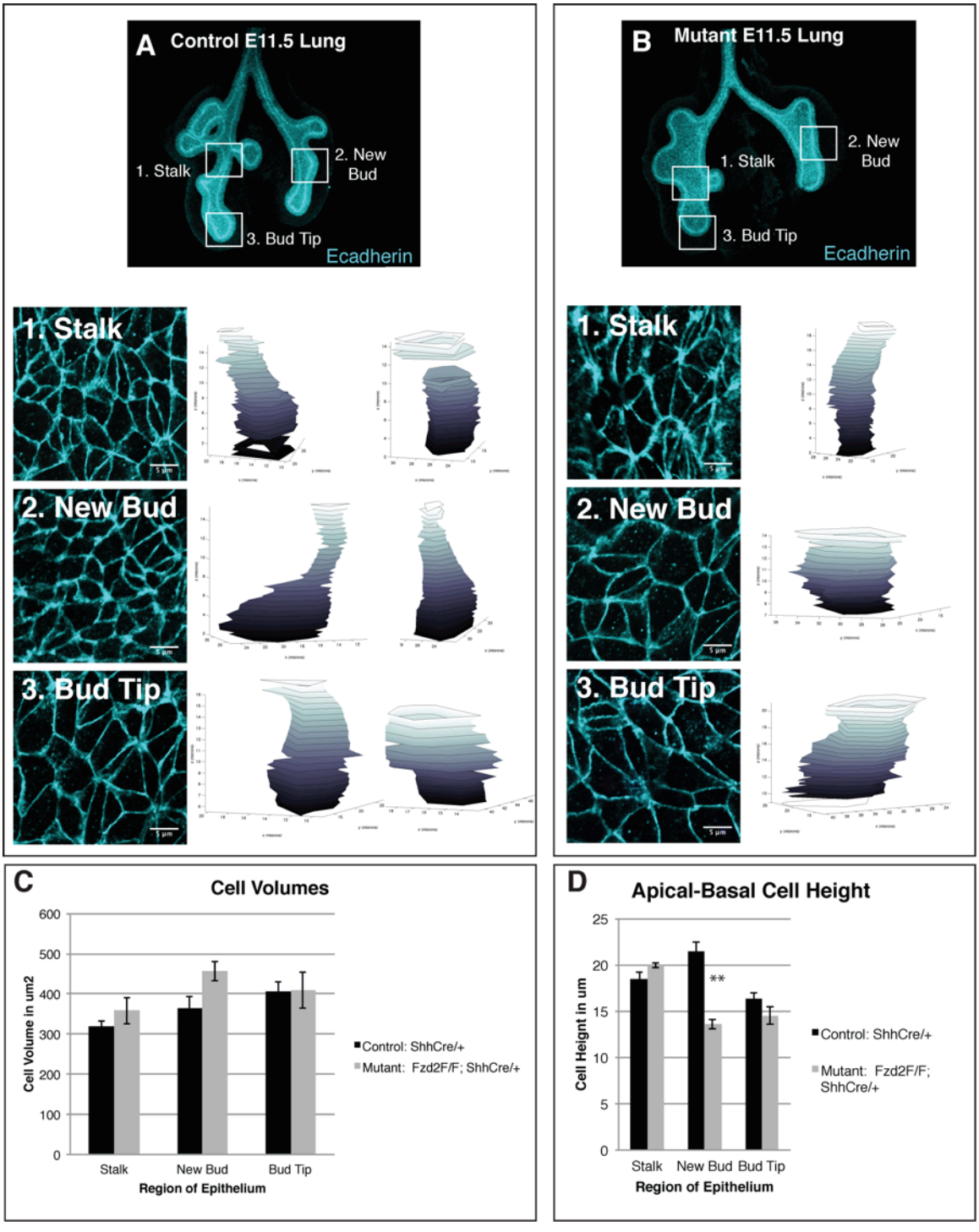

Figure 3.18 Defects in Cell Morphology at Sites of New Branch Formation with Loss of Fzd2

Cell morphology was analyzed using EDGE in three morphologically distinct regions of the lung epithelium: 1. the stalk region, 2. new bud region and 3. bud tip region (A and B). Representative enface images of E-cadherin stain at each region are pictured and at least 3 images per region and genotype were analyzed. In the control lung, the apical surface area of each cell is reduced in the region of new bud formation (2) as compared to the stalk region (1) and the tip region (3). In the mutant (B), the bud tip (3) and the new bud region (2) do not exhibit any difference in apical surface area of each cell. Cell morphology in the mutant lung is primarily short columnar, whereas in the control lung we observe elongated columnar, bottle and short columnar morphology. Measurements of cell volume do not demonstrate a significant difference between mutant and control (C) but apical-basal cell heights in the new bud region are significantly different between mutant and control (E). Error bars are SEM.

Figure 3.19 Defects in Cell-Cell Adhesion Molecules with Loss of Fzd2

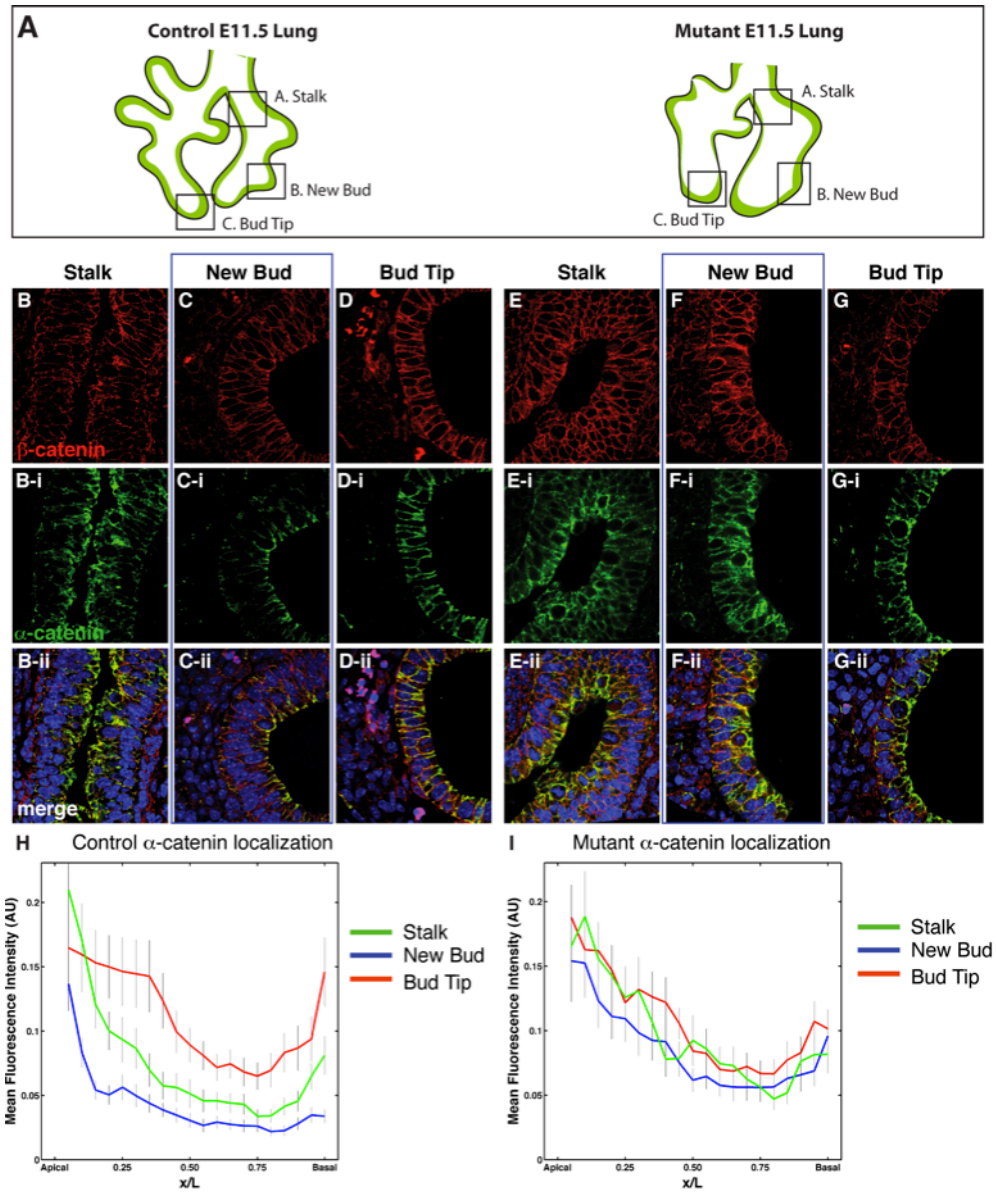

Figure 3.19 Defects in Cell-Cell Adhesion Molecules with Loss of Fzd2

We evaluated α-catenin localization throughout the lung epithelium and found specific α-catenin membrane localization dependent on the spatial region within the developing airways and epithelial cell morphology. In the stalk and new bud region of a wild-type lung, α-catenin localization is enriched at the apical surface and significantly decreased in the basal-lateral cell membrane (Bii, Cii). In contrast, at the bud tip, where the cells adopt a short columnar morphology, α-catenin is more broadly localized throughout the basal-lateral membrane (Di). Throughout the *Shh*^{cre}*:Fzd2*$^{flox/flox}$ mutant epithelium, α-catenin is de-localized and found at both basal-lateral and apical surfaces (Gi-Ii), similar to what is observed only in the bud tip of the control lung. Mean fluorescent intensities (as measured in Matlab) are graphed in E and J and show distinct localization patterns in the control lungs at the stalk, new bud, and bub tip positions, while α-catenin localization patterns are homogenous for all three positions in *Shh*^{cre}*:Fzd2*$^{flox/flox}$ mutant epithelium. Scale bars= 25μm.

Figure 3.20 Components of the RhoA Pathway are Decreased with Loss of Fzd2

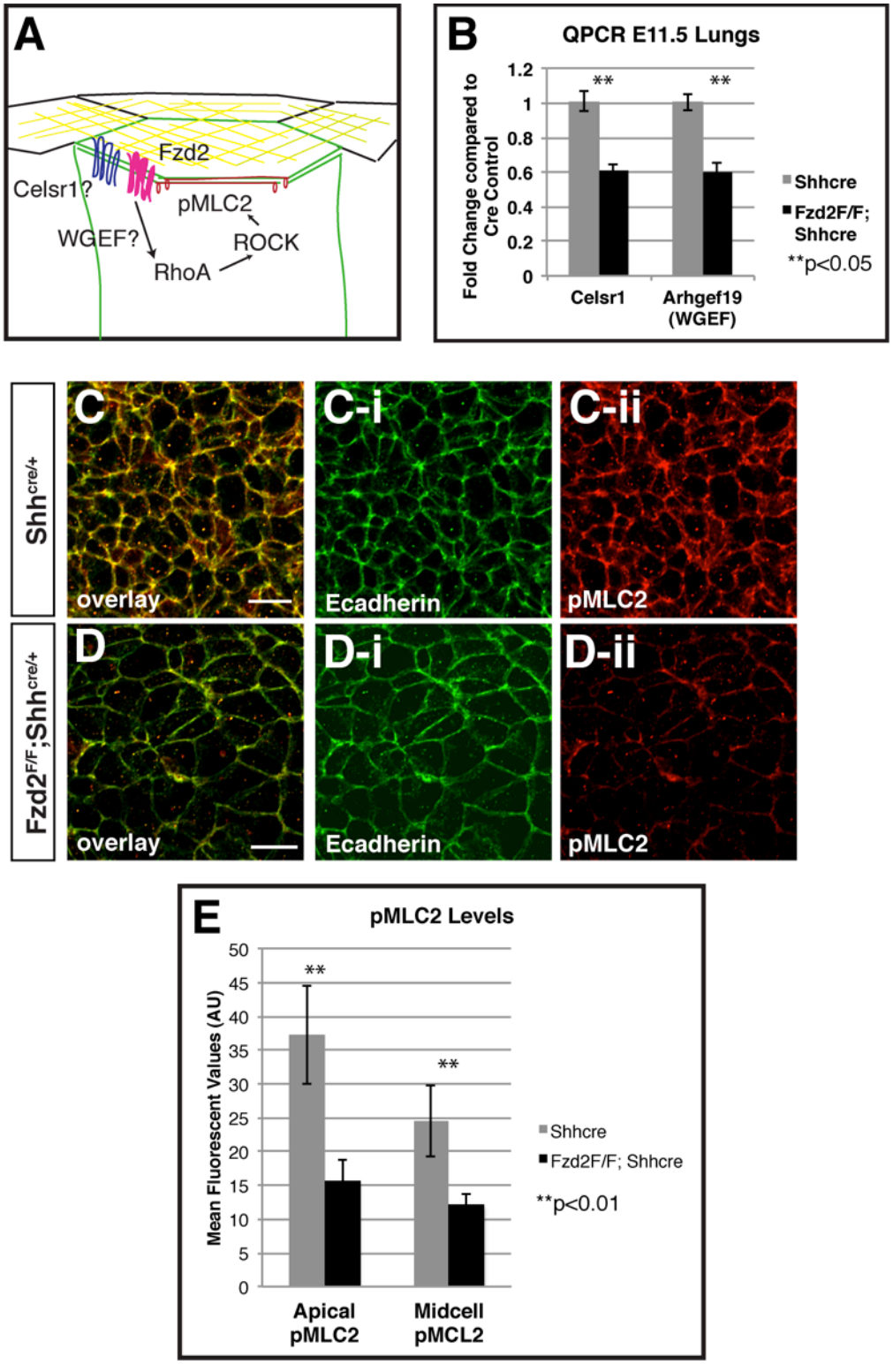

Figure 3.20 Components of the RhoA Pathway are Decreased with Loss of Fzd2

Components of the non-canonical Wnt signaling pathway have been shown to affect changes in cytoskeletal behavior via the Rho pathway (A). Q-PCR data showing decreased Celsr1 and Arhgef19 levels expression in *Shh*^{cre}*:Fzd2*$^{flox/flox}$ mutant lungs at E11.5 (B). E-cadherin was used to outlined the cell shape in *Shh*^{cre}*:Fzd2*$^{flox/flox}$ mutant lungs (C and D). Expression of pMLC2 in *Shh*^{cre} (Cii) and *Shh*^{cre}*:Fzd2*$^{flox/flox}$ mutant lungs (Dii). Expression of pMLC2 and levels are quantitatively decreased in *Shh*^{cre}*:Fzd2*$^{flox/flox}$ mutant lungs (E).

Figure 3.21 Inhibiting or Activating Components of the RhoA Pathway Affects Cell Morphology and Branching Morphogenesis

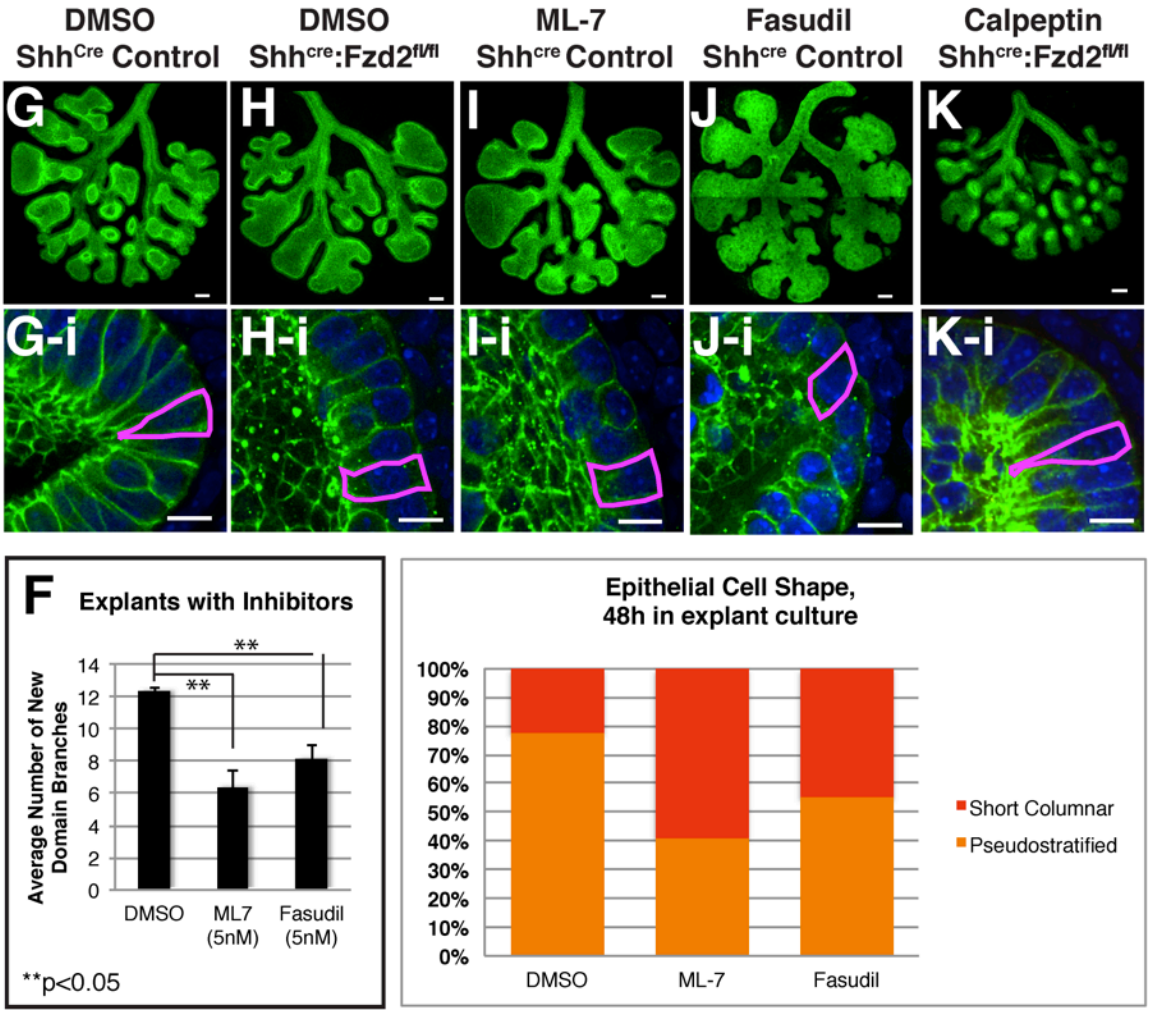

Figure 3.21 Inhibiting or Activating Components of the RhoA Pathway Affects Cell Morphology and Branching Morphogenesis

Quantification of domain branch number of lung explants treated with ML7 or fasudil (F). E-cadherin whole mount immunostaining of *Shh*^{cre} or *Shh*^{cre}*:Fzd2*$^{flox/flox}$ mutant lung explants treated with DMSO, ML7 or fasudil (G-J). Lower panels show cell outlines of after each treatment regime (Gi-Ji). Treatment of Shh^{cre}:Fzd2$^{flox/flox}$ mutant lungs with a RhoA activator calpeptin partially rescues branching morphogenesis and restores bottle cell morphology in Shh^{cre}:Fzd2$^{flox/flox}$ mutant lungs (K and Ki). N=9-12 lungs treated per condition. Confocal images of E-cadherin stained explants after 48hrs in culture were analyzed for epithelial cell morphology. The length of the epithelium exhibiting pseudostratified morphology versus short columnar morphology were measured using ImageJ in DMSO treated controls and lung explants treated with inhibitors as indicated. Treatment with either ML-7 or fasudil expanded the region of short columnar cell types, and decreased the amount of pseudostratified epithelium with a $p<0.01$ using a two-tailed students t-test. Scale bars: C and D=10μm

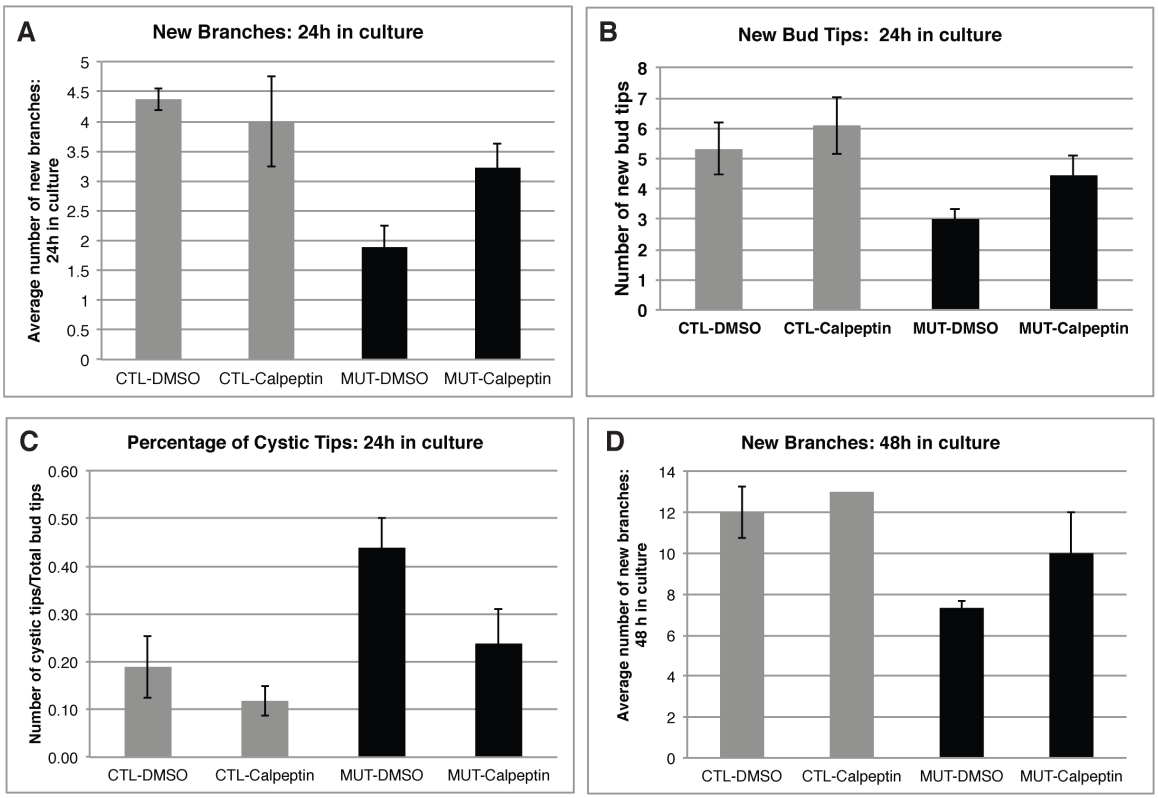

Figure 3.22 Quantification of Calpeptin-mediated rescue of cystic phenotype and branching defect in *Shh^{cre}:Fzd2$^{flox/flox}$* mutant explants.

The number of new domain branches was determined after 24 hours and 48 hours in explant culture (A, B). DMSO-treated *Shh^{cre}:Fzd2$^{flox/flox}$* mutant lung explants show decreased branching as compared to control at both time points. Treatment with calpeptin can partially rescue the defect in branching, $p<0.05$, and increases the number of new bud tips. Cystic tips were determined by the distinctive rounded morphology found in the mutant lungs as opposed to the flattened morphology that leads to new bud formation in the control. *Shh^{cre}:Fzd2$^{flox/flox}$* mutant lungs had approximately 45% of tips exhibiting a cystic phenotype and treatment with calpeptin reduced the number of cystic tips to 23%, $p<0.05$ (B). N=9-12 lungs treated per condition.

Figure 3.23 Model of the effect of loss of Fzd2 on epithelial cell and tissue biology in the developing lung.

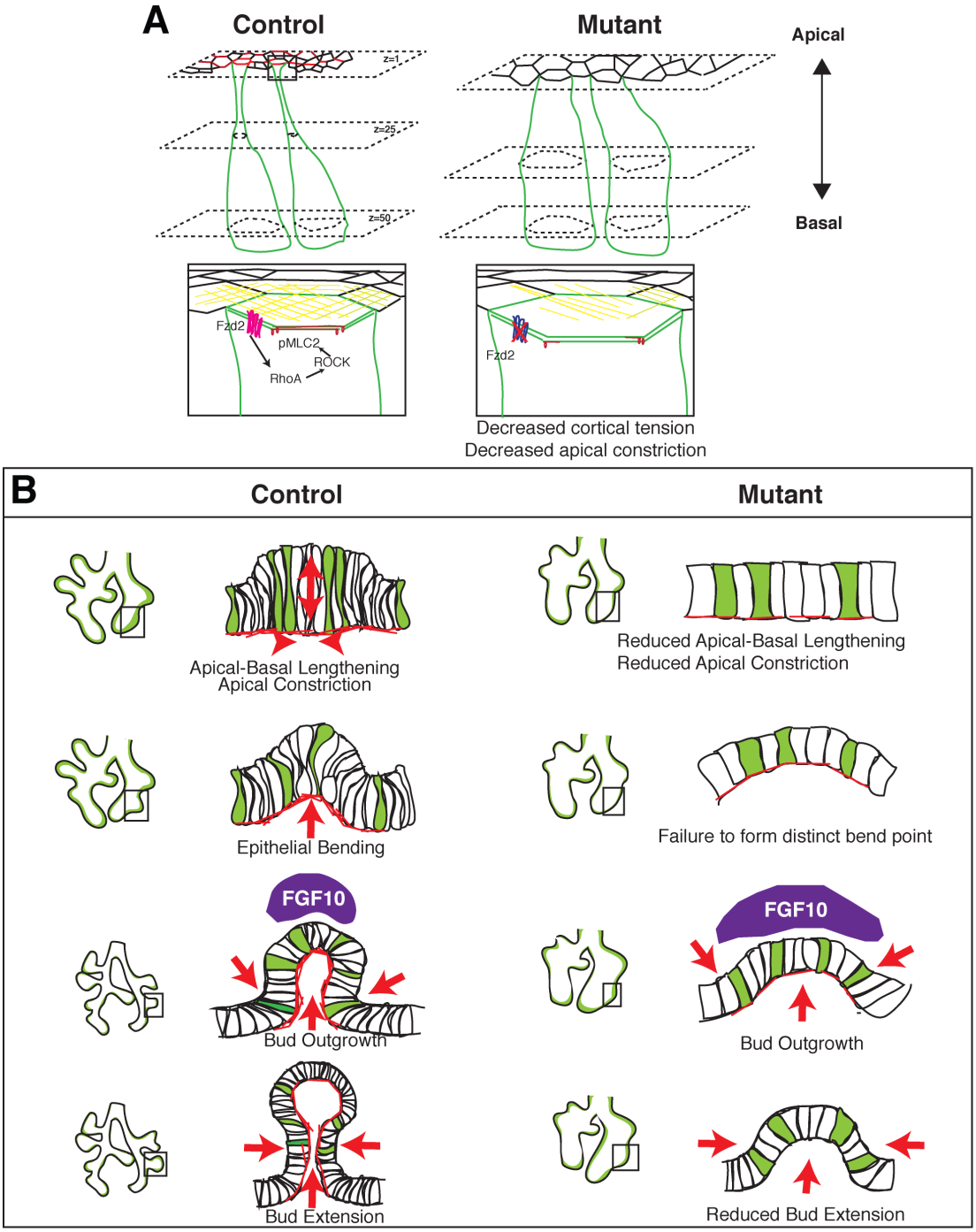

Figure 3.23 Model of the effect of loss of Fzd2 on epithelial cell and tissue biology in the developing lung.

(A) Proposed model of how changes in RhoA activity results in defects in changes in cell shape and apical-basal epithelial cell lengthening. (B) Overall model of how Fzd2 acts to control lung epithelial cell shape leading to defective branch point formation. Cell intrinsic defects as noted in A and the increased and expanded domain of Fgf10 expression both contribute to the defective domain branch formation as well as maintenance of the epithelial tube shape. Red arrows and arrowheads indicate direction of epithelial bending and sculpting of the developing airways to form new branch points.

Chapter 4: Conclusions and Future Directions

Summary

Formation of the structurally complex lung requires coordination of signaling and gene regulatory networks with morphogenetic processes that remodel tissues to give rise to three-dimensional organs. Important work in the last 20-40 years has highlighted the role of a number of signaling pathways in directing lung development, but links between these molecular signals and actual deformations in embryonic tissue remain obscure. Unlike in other branched organs such as the mammary gland, kidney and salivary gland, very little is understood regarding the changes in tissue and cellular morphology that drive new branch formation in the lung. Failure of the lung to properly arborize directly affects its primary function in gas exchange and as such understanding the morphogenesis, as well as the biochemical signaling, underlying this process is of vital importance.

In this dissertation, I provided a detailed analysis of the changes in cell biology in the lung epithelium that accompany new domain branch formation in initial establishment of the respiratory tree. I used this analysis to characterize a mutant for the receptor, Fzd2, in the Wnt signaling pathway. This work highlights a previously unappreciated role for Wnt signaling in branching morphogenesis in the lung and provides much needed insight into the morphological consequences of loss of this signaling pathway in the establishing the branched respiratory tree.

In Chapter 2, I use both live imaging and fixed samples to describe the changes in the lung epithelium that lead to bending of the epithelium and new branch formation. I found that the lung epithelium thickens at the region where a new domain branch will form, and then a distinct kink is formed in the epithelial tube that leads to bending of the

epithelium. I also characterized the cell morphologies in specific regions of the epithelium and found an increase in apically constricted bottle cells at regions undergoing new branch formation. These results provide a model of the changes in cellular and tissue biology that lead to new domain branch formation. This model for new branch formation in the epithelium is distinct from branching morphogenesis processes described in mammary glands and the vascular network, and appears to be more similar to morphological processes that result in bending of an epithelium. While limitations in confocal microscopy and culturing conditions prevented me from investigating the dynamic nature of the cell shape changes that accompany new domain branch formation, advancements in these areas as well as development of improved reporter constructs will build on my findings to provide more insight into branching morphogenesis in the lung.

In Chapter 3, I use the model derived from normal lung epithelial development to characterize the defects in branching morphogenesis observed with loss of a Wnt receptor, Fzd2, in the lung epithelium. I found that when the Fzd2 receptor is specifically lost in the respiratory epithelium early in lung development, the formation of the domain branches is disrupted and the distal epithelium forms cysts rather than branched airways. This defect in domain branch formation is due to epithelium lacking Fzd2 failing to undergo changes in cell shape that are required for bending of the epithelial tube.

These findings represent an important initial foray into understanding the morphological changes in cellular and tissue biology that underlie new branch formation in the lung epithelium. Despite this insight, there remain a number of outstanding questions. In the following chapter, I will outline some remaining questions and some

preliminary data addressing the role of Wnt signaling through Fzd2 in branching morphogenesis. I will also highlight some of the remaining important questions that need to be addressed to further our understanding of branching morphogenesis in the respiratory epithelium. Finally, I have included preliminary data evaluating the requirement for Fzd2 in early embryonic development.

Preliminary Data on complete loss of Fzd2 in the embryo

While we found specific defects in branching morphogenesis with loss of Fzd2 in the foregut endoderm prior to lung specification, we wanted to determine the effect of complete loss of Fzd2 on embryonic development. To address this question, we used the *CMV*^{cre} to excise the *Fzd2* floxed allele throughout the embryo and evaluated Fzd2 null embryos. We found that complete loss of Fzd2 results in early embryonic lethality, in contrast to a previously reported *Fzd2* mutant allele [93]. In addition to description of the Fzd2-null phenotype, I will discuss the potential causes for the observed differences between our findings and the reported Fzd2^{LacZ} mutant.

Wnt signaling is known to have a critical role in gastrulation and axis development based on analysis of loss of function mutations in Wnt3a and β-catenin[141, 142]. Specifically, embryos mutant for the Ctnnb1 allele do not form a primitive streak and fail to form mesoderm or any other defined germ layers[141, 143, 144]. Conditional loss of Wnt3 in the epiblast permits primitive streak formation but function is not maintained and the embryos demonstrate developmental delay [145, 146]. These results demonstrate a vital role for Wnt signaling in promoting primitive streak formation and maintenance early in development.

In addition to the role of canonical Wnt signaling in forming the primitive streak, graded levels of Wnt/β-catenin signaling are thought to promote formation of the

anterior-posterior axis, with highest canonical Wnt activity at the posterior region of the embryo[147]. A gradient of Wnt/β-catenin signaling activity along the anterior-posterior body axis is proposed to be required for anterior development of the head and brain [148]. Specifically, downregulation of Wnt signaling in the anterior neuroectoderm is required for proper forebrain development[149]. Antagonism of Wnt signaling at the anterior region of the embryo negatively modulates the function of the Wnt signaling cascade. Antagonists for the Wnt signaling pathway, Dkk1, Cer1, Sfrp1, and Sfrp5 are expressed in the anterior part of the embryo, and several Wnt ligands, Wnt3, Wnt2b and Wnt8a, are expressed posteriorly. These factors, along with others, act to establish a low to high gradient of Wnt signaling activity across the anterior to posterior plane of the embryo. Loss of antagonism of Wnt signaling through mutant Dkk results in anterior truncation [150]. Fzd8 is expressed in the anterior endoderm[151] and overlaps with Dkk1 and Cer1 expression, but no early embryonic phenotype for Fzd8 null animals has been described. These findings, in aggregate, suggest a link between the regulation of Wnt signaling by anteriorly expressed antagonists and the development of anterior structures of the embryo.

Animals with the *Fzd2*$^{F/F}$ conditional allele were crossed into the *CMV*$^{cre/+}$, which ubiquitously expresses cre-recombinase to generate *Fzd2*$^{d/+}$ heterozygous animals. *Fzd2*$^{d/+}$animals do not exhibit any developmental defects and breed normally. No viable *Fzd2*$^{d/d}$ pups were recovered upon crossing *Fzd2*$^{d/+}$ animals. Severely delayed *Fzd2*$^{d/d}$ embryos are recovered at E7 (Fig4.1, C) but by E7.5, the embryos are necrotic (Fig4.1, X). Whole mount in situ hybridization using an anti-sense Fzd2 probe shows Fzd2 is broadly expressed throughout embryo as early as E6.5. As development proceeds, Fzd2 expression is concentrated primarily at the anterior neural folds by E7.5 and E8 (Fig 4.1,

upper panels 3,4). Cross-sections of E7.5 embryos stained for H&E, or radioactive in situ for Fzd2, shows that by E7.5, *Fzd2*$^{d/d}$ embryos have disorganized tissue organization. Similar to what is seen in the whole mount in situs, radioactive in situ on the cross-section of the E7.5 embryo displays Fzd2 strongly expressed in the neural folds. This dramatic phenotype with loss of Fzd2 is similar to what is observed with loss of Wnt3. In contrast to Wnt3 localization, Fzd2 is expressed primarily in the anterior region, although at the time of primitive streak formation, Fzd2 expression is not yet restricted to the anterior region. These results strongly argue for a role of Wnt signaling through Fzd2 to promote early embryonic development. Given the expression pattern of Fzd2 during this time period, it would be interesting to investigate the requirement for Fzd2 in primitive streak formation and maintenance as well as the requirement for Fzd2 in the anterior region of the developing embryo.

These results are in conflict with a previously reported phenotype for Fzd2$^{LacZ/LacZ}$ animals [93]. This group found Fzd2$^{LacZ/LacZ}$ animals survived to birth at expected Mendelian ratios, but 50% had cleft palate, and died shortly after birth. Of the surviving Fzd2$^{LacZ/LacZ}$ animals, most failed to thrive, with decreased survival and decreased weight gain over the first month of life. Loss of Fzd2 had little effect on canonical Wnt signaling, as assessed by microarray to determine changes in transcriptional profile between mutant and control. But, there was an effect on tissue fusion in the neural tube and orientation of inner ear hair cell development, two processes that require core PCP components for proper development. They also demonstrated loss of Fzd1 in addition to loss of Fzd2 increased the penetrance of the above phenotypes, suggesting some redundancy between the closely related Fzd2 and Fzd1. In additional work, this group found that double mutants of Fzd2$^{LacZ/LacZ}$ and Fzd7$^{LacZ/LacZ}$ (a closely related Frizzled) exhibit a morphological defect consistent with defects in convergent-extension at E8.5

[94]. They also found that $Fzd2^{+/-}Fzd7^{-/-}Wnt5a^{+/-}$ animals fail to survive past E11, but the mechanism of the early embryonic lethality was not examined. These results suggest that Fzd2, and the closely related Fzd1 and Fzd7 all can act, in vivo, through the non-canonical Wnt signaling pathway.

How can we account for this drastically different phenotype with loss of Fzd2? Although this group provided limited information regarding the construction of the LacZ knock-in of the Fzd2 allele, it appears the LacZ gene was knocked-into the 5-prime region of the Fzd2 allele, but the 3-prime region of the gene was not removed. As such, we believe this Fzd2 null allele is a hypomorph and a partial Fzd2 transcript or LacZ-Fzd2 fusion protein may be expressed in these animals, providing partial Fzd2 function. In contrast, the Fzd2 floxed allele we generated has lox-p sites in upstream and downstream of the Fzd2-single exon gene. It would be interesting to obtain these $Fzd2^{LacZ}$ animals to further characterize and compare the different Fzd2 null animals. Additionally, given the similarity between Fzd2 and Fzd7, it would be informative to assess the redundancy between Fzd2 and Fzd7 in early development as well as in lung development.

Figure 4.1 Fzd2 Expression in the Early Embryo and Fzd2 Complete Null Phenotype

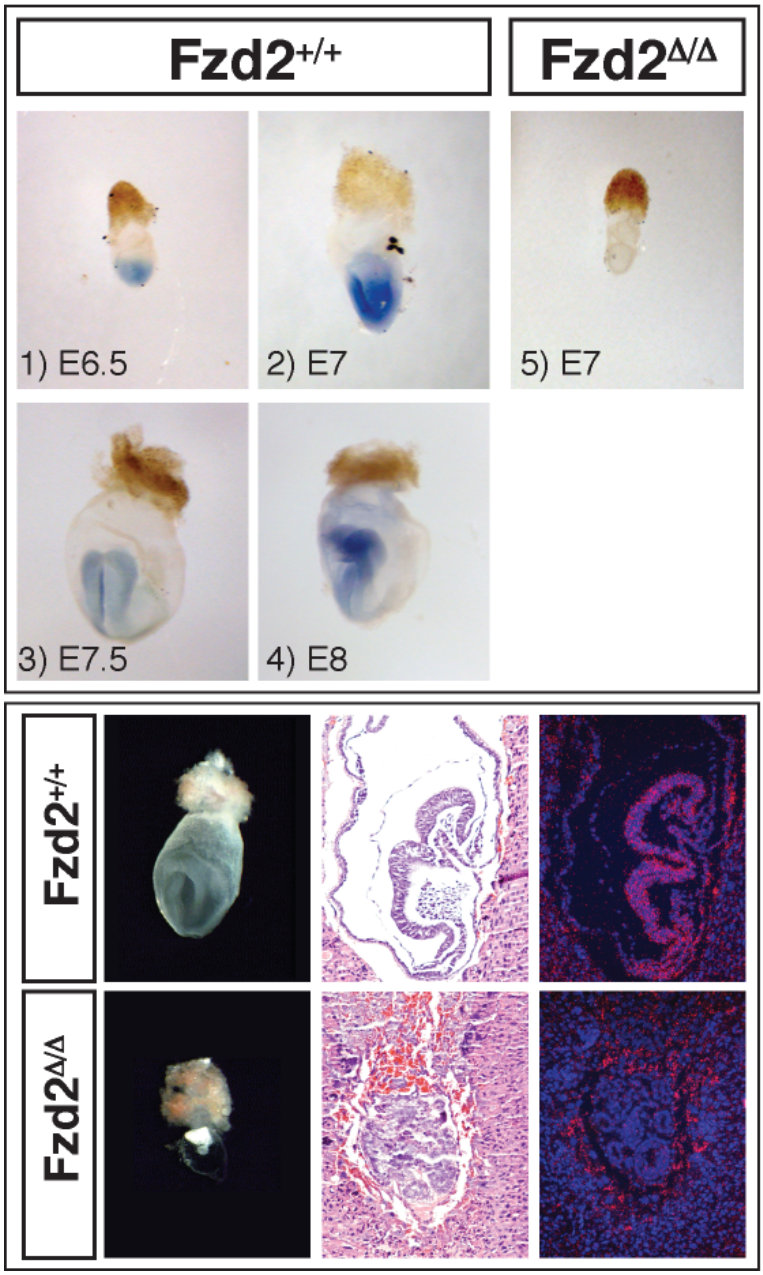

Figure 4.1 Fzd2 Expression in the Early Embryo and Fzd2 Complete Null Phenotype

In situs for Frizzled2 show expression of Frizzled2 throughout the embryos at the early primitive streak stage (1,2). As development proceeds, Frizzled2 expression is localized to the anterior region of the developing embryo, with expression strongest in the neural groove and the neuroectoderm (3-4). CMV-cre mediated excision of the Frizzled2 conditional allele eliminates Frizzled2 expression in the early embryo (5).

Lower Panels: Hematoxilyn and Eosin staining of sections from a uterus containing E7.5 embryos. The mutant embryo (lower panels) failed to form appropriate germ layers and has a generally disorganized appearance. Farthest right panels are in situ hybridization for Frizzled2 on adjacent sections to the H&E stained sections. Frizzled2 is highly expressed in the neural folds, consistent with the whole-mount in situs (1-4). The Frizzled2 null embryo fails to express Frizzled 2. Nuclei are counterstained with Dapi.

Future Directions

What Wnt ligand(s) interact with Fzd2 to promote branching?

In chapter 2, I clearly demonstrated a role for Wnt signaling through Fzd2 for branching morphogenesis in the lung. One aspect of this signaling pathway that was not fully examined was the Wnt ligand acting upstream of Fzd2 signaling in the lung. Additionally, by in situ staining, it appears Fzd2 is expressed ubiquitously both in the epithelium and the mesenchyme (Fig 2.2). If the pattern of protein localization is consistent with the mRNA expression, it is unclear how the specificity of the defect is localized to the distal regions of the epithelium. One potential mechanism for this localization would be spatial specificity of the interaction between the Fzd2 receptor and a spatially restricted Wnt ligand.

A role for Wnt signaling in branching morphogenesis has been suggested by previous studies [14], but the defects in branching morphogenesis have not been well characterized in any of the Wnt mutants evaluated. My results strongly argue for a role for Wnt signaling in branching morphogenesis, but additional work remains to establish the upstream Wnt ligand or ligands responsible for this phenotype. As I described in Chapter 3, Wnt5a has a distinct branching defect early in development that was not previously described, but does not appear to interact with the Wnt/Fzd2 pathway.

Wnt7b has been described as both a canonical and non-canonical Wnt ligand, so we evaluated the loss of one copy of Wnt7b with loss of one copy of Fzd2. Wnt7b is expressed in the lung epithelium, and we noted no difference in Wnt7b localization or expression level with loss of Fzd2 (Fig4.2, I-J). With loss of one copy of each allele, we saw no indication of genetic interaction between Fzd2 and Wnt7b, (Fig 4.2 A-B, E-F). Of interest is that loss of Wnt7b does have a subtle defect in lung lobation. Specifically,

Wnt7b null lungs have delayed appearance of the right medial lobe (Fig 4.2, arrows in C,G). The right medial lobe appears to arise from the right cranial lobe rather than the main right bronchi. Additionally, there are fewer domain branches and the branches that do form are shortened as compared to control. Despite the shortened epithelial tubes, there is no appearance of cystic regions of the lung with loss of Wnt7b. Overall, the branching defect with loss of Wnt7b is distinct from loss of Fzd2, and suggests that there is not a genetic interaction between Fzd2 and Wnt7b. The shortened, but not wider epithelial tubes may be due to the reported defects in proliferation [71] with loss of Wnt7b. We do not observe any significant defects in proliferation with loss of Fzd2 (Fig 3.13), further supporting the hypothesis that Wnt7b and Fzd2 do not genetically interact. While these results strongly argue against Wnt7b and Fzd2 interacting in lung development, analysis of both double nulls or loss of one copy of Wnt7b in addition to complete loss of Fzd2 in the lung epithelium may provide new insights into this potential ligand-receptor interaction.

Two other Wnts expressed in the lung, Wnt2/2a and Wnt11 were not evaluated for interaction with Fzd2. Wnt11 knockout mice have no reported lung phenotype, but do display defects in kidney branching morphogenesis [81]. Wnt2/2a is reported to act through the canonical Wnt signaling pathway, and complete loss of Wnt2/2a causes failure to specify a lung [67]. Wnt2a is required for smooth muscle formation in the lung [70], and this does not appear to be affected with loss of Fzd2 (Fig4.3). The knockout phenotypes of these Wnt ligands do not suggest an interaction with the Fzd2 phenotype. But, because previous defects in branching morphogenesis have been overlooked depending on the method of analysis, evaluation of the interaction between Fzd2 and these Wnt ligands may prove informative. Additionally, there may be other Wnt ligands expressed in the lung that contribute alone, or in concert, to direct branching

morphogenesis. As such, identification of the Wnt ligand(s) that Fzd2 interacts with during lung development is an area open to future study.

What are the physical and mechanical forces acting in the lung during branching morphogenesis?

The results presented both in Chapters 2 and 3 support the hypothesis that changes in cell shape, specifically constriction at the apical surface of the epithelium, are required for the epithelial sheet to bend at specific points for new domain branch formation. Both the constricted cell surface area and the enrichment of actin and pMLC2 at the apical surface strongly suggest that there is increased cortical tension and active constriction mediated by the actin-myosin network localized to the apical surface. But, the presented experiments were unable to establish that apical constriction is required for domain branch formation. Addressing this question is technically challenging in the lung because the area of interest is located at the most interior region of the organ, namely the lumen of the epithelium, which is encased by the mesenchyme. With technical advances in confocal microscopy and improved fluorescent reporters in the future we should be able to perform live imaging studies of regions of new bud formation at the apical surface. This would provide information regarding if the cell surface was dynamically changing in surface area during new bud formation. While this would support the model proposed and would agree with our findings in fixed samples, this still does not address if apical constriction is required for new bud formation.

In order to manipulate the apical surface of the epithelium to determine the required factors for branching morphogenesis, establishment of a cell culture system to study lung epithelial bending is needed. A '2.5D' cell culture system using MDCK cells co-cultured with fibroblasts embedded in collagen has been used to study tubulogenesis

in culture [133]. A lung cell line, Calu3, can form a polarized monolayer and maybe amenable to similar culture conditions. The changes in cell morphology that promote tube formation in this system are reminiscent of vasculogenesis, with basal extensions promoting invasion of the epithelial cells during tubulogenesis. Because the lung epithelium bends into rather than invading the surrounding mesenchyme, optimization of the stiffness of the extracellular matrix will likely be needed to promote this specific morphogenetic change. Additionally, as the apical surface of the lung is subject to interluminal pressure, use of a microfluidic chamber to modulate pressure on the apical and basal regions of the cells will likely be required. These caveats aside, if a cell-culture system could be established, it would allow for investigation into a number of questions about the components required for new branch formation. Changing the pressure and pressure differential between the apical and basal regions could provide information about the forces acting in these respective regions during branch formation. Additional manipulation of the basal environment, through inclusion of particular cell types such as smooth muscle cells will also prove informative regarding the mesenchymal requirements for branching morphogenesis. If our proposed model is correct, then Rho activation at the apical surface is required for constriction and bending of the epithelium to occur. Activation or inactivation of Rho at the apical surface in the cell culture conditions could conceivably be accomplished through a photo-activatable [152]or de-activatable form of Rho, which could be activated in a specific region of the epithelial sheet and evaluated for the ability to induce or block bending.

Several groups have evaluated tension at the apical surface in Drosophila by laser ablating cell-cell junctions and measuring the speed of recoil from the point of sectioning [153, 154]. They found that at regions under increased tension, there is increased speed of retraction. This technique could be used to address several questions raised by my

work. Using the cell culture system outlined above, cutting cell-cell junctions at different time points during bending of the epithelium would provide information regarding the amount of cortical tension present during thickening of the epithelium and bending of the epithelium, as well as during the extension phase of bud formation. Additionally, disrupting cell-cell junctions during folding of the epithelium would allow us to evaluate the effect of loss of cortical tension on the bending process. If efficient bending of the epithelium could still occur, this would suggest that cortical tension is not required, and furthermore, that either forces elsewhere in the epithelium, or forces in the mesenchyme are required for epithelial bending to occur.

While the work detailed in this dissertation has focused on the changes in cell shape and morphology in the lung epithelium, branching morphogenesis of the airways occurs in a complex environment and likely involves physical forces arising from the surrounding mesenchyme, epithelium and interluminal pressure [155]. The role of the mesenchyme in directing new branch formation remains an area requiring further investigation. Imaging of phalloidin staining to visualize actin at the basal surface of the developing lung epithelium shows actin wrapping around the developing stalk perpendicular to the direction of growth (Fig 4.3). Smooth muscle cells are spindle shaped and also wrapped around the stalk in the same direction. This localization of the smooth muscle cells and actin is restricted to the stalk region of the lung and is not found at the regions undergoing new domain branch formation or the bud tip (Fig 4.3). This 'corset-like' arrangement of smooth muscle cells and actin could provide a compressive force on the developing epithelial tube. While we do not see a difference in smooth muscle or basal actin localization with loss of Fzd2 (Fig. 4.3), these factors likely play a role in tissue morphogenesis in the lung at this stage and analysis of branching morphogenesis in animals with defects in smooth muscle formation is needed. It has

been noted that the lung undergoes peristalsis during development, presumably mediated through the surrounding smooth muscle and this constrictive motion has been proposed to effect lung development and growth[156, 157]. Physical modeling taking into account the forces produced by the actin and smooth muscle, the internal pressure of the lung, and the epithelial sheet itself are needed to provide insight into the roles and contributions of the various forces acting in the lung during branch formation. These questions regarding the physical constraints and forces involved in branching morphogenesis highlight the need for further analysis of both the role of internal pressure on branching morphogenesis as well as the forces arising from the mesenchyme during this process. Taking a similar approach to the evaluation completed in this work to identify the changes in cell behavior in the lung epithelium, labeling of individual cells and cell types in the mesenchyme, and analysis of changes in cell behavior over the course of new branch formation would be a place to start.

What constitutes the periodicity generator for stereotyped domain branch formation?

As described above, the stereotyped branching pattern of the lung, and in particular, the regularly patterned emergence of domain branches along the main bronchus is highly suggestive of a periodicity generator used to set the pattern of branches in the lung. There are a number of models in biology that can be referred to that could create a periodic pattern in developing tissues such as the molecular oscillator used in somite formation [158] or a Turing network, recently shown to be used in establishing the pattern of digit formation in the limb [159]. While the proposed Fgf signaling network has a number of properties that make it attractive as the periodicity generator in the lung, much work remains to be completed to establish how this network operates and the intersecting signaling pathways that influence its behavior. Below, I

propose a number of experiments that could establish the nature of the periodicity generator, and then I outline how these tools could be used to evaluate mutants defective in aspects of branching morphogenesis to address the basis of the defect.

I have shown that loss of Fzd2 in the lung epithelium causes a defect in establishing the domain branching pattern in early lung development. Without a clearer picture of the required components of the periodicity generator in the lung, it is difficult to determine if the defects in branching are due to a role of Wnt signaling in the periodicity generator or if the observed defect in Fgf10 expression is a secondary effect of defects in epithelial organization arising from a requirement for Wnt signaling to promote changes in epithelial cell behavior. In order to establish the nature of the periodicity generator in the lung, the first and simplest step would require in situ or antibody staining of both the mesenchyme and the epithelium to establish the molecular components that have both in-phase and out-of-phase expression patterns. The proposed major molecular players in the molecular branching circuitry have been analyzed in isolation and the spatial and temporal relationship between their respective expression patterns have not been evaluated. Dual in-situs for Sprouty2 and Fgf10, Shh and Fgf10, p-ERK (antibody staining for downstream Fgf10 target) with Bmp signaling (antibody staining for pSMAD), and Wnt/β-catenin signaling (using an Axin2 reporter) with p-ERK staining, would be good places to start to establish the temporal and spatial relationship between these proposed interacting factors and the emergence of new branches. These experiments evaluating the expression pattern of the proposed components of the molecular branching circuitry in the epithelium and mesenchyme just prior to and during bending of the epithelium will provide needed information about the

spatial and temporal relationship between the multiple signaling pathways involved in branch formation.

To visualize the activity of the periodicity generator in vivo, fluorescent reporters for down-stream targets of the generator could be used. There are two systems that would be amenable to this type of analysis. In visualizing the activity of the somitogenesis clock, an ubiquitin-destabilized luciferase bioluminescence reporter has been used [160, 161]. This reporter construct placed downstream of the Sprouty2 promoter would allow for live imaging of the signaling oscillator in the epithelium if Fgf10 signaling acts as the driver of the periodicity generator. A similar approach could make use of the MS-2 system for live imaging transcriptional bursts of RNA production in a temporally specific manner. This system makes use of the specific binding between the MS2 bacteriophage capsid protein and the MS2 binding site RNA stem-loops to fluorescently label mRNA of interest. This system has been used to image RNA production of the β-actin gene in the mouse [162, 163]. If a transcriptional target or readout of the periodicity generator could be established (and Sprouty2 would be a good initial candidate), this system would allow for observing temporal activation of the gene of interest. Use of either of these tools would require advancement in detection and analysis methods, but once established, would provide powerful tools for evaluating the gene activity during the morphogenetic process of branching morphogenesis. Once an appropriate readout of the periodicity generator was established, this could be used to analyze defects in failure to branch, such as observed with loss of Fzd2, as well as analyzing mutants with reported over-branching phenotypes [4, 155].

Finally, work evaluating the components of the genetic circuitry required for secondary and tertiary branching morphogenesis has been hampered by use of straight

knock-outs that exhibit early defects in lung formation or early branching processes. My experience using the Shh-cre-ERT2 inducible system demonstrated that while this system does allow for some temporal control of gene activation and inactivation, there is high variability in the number of cells induced. Use of optogenetics to either activate or deactivate genes of interest in specific regions and at specific times [164] in epithelial branching in explants would allow us to directly address the requirement for particular gene products in branch formation. This would also allow for evaluation of genes that can induce folding of the epithelium when activated. Use of this system would also allow for a patch of cells to be induced and labeled, which has proved to be difficult to achieve using tamoxifen-inducible systems. Inducing a patch of cells with a fluorescent label would then allow us to follow these cells over time to determine individual cell movements as branch formation and extension occurs. Development of a system that allows for more robust and specific manipulation of genes in a spatial and temporal manner will allow for additional insight into the genetic requirements for the dynamic process of branching morphogenesis in the lung.

Concluding Remarks

In this dissertation I have provided data that demonstrates a role for Wnt signaling through Fzd2 to promote changes in cell shape in the lung epithelium that are required for new domain branch formation. Using newly available mouse lines and improved imaging and analysis techniques, I was able to complete a detailed description of the cell morphologies in the epithelium during new bud formation, providing insight into the cellular changes that accompany deformation of the airway tubules during construction of the respiratory network. These results make significant contributions to

our understanding of the changes in cell morphology that accompany new domain branch formation. Through analysis of lungs lacking Fzd2 expression in the epithelium, I demonstrated that Wnt signaling through Fzd2 is required for the lung epithelium to undergo these changes in cell morphology. This work presents evidence for intersection of the Wnt signaling pathway and changes in cellular morphology that drive tissue level changes required for establishment of the respiratory tree. This analysis provides new insights into signaling pathways and cellular biology that effect branching morphogenesis. Future investigations building on my findings and using the novel approaches detailed in this dissertation will allow for significant advances in understanding the role of signaling and physical forces in constructing a functional respiratory tree.

Figure 4.2 Wnt7b Mutant Branching Defect and Wnt7b and Wnt2 Expression

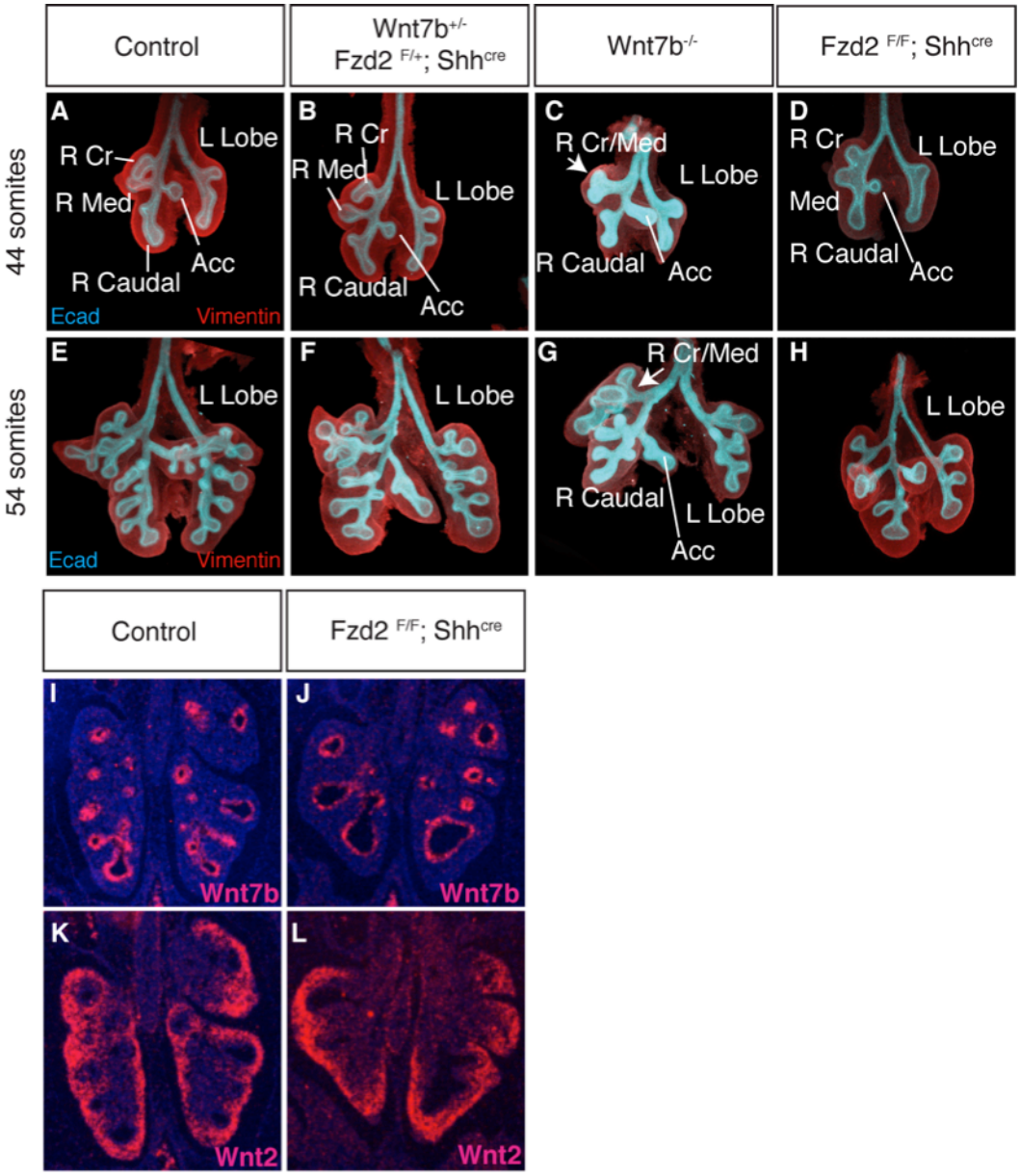

Figure 4.2 Wnt7b Mutant Branching Defect and Wnt7b and Wnt2 Expression

Whole mount lungs were antibody stained for Ecadherin (blue) and Vimentin (red) to visualize the epithelium and mesenchyme respectively. Double heterozygotes for Wnt7b and Fzd2 did not exhibit defects in branching morphogenesis or epithelial tube morphology at either E11.5 (44 somites) or E12.5 (54 somites). Wnt7b mutants exhibit defects in lung epithelial development, with fewer and shorter domain branches at both E11.5 and E12.5 (C, G). Additionally, the right medial lobe does not branch from the main right bronchi, rather the right cranial and medial lobes share a common branch from the parent branch. In situ for Wnt7b transcripts demonstrate expression in the lung epithelium at E12.5 (I). Loss of Fzd2 in the lung epithelium does not have a significant effect on Wnt7b expression or localization pattern (J). Additionally, Wnt2, which is expressed in the lung mesenchyme also does not show a change in expression level or localization with loss of Fzd2 in the lung epithelium.

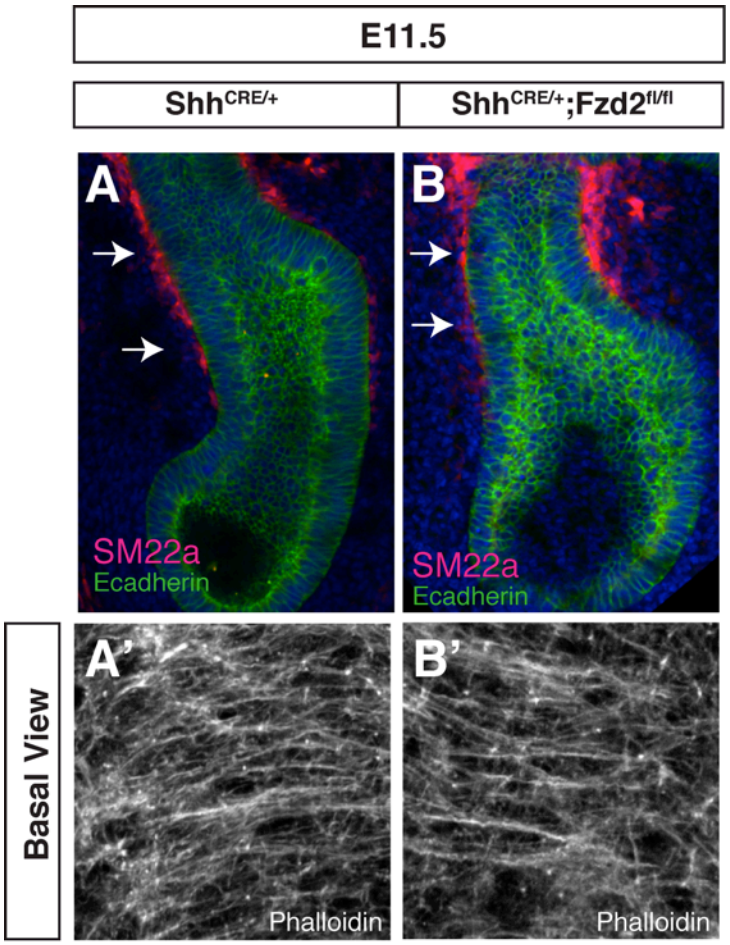

Figure 4.3 Smooth Muscle Development and basal actin organization and localization is normal in Shh$^{cre/+}$; Fzd2$^{F/F}$ mutant lungs.

SM22a immunostaining shows development of smooth muscle surrounding the proximal regions of the developing airway tree at E11.5. Note that SM22a staining extends distally to approximately the same level in the Fzd2 mutants as the control lungs (arrows in A and B). Imaging phalloidin staining of the basal surface of the lung epithelium demonstrates actin fibers organized perpendicular to the direction of growth of the extending stalk (A'-B'). There is no significant difference in actin levels or organization in the mutant lungs as compared to control.

BIBLIOGRAPHY

1. Kadzik, R.S. and E.E. Morrisey, *Directing lung endoderm differentiation in pluripotent stem cells*. Cell stem cell, 2012. **10**(4): p. 355-61.
2. Morrisey, E.E. and B.L. Hogan, *Preparing for the first breath: genetic and cellular mechanisms in lung development*. Developmental cell, 2010. **18**(1): p. 8-23.
3. Shannon, J.M. and B.A. Hyatt, *Epithelial-mesenchymal interactions in the developing lung*. Annual review of physiology, 2004. **66**: p. 625-45.
4. Metzger, R.J., et al., *The branching programme of mouse lung development*. Nature, 2008. **453**(7196): p. 745-50.
5. Zorn, A.M. and J.M. Wells, *Vertebrate endoderm development and organ formation*. Annual review of cell and developmental biology, 2009. **25**: p. 221-51.
6. Domyan, E.T., et al., *Signaling through BMP receptors promotes respiratory identity in the foregut via repression of Sox2*. Development, 2011. **138**(5): p. 971-81.
7. Patel, N., P.T. Sharpe, and I. Miletich, *Coordination of epithelial branching and salivary gland lumen formation by Wnt and FGF signals*. Developmental biology, 2011. **358**(1): p. 156-67.
8. Ewald, A.J., et al., *Mammary collective cell migration involves transient loss of epithelial features and individual cell migration within the epithelium*. Journal of cell science, 2012. **125**(Pt 11): p. 2638-54.
9. Que, J., et al., *Multiple roles for Sox2 in the developing and adult mouse trachea*. Development, 2009. **136**(11): p. 1899-907.
10. Tompkins, D.H., et al., *Sox2 is required for maintenance and differentiation of bronchiolar Clara, ciliated, and goblet cells*. PloS one, 2009. **4**(12): p. e8248.
11. Rawlins, E.L., et al., *The Id2+ distal tip lung epithelium contains individual multipotent embryonic progenitor cells*. Development, 2009. **136**(22): p. 3741-5.
12. Chang, D.R., et al., *Lung epithelial branching program antagonizes alveolar differentiation*. Proceedings of the National Academy of Sciences of the United States of America, 2013. **110**(45): p. 18042-51.
13. Rockich, B.E., et al., *Sox9 plays multiple roles in the lung epithelium during branching morphogenesis*. Proceedings of the National Academy of Sciences of the United States of America, 2013. **110**(47): p. E4456-64.
14. Mucenski, M.L., et al., *beta-Catenin is required for specification of proximal/distal cell fate during lung morphogenesis*. The Journal of biological chemistry, 2003. **278**(41): p. 40231-8.
15. Weaver, M., et al., *Bmp signaling regulates proximal-distal differentiation of endoderm in mouse lung development*. Development, 1999. **126**(18): p. 4005-15.
16. Morimoto, M., et al., *Canonical Notch signaling in the developing lung is required for determination of arterial smooth muscle cells and selection of Clara versus ciliated cell fate*. Journal of cell science, 2010. **123**(Pt 2): p. 213-24.
17. Hsia, C.C. and M.H. Tawhai, *What can imaging tell us about physiology? Lung growth and regional mechanical strain*. Journal of applied physiology, 2012. **113**(6): p. 937-46.
18. Alescio, T. and A. Cassini, *Induction in vitro of tracheal buds by pulmonary mesenchyme grafted on tracheal epithelium*. The Journal of experimental zoology, 1962. **150**: p. 83-94.

19. Masters, J.R., *Epithelial-mesenchymal interaction during lung development: the effect of mesenchymal mass*. Developmental biology, 1976. **51**(1): p. 98-108.
20. Taderera, J.V., *Control of lung differentiation in vitro*. Developmental biology, 1967. **16**(5): p. 489-512.
21. Park, W.Y., et al., *FGF-10 is a chemotactic factor for distal epithelial buds during lung development*. Developmental biology, 1998. **201**(2): p. 125-34.
22. Bellusci, S., et al., *Fibroblast growth factor 10 (FGF10) and branching morphogenesis in the embryonic mouse lung*. Development, 1997. **124**(23): p. 4867-78.
23. Dorey, K. and E. Amaya, *FGF signalling: diverse roles during early vertebrate embryogenesis*. Development, 2010. **137**(22): p. 3731-42.
24. Izvolsky, K.I., et al., *Heparan sulfate-FGF10 interactions during lung morphogenesis*. Developmental biology, 2003. **258**(1): p. 185-200.
25. Izvolsky, K.I., et al., *Heparan sulfates expressed in the distal lung are required for Fgf10 binding to the epithelium and for airway branching*. American journal of physiology. Lung cellular and molecular physiology, 2003. **285**(4): p. L838-46.
26. Yin, Y., F. Wang, and D.M. Ornitz, *Mesothelial- and epithelial-derived FGF9 have distinct functions in the regulation of lung development*. Development, 2011. **138**(15): p. 3169-77.
27. Cardoso, W.V., et al., *FGF-1 and FGF-7 induce distinct patterns of growth and differentiation in embryonic lung epithelium*. Developmental dynamics : an official publication of the American Association of Anatomists, 1997. **208**(3): p. 398-405.
28. Post, M., et al., *Keratinocyte growth factor and its receptor are involved in regulating early lung branching*. Development, 1996. **122**(10): p. 3107-15.
29. Finch, P.W., et al., *Pattern of keratinocyte growth factor and keratinocyte growth factor receptor expression during mouse fetal development suggests a role in mediating morphogenetic mesenchymal-epithelial interactions*. Developmental dynamics : an official publication of the American Association of Anatomists, 1995. **203**(2): p. 223-40.
30. Peters, K., et al., *Targeted expression of a dominant negative FGF receptor blocks branching morphogenesis and epithelial differentiation of the mouse lung*. The EMBO journal, 1994. **13**(14): p. 3296-301.
31. Ohuchi, H., et al., *FGF10 acts as a major ligand for FGF receptor 2 IIIb in mouse multi-organ development*. Biochemical and biophysical research communications, 2000. **277**(3): p. 643-9.
32. Francavilla, C., et al., *Functional proteomics defines the molecular switch underlying FGF receptor trafficking and cellular outputs*. Molecular cell, 2013. **51**(6): p. 707-22.
33. Guo, L., Q.C. Yu, and E. Fuchs, *Targeting expression of keratinocyte growth factor to keratinocytes elicits striking changes in epithelial differentiation in transgenic mice*. The EMBO journal, 1993. **12**(3): p. 973-86.
34. Celli, G., et al., *Soluble dominant-negative receptor uncovers essential roles for fibroblast growth factors in multi-organ induction and patterning*. The EMBO journal, 1998. **17**(6): p. 1642-55.
35. Abler, L.L., S.L. Mansour, and X. Sun, *Conditional gene inactivation reveals roles for Fgf10 and Fgfr2 in establishing a normal pattern of epithelial*

branching in the mouse lung. Developmental dynamics : an official publication of the American Association of Anatomists, 2009. **238**(8): p. 1999-2013.
36. Min, H., et al., *Fgf-10 is required for both limb and lung development and exhibits striking functional similarity to Drosophila branchless*. Genes & development, 1998. **12**(20): p. 3156-61.
37. Sekine, K., et al., *Fgf10 is essential for limb and lung formation*. Nature genetics, 1999. **21**(1): p. 138-41.
38. Ramasamy, S.K., et al., *Fgf10 dosage is critical for the amplification of epithelial cell progenitors and for the formation of multiple mesenchymal lineages during lung development*. Developmental biology, 2007. **307**(2): p. 237-47.
39. Tang, N., et al., *Control of mitotic spindle angle by the RAS-regulated ERK1/2 pathway determines lung tube shape*. Science, 2011. **333**(6040): p. 342-5.
40. Minowada, G., et al., *Vertebrate Sprouty genes are induced by FGF signaling and can cause chondrodysplasia when overexpressed*. Development, 1999. **126**(20): p. 4465-75.
41. Tefft, J.D., et al., *Conserved function of mSpry-2, a murine homolog of Drosophila sprouty, which negatively modulates respiratory organogenesis*. Current biology : CB, 1999. **9**(4): p. 219-22.
42. Mailleux, A.A., et al., *Evidence that SPROUTY2 functions as an inhibitor of mouse embryonic lung growth and morphogenesis*. Mechanisms of development, 2001. **102**(1-2): p. 81-94.
43. Tefft, D., et al., *mSprouty2 inhibits FGF10-activated MAP kinase by differentially binding to upstream target proteins*. American journal of physiology. Lung cellular and molecular physiology, 2002. **283**(4): p. L700-6.
44. Taniguchi, K., et al., *Sprouty2 and Sprouty4 are essential for embryonic morphogenesis and regulation of FGF signaling*. Biochemical and biophysical research communications, 2007. **352**(4): p. 896-902.
45. Pepicelli, C.V., P.M. Lewis, and A.P. McMahon, *Sonic hedgehog regulates branching morphogenesis in the mammalian lung*. Current biology : CB, 1998. **8**(19): p. 1083-6.
46. Bellusci, S., et al., *Involvement of Sonic hedgehog (Shh) in mouse embryonic lung growth and morphogenesis*. Development, 1997. **124**(1): p. 53-63.
47. Lebeche, D., S. Malpel, and W.V. Cardoso, *Fibroblast growth factor interactions in the developing lung*. Mechanisms of development, 1999. **86**(1-2): p. 125-36.
48. Volckaert, T., et al., *Localized Fgf10 expression is not required for lung branching morphogenesis but prevents differentiation of epithelial progenitors*. Development, 2013. **140**(18): p. 3731-42.
49. Ghabrial, A., et al., *Branching morphogenesis of the Drosophila tracheal system*. Annual review of cell and developmental biology, 2003. **19**: p. 623-47.
50. Schnatwinkel, C. and L. Niswander, *Multiparametric image analysis of lung-branching morphogenesis*. Developmental dynamics : an official publication of the American Association of Anatomists, 2013. **242**(6): p. 622-37.
51. Clevers, H. and R. Nusse, *Wnt/beta-catenin signaling and disease*. Cell, 2012. **149**(6): p. 1192-205.
52. Strutt, D.I., U. Weber, and M. Mlodzik, *The role of RhoA in tissue polarity and Frizzled signalling*. Nature, 1997. **387**(6630): p. 292-5.
53. Habas, R., Y. Kato, and X. He, *Wnt/Frizzled activation of Rho regulates vertebrate gastrulation and requires a novel Formin homology protein Daam1*. Cell, 2001. **107**(7): p. 843-54.

54. Tahinci, E. and K. Symes, *Distinct functions of Rho and Rac are required for convergent extension during Xenopus gastrulation*. Developmental biology, 2003. **259**(2): p. 318-35.
55. Schlessinger, K., A. Hall, and N. Tolwinski, *Wnt signaling pathways meet Rho GTPases*. Genes & development, 2009. **23**(3): p. 265-77.
56. Mason, F.M., M. Tworoger, and A.C. Martin, *Apical domain polarization localizes actin-myosin activity to drive ratchet-like apical constriction*. Nature cell biology, 2013. **15**(8): p. 926-36.
57. Slusarski, D.C., et al., *Modulation of embryonic intracellular Ca2+ signaling by Wnt-5A*. Developmental biology, 1997. **182**(1): p. 114-20.
58. Slusarski, D.C., V.G. Corces, and R.T. Moon, *Interaction of Wnt and a Frizzled homologue triggers G-protein-linked phosphatidylinositol signalling*. Nature, 1997. **390**(6658): p. 410-3.
59. Kuhl, M., et al., *Ca(2+)/calmodulin-dependent protein kinase II is stimulated by Wnt and Frizzled homologs and promotes ventral cell fates in Xenopus*. The Journal of biological chemistry, 2000. **275**(17): p. 12701-11.
60. Sheldahl, L.C., et al., *Protein kinase C is differentially stimulated by Wnt and Frizzled homologs in a G-protein-dependent manner*. Current biology : CB, 1999. **9**(13): p. 695-8.
61. Saneyoshi, T., et al., *The Wnt/calcium pathway activates NF-AT and promotes ventral cell fate in Xenopus embryos*. Nature, 2002. **417**(6886): p. 295-9.
62. Liao, G., et al., *Jun NH2-terminal kinase (JNK) prevents nuclear beta-catenin accumulation and regulates axis formation in Xenopus embryos*. Proceedings of the National Academy of Sciences of the United States of America, 2006. **103**(44): p. 16313-8.
63. Topol, L., et al., *Wnt-5a inhibits the canonical Wnt pathway by promoting GSK-3-independent beta-catenin degradation*. The Journal of cell biology, 2003. **162**(5): p. 899-908.
64. Ishitani, T., et al., *The TAK1-NLK mitogen-activated protein kinase cascade functions in the Wnt-5a/Ca(2+) pathway to antagonize Wnt/beta-catenin signaling*. Molecular and cellular biology, 2003. **23**(1): p. 131-9.
65. Lako, M., et al., *Isolation, characterisation and embryonic expression of WNT11, a gene which maps to 11q13.5 and has possible roles in the development of skeleton, kidney and lung*. Gene, 1998. **219**(1-2): p. 101-10.
66. Miller, M.F., et al., *Wnt ligands signal in a cooperative manner to promote foregut organogenesis*. Proceedings of the National Academy of Sciences of the United States of America, 2012. **109**(38): p. 15348-53.
67. Goss, A.M., et al., *Wnt2/2b and beta-catenin signaling are necessary and sufficient to specify lung progenitors in the foregut*. Developmental cell, 2009. **17**(2): p. 290-8.
68. Harris-Johnson, K.S., et al., *beta-Catenin promotes respiratory progenitor identity in mouse foregut*. Proceedings of the National Academy of Sciences of the United States of America, 2009. **106**(38): p. 16287-92.
69. Okubo, T. and B.L. Hogan, *Hyperactive Wnt signaling changes the developmental potential of embryonic lung endoderm*. Journal of biology, 2004. **3**(3): p. 11.
70. Goss, A.M., et al., *Wnt2 signaling is necessary and sufficient to activate the airway smooth muscle program in the lung by regulating myocardin/Mrtf-B and Fgf10 expression*. Developmental biology, 2011. **356**(2): p. 541-52.

71. Rajagopal, J., et al., *Wnt7b stimulates embryonic lung growth by coordinately increasing the replication of epithelium and mesenchyme*. Development, 2008. **135**(9): p. 1625-34.
72. Shu, W., et al., *Wnt7b regulates mesenchymal proliferation and vascular development in the lung*. Development, 2002. **129**(20): p. 4831-42.
73. Wang, Z., et al., *Wnt7b activates canonical signaling in epithelial and vascular smooth muscle cells through interactions with Fzd1, Fzd10, and LRP5*. Molecular and cellular biology, 2005. **25**(12): p. 5022-30.
74. Du, S.J., et al., *Identification of distinct classes and functional domains of Wnts through expression of wild-type and chimeric proteins in Xenopus embryos*. Molecular and cellular biology, 1995. **15**(5): p. 2625-34.
75. Mikels, A.J. and R. Nusse, *Purified Wnt5a protein activates or inhibits beta-catenin-TCF signaling depending on receptor context*. PLoS biology, 2006. **4**(4): p. e115.
76. Li, C., et al., *Wnt5a participates in distal lung morphogenesis*. Developmental biology, 2002. **248**(1): p. 68-81.
77. Li, C., et al., *Wnt5a regulates Shh and Fgf10 signaling during lung development*. Developmental biology, 2005. **287**(1): p. 86-97.
78. van Amerongen, R., *Alternative Wnt pathways and receptors*. Cold Spring Harbor perspectives in biology, 2012. **4**(10).
79. Karner, C.M., et al., *Wnt9b signaling regulates planar cell polarity and kidney tubule morphogenesis*. Nature genetics, 2009. **41**(7): p. 793-9.
80. Habib, S.J., et al., *A localized Wnt signal orients asymmetric stem cell division in vitro*. Science, 2013. **339**(6126): p. 1445-8.
81. Majumdar, A., et al., *Wnt11 and Ret/Gdnf pathways cooperate in regulating ureteric branching during metanephric kidney development*. Development, 2003. **130**(14): p. 3175-85.
82. Yates, L.L., et al., *The planar cell polarity gene Vangl2 is required for mammalian kidney-branching morphogenesis and glomerular maturation*. Human molecular genetics, 2010. **19**(23): p. 4663-76.
83. Yates, L.L., et al., *The PCP genes Celsr1 and Vangl2 are required for normal lung branching morphogenesis*. Human molecular genetics, 2010. **19**(11): p. 2251-67.
84. Yates, L.L., et al., *Scribble is required for normal epithelial cell-cell contacts and lumen morphogenesis in the mammalian lung*. Developmental biology, 2013. **373**(2): p. 267-80.
85. White, A.C., et al., *FGF9 and SHH signaling coordinate lung growth and development through regulation of distinct mesenchymal domains*. Development, 2006. **133**(8): p. 1507-17.
86. Lu, J., et al., *Identification of FGF10 targets in the embryonic lung epithelium during bud morphogenesis*. The Journal of biological chemistry, 2005. **280**(6): p. 4834-41.
87. Shu, W., et al., *Wnt/beta-catenin signaling acts upstream of N-myc, BMP4, and FGF signaling to regulate proximal-distal patterning in the lung*. Developmental biology, 2005. **283**(1): p. 226-39.
88. Huang, H.C. and P.S. Klein, *The Frizzled family: receptors for multiple signal transduction pathways*. Genome biology, 2004. **5**(7): p. 234.
89. Zhang, Y., et al., *A Gata6-Wnt pathway required for epithelial stem cell development and airway regeneration*. Nature genetics, 2008. **40**(7): p. 862-70.

90. Sato, A., et al., *Wnt5a regulates distinct signalling pathways by binding to Frizzled2*. The EMBO journal, 2010. **29**(1): p. 41-54.
91. Verkaar, F., et al., *Stably overexpressed human Frizzled-2 signals through the beta-catenin pathway and does not activate Ca2+-mobilization in Human Embryonic Kidney 293 cells*. Cellular signalling, 2009. **21**(1): p. 22-33.
92. Li, C., et al., *Ror2 modulates the canonical Wnt signaling in lung epithelial cells through cooperation with Fzd2*. BMC molecular biology, 2008. **9**: p. 11.
93. Yu, H., et al., *Frizzled 1 and frizzled 2 genes function in palate, ventricular septum and neural tube closure: general implications for tissue fusion processes*. Development, 2010. **137**(21): p. 3707-17.
94. Yu, H., et al., *Frizzled 2 and frizzled 7 function redundantly in convergent extension and closure of the ventricular septum and palate: evidence for a network of interacting genes*. Development, 2012. **139**(23): p. 4383-94.
95. Kadzik, R.S., et al., *Wnt ligand/Frizzled 2 receptor signaling regulates tube shape and branch-point formation in the lung through control of epithelial cell shape*. Proceedings of the National Academy of Sciences of the United States of America, 2014.
96. Varner, V.D. and C.M. Nelson, *Cellular and physical mechanisms of branching morphogenesis*. Development, 2014. **141**(14): p. 2750-9.
97. Weaver, M., N.R. Dunn, and B.L. Hogan, *Bmp4 and Fgf10 play opposing roles during lung bud morphogenesis*. Development, 2000. **127**(12): p. 2695-704.
98. Kim, H.Y., V.D. Varner, and C.M. Nelson, *Apical constriction initiates new bud formation during monopodial branching of the embryonic chicken lung*. Development, 2013.
99. Nogawa, H., K. Morita, and W.V. Cardoso, *Bud formation precedes the appearance of differential cell proliferation during branching morphogenesis of mouse lung epithelium in vitro*. Developmental dynamics : an official publication of the American Association of Anatomists, 1998. **213**(2): p. 228-35.
100. Packard, A., et al., *Luminal mitosis drives epithelial cell dispersal within the branching ureteric bud*. Developmental cell, 2013. **27**(3): p. 319-30.
101. Hardin, J. and R. Keller, *The behaviour and function of bottle cells during gastrulation of Xenopus laevis*. Development, 1988. **103**(1): p. 211-30.
102. Lee, J.Y. and R.M. Harland, *Actomyosin contractility and microtubules drive apical constriction in Xenopus bottle cells*. Developmental biology, 2007. **311**(1): p. 40-52.
103. Rolo, A., P. Skoglund, and R. Keller, *Morphogenetic movements driving neural tube closure in Xenopus require myosin IIB*. Developmental biology, 2009. **327**(2): p. 327-38.
104. Liu, W., et al., *MIM regulates vertebrate neural tube closure*. Development, 2011. **138**(10): p. 2035-47.
105. Svoboda, K.K. and K.S. O'Shea, *An analysis of cell shape and the neuroepithelial basal lamina during optic vesicle formation in the mouse embryo*. Development, 1987. **100**(2): p. 185-200.
106. Girdler, G.C. and K. Roper, *Controlling cell shape changes during salivary gland tube formation in Drosophila*. Seminars in cell & developmental biology, 2014. **31C**: p. 74-81.
107. Yokomizo, T., et al., *Whole-mount three-dimensional imaging of internally localized immunostained cells within mouse embryos*. Nature protocols, 2012. **7**(3): p. 421-31.

108. Del Moral, P.M. and D. Warburton, *Explant culture of mouse embryonic whole lung, isolated epithelium, or mesenchyme under chemically defined conditions as a system to evaluate the molecular mechanism of branching morphogenesis and cellular differentiation*. Methods in molecular biology, 2010. **633**: p. 71-9.
109. Cardoso, W.V. and J. Lu, *Regulation of early lung morphogenesis: questions, facts and controversies*. Development, 2006. **133**(9): p. 1611-24.
110. Zallen, J.A. and E. Wieschaus, *Patterned gene expression directs bipolar planar polarity in Drosophila*. Developmental cell, 2004. **6**(3): p. 343-55.
111. Wang, Y. and J. Nathans, *Tissue/planar cell polarity in vertebrates: new insights and new questions*. Development, 2007. **134**(4): p. 647-58.
112. Nishimura, T., H. Honda, and M. Takeichi, *Planar cell polarity links axes of spatial dynamics in neural-tube closure*. Cell, 2012. **149**(5): p. 1084-97.
113. Harfe, B.D., et al., *Evidence for an expansion-based temporal Shh gradient in specifying vertebrate digit identities*. Cell, 2004. **118**(4): p. 517-28.
114. Wang, Y., et al., *Development and regeneration of Sox2+ endoderm progenitors are regulated by a Hdac1/2-Bmp4/Rb1 regulatory pathway*. Developmental cell, 2013. **24**(4): p. 345-58.
115. Gontan, C., et al., *Sox2 is important for two crucial processes in lung development: branching morphogenesis and epithelial cell differentiation*. Developmental biology, 2008. **317**(1): p. 296-309.
116. Ishii, Y., et al., *Region-specific expression of chicken Sox2 in the developing gut and lung epithelium: regulation by epithelial-mesenchymal interactions*. Developmental dynamics : an official publication of the American Association of Anatomists, 1998. **213**(4): p. 464-75.
117. Liu, Y. and B.L. Hogan, *Differential gene expression in the distal tip endoderm of the embryonic mouse lung*. Gene expression patterns : GEP, 2002. **2**(3-4): p. 229-33.
118. DasGupta, R. and E. Fuchs, *Multiple roles for activated LEF/TCF transcription complexes during hair follicle development and differentiation*. Development, 1999. **126**(20): p. 4557-68.
119. Al Alam, D., et al., *Contrasting expression of canonical Wnt signaling reporters TOPGAL, BATGAL and Axin2(LacZ) during murine lung development and repair*. PloS one, 2011. **6**(8): p. e23139.
120. Gonzaga, S., et al., *Cystic adenomatoid malformations are induced by localized FGF10 overexpression in fetal rat lung*. American journal of respiratory cell and molecular biology, 2008. **39**(3): p. 346-55.
121. Grindley, J.C., et al., *Evidence for the involvement of the Gli gene family in embryonic mouse lung development*. Developmental biology, 1997. **188**(2): p. 337-48.
122. Liu, T.C., Z.P. Wang, and Z.T. Zhao, *[Meta analysis on the association between parental 5,10-methylenetetrahydrofolate reductase C677T polymorphism and the neural tube defects of their offspring]*. Zhonghua liu xing bing xue za zhi = Zhonghua liuxingbingxue zazhi, 2011. **32**(1): p. 60-7.
123. Mason, F.M. and A.C. Martin, *Tuning cell shape change with contractile ratchets*. Current opinion in genetics & development, 2011. **21**(5): p. 671-9.
124. Drees, F., et al., *Alpha-catenin is a molecular switch that binds E-cadherin-beta-catenin and regulates actin-filament assembly*. Cell, 2005. **123**(5): p. 903-15.

125. Sarpal, R., et al., *Mutational analysis supports a core role for Drosophila alpha-catenin in adherens junction function*. Journal of cell science, 2012. **125**(Pt 1): p. 233-45.
126. Benjamin, J.M., et al., *AlphaE-catenin regulates actin dynamics independently of cadherin-mediated cell-cell adhesion*. The Journal of cell biology, 2010. **189**(2): p. 339-52.
127. Tanegashima, K., H. Zhao, and I.B. Dawid, *WGEF activates Rho in the Wnt-PCP pathway and controls convergent extension in Xenopus gastrulation*. The EMBO journal, 2008. **27**(4): p. 606-17.
128. Schoenwaelder, S.M., et al., *The protein tyrosine phosphatase Shp-2 regulates RhoA activity*. Current biology : CB, 2000. **10**(23): p. 1523-6.
129. Sawyer, J.M., et al., *Apical constriction: a cell shape change that can drive morphogenesis*. Developmental biology, 2010. **341**(1): p. 5-19.
130. Lee, J.Y., et al., *Wnt/Frizzled signaling controls C. elegans gastrulation by activating actomyosin contractility*. Current biology : CB, 2006. **16**(20): p. 1986-97.
131. Kumburegama, S., et al., *Strabismus-mediated primary archenteron invagination is uncoupled from Wnt/beta-catenin-dependent endoderm cell fate specification in Nematostella vectensis (Anthozoa, Cnidaria): Implications for the evolution of gastrulation*. EvoDevo, 2011. **2**(1): p. 2.
132. Choi, S.C. and S.Y. Sokol, *The involvement of lethal giant larvae and Wnt signaling in bottle cell formation in Xenopus embryos*. Developmental biology, 2009. **336**(1): p. 68-75.
133. Kwon, S.H., P.I. Nedvetsky, and K.E. Mostov, *Transcriptional profiling identifies TNS4 function in epithelial tubulogenesis*. Current biology : CB, 2011. **21**(2): p. 161-6.
134. Gelbart, M.A., et al., *Volume conservation principle involved in cell lengthening and nucleus movement during tissue morphogenesis*. Proceedings of the National Academy of Sciences of the United States of America, 2012. **109**(47): p. 19298-303.
135. Winter, C.G., et al., *Drosophila Rho-associated kinase (Drok) links Frizzled-mediated planar cell polarity signaling to the actin cytoskeleton*. Cell, 2001. **105**(1): p. 81-91.
136. Muzumdar, M.D., et al., *A global double-fluorescent Cre reporter mouse*. Genesis, 2007. **45**(9): p. 593-605.
137. Li, S., et al., *Foxp1/4 control epithelial cell fate during lung development and regeneration through regulation of anterior gradient 2*. Development, 2012. **139**(14): p. 2500-9.
138. Kim, S., et al., *A serum response factor-dependent transcriptional regulatory program identifies distinct smooth muscle cell sublineages*. Molecular and cellular biology, 1997. **17**(4): p. 2266-78.
139. Winnier, G., et al., *Bone morphogenetic protein-4 is required for mesoderm formation and patterning in the mouse*. Genes & development, 1995. **9**(17): p. 2105-16.
140. Kuo, C.T., et al., *GATA4 transcription factor is required for ventral morphogenesis and heart tube formation*. Genes & development, 1997. **11**(8): p. 1048-60.
141. Huelsken, J., et al., *Requirement for beta-catenin in anterior-posterior axis formation in mice*. The Journal of cell biology, 2000. **148**(3): p. 567-78.

142. Liu, P., et al., *Requirement for Wnt3 in vertebrate axis formation*. Nature genetics, 1999. **22**(4): p. 361-5.
143. Haegel, H., et al., *Lack of beta-catenin affects mouse development at gastrulation*. Development, 1995. **121**(11): p. 3529-37.
144. Valenta, T., et al., *Probing transcription-specific outputs of beta-catenin in vivo*. Genes & development, 2011. **25**(24): p. 2631-43.
145. Tortelote, G.G., et al., *Wnt3 function in the epiblast is required for the maintenance but not the initiation of gastrulation in mice*. Developmental biology, 2013. **374**(1): p. 164-73.
146. Barrow, J.R., et al., *Wnt3 signaling in the epiblast is required for proper orientation of the anteroposterior axis*. Developmental biology, 2007. **312**(1): p. 312-20.
147. Arkell, R.M., N. Fossat, and P.P. Tam, *Wnt signalling in mouse gastrulation and anterior development: new players in the pathway and signal output*. Current opinion in genetics & development, 2013. **23**(4): p. 454-60.
148. Fossat, N., et al., *Stringent requirement of a proper level of canonical WNT signalling activity for head formation in mouse embryo*. Development, 2011. **138**(4): p. 667-76.
149. Lewis, S.L., et al., *Dkk1 and Wnt3 interact to control head morphogenesis in the mouse*. Development, 2008. **135**(10): p. 1791-801.
150. Mukhopadhyay, M., et al., *Dickkopf1 is required for embryonic head induction and limb morphogenesis in the mouse*. Developmental cell, 2001. **1**(3): p. 423-34.
151. Lu, C.C., E.J. Robertson, and J. Brennan, *The mouse frizzled 8 receptor is expressed in anterior organizer tissues*. Gene expression patterns : GEP, 2004. **4**(5): p. 569-72.
152. Wu, Y.I., et al., *Spatiotemporal control of small GTPases with light using the LOV domain*. Methods in enzymology, 2011. **497**: p. 393-407.
153. Martin, A.C., et al., *Integration of contractile forces during tissue invagination*. The Journal of cell biology, 2010. **188**(5): p. 735-49.
154. Rauskolb, C., et al., *Cytoskeletal tension inhibits Hippo signaling through an Ajuba-Warts complex*. Cell, 2014. **158**(1): p. 143-56.
155. Unbekandt, M., et al., *Tracheal occlusion increases the rate of epithelial branching of embryonic mouse lung via the FGF10-FGFR2b-Sprouty2 pathway*. Mechanisms of development, 2008. **125**(3-4): p. 314-24.
156. Jesudason, E.C., et al., *Developing rat lung has a sided pacemaker region for morphogenesis-related airway peristalsis*. American journal of respiratory cell and molecular biology, 2005. **32**(2): p. 118-27.
157. Jesudason, E.C., et al., *Peristalsis of airway smooth muscle is developmentally regulated and uncoupled from hypoplastic lung growth*. American journal of physiology. Lung cellular and molecular physiology, 2006. **291**(4): p. L559-65.
158. Pourquie, O., *Vertebrate segmentation: from cyclic gene networks to scoliosis*. Cell, 2011. **145**(5): p. 650-63.
159. Raspopovic, J., et al., *Modeling digits. Digit patterning is controlled by a Bmp-Sox9-Wnt Turing network modulated by morphogen gradients*. Science, 2014. **345**(6196): p. 566-70.
160. Takashima, Y., et al., *Intronic delay is essential for oscillatory expression in the segmentation clock*. Proceedings of the National Academy of Sciences of the United States of America, 2011. **108**(8): p. 3300-5.

161. Cinquin, O., *Understanding the somitogenesis clock: what's missing?* Mechanisms of development, 2007. **124**(7-8): p. 501-17.
162. Lionnet, T., et al., *A transgenic mouse for in vivo detection of endogenous labeled mRNA*. Nature methods, 2011. **8**(2): p. 165-70.
163. Park, H.Y., et al., *Visualization of dynamics of single endogenous mRNA labeled in live mouse*. Science, 2014. **343**(6169): p. 422-4.
164. Konermann, S., et al., *Optical control of mammalian endogenous transcription and epigenetic states*. Nature, 2013. **500**(7463): p. 472-6.